The development of photosensitive surfaces to control cell adhesion and form cell patterns

by

Nan Cheng

A thesis submitted to the Faculty of Graduate and Postdoctoral Studies in fulfilment of the requirement for

The Doctor Degree of Philosophy in Chemical Engineering

Statement of contributions of collaborators

I hereby declare that I am the sole author of this thesis. I performed all the synthesis and cell culture experiments, and all data analysis for all the papers. The scientific guidance throughout the project and editorial comments for the written work were provided by my supervisor Dr. Xudong Cao.

Abstract

Cell adhesion is the first step of cell response to materials and the extracellular matrix (ECM), and is essential to all cell behaviours such as cell proliferation, differentiation, migration and apoptosis for anchor-dependent cells. Therefore, studies of cell attachment have important implications to control and study cell behaviours. During many developed techniques for cell attachment, the manipulation of surface chemistry is a very important method to control initial cell attachment. To control cell adhesion on a two-dimensional surface is a simple model to study cell behaviours, and is a fundamental topic for cell biology, tissue engineering, and the development of biosensors. From the engineering point of view, the preparation of a material with controllable surface chemistry can help studies of cell behaviours and help scientists understand how surface features and chemistry influence cell behaviours. During the fabrication, the challenge is to create a surface with heterogeneous surface properties in the micro scale and subsequently to guide cell initial adhesion.

In order to control cell adhesion in a spatial and temporal manner, a photochemical method to control surface chemistry was employed to control the surface property for cell adhesion in this project. Two photocleavable derivatives of the nitrobenzyl group were tried on two types of surfaces: a model self-assembled monolayer (SAM) with alkanethiol-gold surface and biodegradable chitosan. Reactive functional groups on two different surfaces can be inactivated by covalent binding with these photocleavable molecules, and light can be further introduced into the system as a stimulus to recover their reactivity. By simply applying a photomask with different patterns, the deprotection of the surface functional groups on both SAM and chitosan can be controlled in a spatial and temporal manner and for further biomolecule immobilization. To control cell adhesions, poly(ethylene glycol) (PEG) was used to create a non-fouling surface or regions and resist cell attachment; cell adhesive peptide sequences or proteins were immobilized through deprotected functional groups on a surface or on designed regions of one surface to promote cell adhesion. Due to the immobilization of different biomolecules after light irradiations, the surface or specific regions on one surface was rendered cell adhesive or cell non-adhesive. Different surface characterization methods were utilized to demonstrate the surface functionality, wettability, and microstructure during the fabrication and photolysis. NIH/3T3 fibroblast and PC12

pheochromocytoma cell lines were cultured on the resulting surfaces with heterogeneous immobilized biomolecules in a pattern. The cell patterning shown on these surfaces indicated the successful control over surface chemistry and properties on one surface and also two cell types' response to the heterogeneous properties.

Résumé

L'adhésion cellulaire est entreprise par les cellules dépendantes d'ancrage lorsqu'elles sont misent en contact avec certains matériaux ou avec la matrice extracellulaire. Cette étape d'adhésion est essentielle, étant impliquée dans tous les mécanismes cellulaires, notamment la prolifération, la différentiation, la migration, et l'apoptose de ces cellules. L'adhésion cellulaire a donc d'importantes implications lors de l'étude ou du contrôle de ces mécanismes. Plusieurs méthodes établies pour induire l'adhésion cellulaire impliquent la manipulation des caractéristiques chimiques de la surface des substrats ciblés. L'adhésion contrôlée de cellules sur des surfaces deux-dimensionnelles représente un modèle simple pour étudier le comportement cellulaire, qui est un des aspects fondamentaux de la biologie cellulaire, du génie tissulaire, et du développement de biocapteurs. Du côté de l'ingénierie, la préparation d'un matériel avec une surface ayant des propriétés chimiques contrôlables aiderait à étudier différents éléments du comportement cellulaire et à mieux comprendre comment ceux-ci sont affectés par les caractéristiques de cette surface. Lors de la fabrication de ce matériel, le défi principal est de créer une surface ayant des propriétés chimiques hétérogènes et définies à l'échelle microscopique, et ensuite guider l'adhésion initiale des cellules.

Afin de contrôler l'adhésion spatio-temporelle des cellules, une méthode photochimique fut utilisée au cours de ce projet pour modifier les propriétés chimiques de la surface des substrats étudiés. Deux dérivés photoclivables de groupements nitrobenzyle furent examinés sur deux surfaces différentes, soit une monocouche modèle auto-assemblée avec une surface or-alcanethiol, et une surface de chitosane biodégradable. Les groupements fonctionnels réactifs sur les deux surfaces peuvent être inactivés par liaison covalente avec les molécules photoclivables, et de la lumière peut ensuite être ré-introduite dans le système pour rétablir la réactivité. En appliquant des photomasques ayant différents patrons, la déprotection des groupements fonctionnels à la surface de la monocouche auto-assemblée et de la chitosane peuvent être contrôlés spatio-temporellement. Afin de contrôler l'adhésion cellulaire, du polyéthylèneglycol (PEG) fut utilisé sur la surface des substrats pour créer des régions inencrassable ou résistantes à l'attachement cellulaire. Des séquences peptidiques ou protéines adhérentes furent immobilisées sur des groupements fonctionnels déprotégés pour

promouvoir l'adhésion cellulaire. Grâce à l'immobilisation de différentes biomolécules suivant l'irradiation lumineuse, la surface, ou des régions spécifiques d'une surface, furent rendues adhésives ou non-adhésives pour les cellules. Différentes méthodes furent utilisées pour caractériser la fonctionnalité, la mouillabilité, et la microstructure des surfaces durant leur fabrication et photolyse. Des fibroblastes NIH/3T3 et des lignes de cellules phéochromocytome PC12 furent cultivés sur les surfaces modifiées avec des biomolécules hétérogènes immobilisées selon un patron. L'agencement spécifique des cellules sur ces surfaces indiquent que les propriétés chimiques des surfaces étudiées, ainsi que le comportement de deux types de cellules sur ces surfaces hétérogènes, furent efficacement contrôlés.

Acknowledgment

I would like to express my sincere appreciation to my supervisor Dr. Xudong Cao for his guidance, continued encouragement, and constructive criticism throughout my whole PhD study. Thanks to give me the opportunity to work in your lab.

I also wish to thank my colleagues, faculty members and many friends in the department. Many thanks to Cathy Goubko, Sagedeh Sadat Shahabi, Zijun Liu, Yiping Tian, Benu Sethi, Warren Sun, Yan Du, and other lab members for the great help and encouragement through my study. Thank Louis Tremblay, Gérard Nina, and Franco Ziroldo for their help in all the experimental setup and maintaining. Thank Gabriel Potvin for the translation of the abstract.

I also would like to take the opportunity to thank Prof. Marc Dubé, Prof. Jules Thibault, Prof. Elena Baranova, Prof. Jason Zhang and Prof. R. Tom Baker for the access of their equipments.

Lastly, sincere thank goes to my dear family members and friends for your continued support and encouragement. Special thank to my great mother, father and sister.

Table of content

List of Figures

Chapter 2

Chapter 3

Chapter 4

Chapter 5

List of Tables

Chapter 2

Chapter 3

Chapter 5

List of Abbreviations

μCP	Micro-contact printing
2D	Two dimensional
3D	Three dimensional
ACA	Advancing contact angle
AFM	Atomic force microscopy
Al	Aluminum
ATR-FTIR	Attenuated total reflectance Fourier transform infrared spectroscopy
AUT	11-Amine-1-undecanethiol hydrochloride
AWCA	Advancing water contact angle
BE	Binding energy
bFGF	Basic fibroblast growth factor
BMP-2	Bone morphogenetic protein -2
BMSC	Bone marrow-derived mesenchymal stem cell
BNBA	4-Bromomethyl-3-nitrobenzoic acid
BS^3	Bis[sulfosuccinimidyl] suberate
BSA	Bovine serum albumin
CG	Collagen-glycosaminoglycan
ChABC	Chondroitinase
CNTF	Ciliary neurotrophic factor
CO_2	Carbon dioxide
Col/HAp	Collagen I/hydroxyapatite
CPAE	Calf pulmonary artery endothelial cell
CS	Chitosan
CV	Cyclic voltammetry
DD	Degree of deacetylation
ddH_2O	Deionized distilled woater
DGEA	Asp-Gly-Glu-Ala sequence
DIEA	*N*,*N*-Diisopropylethylamine
DMEM	Dulbecco's modified Eagle's medium
DMPE	Dimyristoylphosphatidylethanolamine
DMSO	Dimethyl sulfoxide
DT	1,8-Octanedithiol
ECM	The extracellular matrix
EDC	1-Ethyl-3-(3-dimethylaminopropyl) carbodiiminde
EG	Ethylene glycol
EGF	Epidermal growth factor
FBS	Fetal bovine serum
FDA	Food and Drug Administration

FGF	Fibroblast growth factor
FTIR	Fourier transform infrared spectroscopy
GA	Glutaradehyde
GAG	Glycosaminoglycan
H_2O_2	Hydrogen peroxide
H_2SO_4	Sulfuric acid
HCl	Hydrochloric acid
hECS	Human embryonic stem cell
Hg	Mercury
Hg_2SO_4	Mercury(I) sulfate
hTGF-β1	Human transforming growth factor beta 1
HUVEC	Human umbilical vein endothelial cell
K_2SO_4	Potassium sulfate
LAM	Laminin
MC3T3	Mouse clonal osteogenic cell
MPC	2-methyacryloyloxyethyl phosphorylcholine
MSC	Mesenchymal stem cell
Na_2SO_4	Sodium sulfate
NaCl	Sodium chloride
$NaHCO_3$	Sodium bicarbonate
$NaHCO_3$	Sodium biocarbonate
NGF	Nerve growth factor
NGF-β	Nerve growth factor beta
NHS	N-hydroxysuccinimide
NT-3	Neurotrophin-3
NVOC	4,5-Dimethoxy-2-nitrobenzyl chloroformate/Nitroveratryloxycarbonyl
PBS	Phosphate buffered saline
PDM-AEMA	Poly(dimethyaminothyl methacrylate)
PEC	Polyelectrolyte
PEG	Poly(ethylene glycol)
PLGA	Poly(lactide-co-glycotide)
PLLA	Poly-l-lactic acid
PMAA	Poly(methacrylic acid)
RGD	Arg-Gly-Asp sequence
RGDS	Arg-Gly-Asp-Ser sequence
RWCA	Receding water contact angle
SAM	Self-assembled monolayer
SCI	Spinal cord injury
SI-ATRP	Surface initiated atomic transfer radical polymerization

STM	Scanning tunnelling microscopy
TCPS	Tissue culture polystyrene
UV	Ultraviolet
VEGF	Vascular endothelial growth factor
WCA	Water contact angle
XPS	X-ray photoelectron spectroscopy
YIGSR	Tyr-Ile-Gly-Ser-Arg sequence

Chapter 1 General Introduction

1.1 Introduction

The ultimate goal of tissue engineering is to understand and restore the functions of tissues *in vitro* and *in vivo*. A highly ordered structure of cells is a defining feature for tissues, and it is vital to study these spatial organizations of cells and their interactions with the surrounding extracellular matrix (ECM) for the understanding of cell functions and subsequently tissue functions. It is clear that the development of a heterogeneous environment is essential to mimic and recapitulate the complex tissue structures and cell-cell/ECM interactions. Well-accepted strategies for these kinds of studies are to expose cells in culture with different physical and chemical cues that have been observed *in vivo* and to investigate the interactions of cells with these different microenvironments. It is evident that a homogeneous environment cannot yield a complex microenvironment like native tissues and cannot mimic the cell-cell/ECM interaction *in vivo*. The strategy to generate a heterogeneous environment for cell culture is crucial for the studies related to cell and tissue functions. Surface patterning with different cues for cell culture is one strategy to realize this heterogeneity on a material and is of great importance in studies dealing with cell shape and microenvironment effects on the motility, proliferation, differentiation and migration of cells [1].

To date, surface patterning with immobilized adhesive cues, especially immobilized biomolecules, is considered as an effective way to create a patterned surface for cell culture. Cell adhesion is the first response to its microenvironment for many cell types. Without adhesion, many cells cannot respond to the neighbouring cells or ECM and face the fate of death. The adhesive molecules, particularly certain ligands, play a critical role in cell adhesion. Based on these, researchers have used ligands and other cell non-adhesive molecules, like hydrophilic poly(ethylene glycol) (PEG), to create a patterned surface with cell-adhesive regions and cell non-adhesive regions, and used these micropatterned surfaces to regulate cell shape and its contact with materials. Until now, many cell processes could be modulated *in vitro* with patterned surfaces, including endothelial cell proliferation and apoptosis [2], mesenchymal stem cell (MSCs) differentiation [3], and the fate of human embryonic stem cells (hECSs) [4].

The methodology to pattern a surface for cell biology has developed rapidly and many traditional fabrication techniques have been employed into these researches, like micro-contact printing techniques [5] and photolithography [6, 7]. Meanwhile, some new techniques have also been pursued including dip-pen technique [8, 9], inkjet printing [10], and laser-guided direct writing [11, 12].

Among all the methodologies, the introduction of photochemistry and photolabile molecules to achieve surface patterning and subsequently protein/cell patterning is one of the important approaches applied in these areas as well as other techniques. Compared with other techniques, the major advantage of using photolabile molecules is that it can provide both spatial and temporal control to the surfaces by using light as a stimulus. In addition, it can avoid the utility of harsh solvents in the system, which could cause denaturation of biomolecules. Particularly for photocleavable molecules (photocages) that are incorporated onto the surfaces, the photolysis will leave no residue on the surface and the desired protected molecule is variable and depending on different functional groups on photocages. Among a series of photocages, *o*-nitrobenzyl groups and its derivatives are the most commonly used and well-studied photocages for biological applications and surface patterning. They have been used to protect and control-release amine, carboxyl, hydroxyl and thiol groups for future reactions when exposed to UV light and help generate complex exposure areas with high spatial resolution by simply using photomasks, microarrays or lasers [13-15].

To control the surface properties that either favor or repel cell adhesion, subsequent immobilization of cell adhesive or non-adhesive molecules to a photo-deprotected surface or region is a common strategy to better define a whole substrate or its local property. PEG is the most efficient and well-accepted molecule that can prevent non-specific binding of proteins and cells. It has been applied in different areas related to its protein/cell-resistance. The mechanism of PEG's protein and cell resistance is still not completely understood. However, PEG is nontoxic and widely available through direct synthesis or purchase and with appropriate chemical derivatization. As a cell adhesive molecule, the RGD (Arg-Glu-Asp) peptide sequence is well-known for its recognition binding to integrins since it has been found to promote cell adhesion in 1984 [16], and it is widely distributed and used throughout

the organism. It has been extensively used in the research of tissue engineering, biosensor and fundamental study of cell biology.

The attempt to incorporate photocleavage into a substrate and subsequently cell adhesive/non-adhesive molecules to create cell-specific binding regions is a good and non-invasive approach to create heterogeneity on the substrate for the study of cell behaviour. Some attempt has been made by other researchers and successful patterns have been observed [13, 17]. Here in my project, two kinds of photocaged surfaces were developed: photocaged SAM was fabricated with two different *o*-nitrobenzyl derivatives to control cell attachment and create cell patterns; a photocaged chitosan film was achieved to direct cell adhesion and growth.

1.2 Project objective

Generally, the objective of this project is to develop and analyze surfaces for controllable cell attachment. Two materials were used in this project: self-assembled monolayers (SAMs) on gold based gold-alkanethiol interaction, and biocompatible and biodegradable polycationic chitosan. These two substrates are representative materials for *in vitro* and *in vivo* applications, separately. SAMs are a good base surface for *in vitro* applications. Different surface techniques like water contact angle (WCA), atomic force microscopy (AFM), X-ray photoelectron spectroscopy (XPS) and cyclic voltammetry (CV) can be used on SAMs to demonstrate the change of surface properties during fabrications. The highly-ordered single layer on SAM can help avoid topographical effects of the surface on cell adhesion and minimize non-specific binding of cell-material. Chitosan is an implantable biopolymer that has been used for drug delivery and tissue engineering *in vivo*. The controllable cell attachment on chitosan was specifically designed for potential *in vivo* applications because of its biocompatibility and biodegradability.

(1). To study the control of cell adhesion on a model surface for *in vitro* applications, a photocleavable and bifunctional *o*-nitrobenzyl derivative, 4-bromomethyl-3-nitrobenzoic acid (BNBA), was tried on a model SAM. In order to control surface properties, layer-by-layer (LBL) technique was applied to synthesize the photocleavable SAM. To provide

surface cell non-adhesiveness or cell adhesiveness, PEG was introduced into this system to resist cell attachment while a bioactive RGD sequence was introduced for cell adhesiveness.

BNBA was designed to work as a photo-switch between the self-assembled molecule, dithiol, and cell non-adhesive PEG. BNBA was chosen because of its bifunctionality. The existence of carboxyl groups on BNBA makes it possible for the future linkage of PEG. The surface properties can be controlled by simply applying a photomask to control light pathway. The capability of the resulting surfaces on control of cell adhesion was examined by cell culture experiments of a well-studied cell line for cell-material interaction, NIH/3T3 fibroblast.

(2). To successfully control cell attachment on one surface and create cell patterns, another widely used *o*-nitrobenzyl derivative, 4,5-dimethoxy-2-nitrobenzyl chloroformate (NVOC), was tried on the SAM for cell patterning. Due to the single functionality of NVOC, a double exposure strategy was applied to create heterogeneity of surface functionality and cell adhesive/non-adhesive molecule immobilization.

The self-assembled molecule, an alkanethiol with a terminal amine group, was needed for NVOC immobilization on the SAM. As described and investigated above, PEG was an efficient cell non-adhesive molecule and introduced to provide surface cell non-adhesiveness. Laminin was chosen as the cell adhesive molecule depending on the cell type cultured on the surface. To evaluate cell adhesion and cell response on this material, a specific cell line, PC12 cell, instead of the NIH/3T3 fibroblast, was cultured onto the surface and used as a model for specific applications to mimic neurons.

(3). To further control surface properties and provide a cell adhesion-controllable surface for tissue engineering and *in vivo* applications, biocompatible chitosan, instead of SAM, was chosen as the substrate. The synthesis of NVOC modified chitosan was studied. The cell culture experiments were carried out with the NIH/3T3 fibroblast to elucidate the formation of 2D cell patterns on this biocompatible chitosan film.

1.3 The organization of the thesis and the significance of scientific contributions

According to the project objectives, the dissertation is comprised of six chapters. Chapter 3 through 5 are independent research publications published or submitted to the referred scientific journal. Chapter 2 is an overview of the development of biomaterials and techniques studied in this project. Chapter 1 and chapter 6 are about general introduction, general discussion, conclusions, recommendations and contributions, respectively related to the entire thesis.

Chapter 3 Nan Cheng, Xudong Cao. Photoactive SAM surface for control of cell attachment. Journal of Colloid and Interface Science, 2010. 348(1): 71-79.

The new approach for controlling cell attachment using photochemistry and a SAM was developed with photocleavable and bifunctional BNBA and a model surface, alkanethiol-gold SAM. PEG was introduced onto the surface to initially create cell non-adhesiveness via photocleavable BNBA. To characterize the surface changes during the fabrication, different surface characterization techniques, such as WCA measurement, XPS and AFM, were employed to elucidate the difference of the properties on the intermediate surfaces and resulting surfaces. NIH/3T3 fibroblast cells were used for cell culture experiments and the results showed the successful control of surface properties by UV exposure for cell attachment. The resulting surfaces were effective to control cell attachment for up to 5 days.

Chapter 4 Nan Cheng, Xudong Cao. Neuron-like PC12 cell patterning on a photoactive self-assembled monolayer (SAM). Submitted to Journal of Colloid and Interface Science.

This approach is also based on an *o*-nitrobenzyl derivative (NVOC) modified SAM. Instead of LBL technique, in order to increase the yield of caging reaction, the amine group on an alkanethiol molecule was modified with NVOC to protect it. The caged self-assembled molecule was fabricated on gold surfaces. A double exposure strategy was applied to completely remove the photocages from the surface. The surface properties can be

demonstrated by WCA, AFM, cyclic voltammetry (CV) and XPS. A neuron-like cell line, PC12 cell, was cultured on the resulting surfaces for cell patterning. Different shapes of PC12 cell patterns were observed. Further control over cell behaviours was achieved by both the selective immobilization of laminin (LAM) and the addition of nerve growth factor (NGF) after cell initial attachment.

Chapter 5 Nan Cheng, Xudong Cao. Photosensitive chitosan to control cell attachment. Journal of Colloid and Interface Science, 2011. 361(1): 71-78.

The approach to control cell adhesion using a photocleavable molecule on chitosan was addressed. To demonstrate the synthesis of photocage (i.e. NVOC) modified chitosan, Fourier transform infrared spectroscopy (FTIR) was used to identify the presence of different characteristic peaks of functional groups. To examine the surface properties during fabrication, the WCA measurement was applied to check the wettability. At the same time, UV-Vis spectra were provided to elucidate the photocleavage of NVOC from chitosan. PEG and a cell adhesive sequence, RGDS (Arg-Gly-Asp-Ser), were used in this chapter as cell non-adhesive and adhesive molecules. Cell culture of a NIH/3T3 fibroblast was conducted for cell attachment and cell patterning. Cell number and morphology were investigated. The strip cell patterned on this modified chitosan film was observed.

1.4 References

1. Shen, C.J., J.P. Fu, and C.S. Chen, *Patterning Cell and Tissue Function.* Cellular and Molecular Bioengineering, 2008. **1**(1): p. 15-23.
2. Chen, C.S., et al., *Geometric control of cell life and death.* Science, 1997. **276**(5317): p. 1425-1428.
3. Peng, R., X. Yao, and J.D. Ding, *Effect of cell anisotropy on differentiation of stem cells on micropatterned surfaces through the controlled single cell adhesion.* Biomaterials, 2011. **32**(32): p. 8048-8057.
4. Lee, L.H., et al., *Micropatterning of human embryonic stem cells dissects the mesoderm and endoderm lineages.* Stem Cell Research, 2009. **2**(2): p. 155-162.
5. Kane, R.S., et al., *Patterning proteins and cells using soft lithography.* Biomaterials, 1999. **20**(23-24): p. 2363-2376.
6. Kleinfeld, D., K.H. Kahler, and P.E. Hockberger, *CONTROLLED OUTGROWTH OF DISSOCIATED NEURONS ON PATTERNED SUBSTRATES.* Journal of Neuroscience, 1988. **8**(11): p. 4098-4120.
7. Chang, J.C., G.J. Brewer, and B.C. Wheeler, *Modulation of neural network activity by patterning.* Biosensors & Bioelectronics, 2001. **16**(7-8): p. 527-533.
8. Piner, R.D., et al., *"Dip-pen" nanolithography.* Science, 1999. **283**(5402): p. 661-663.

9. Sekula, S., et al., *Multiplexed Lipid Dip-Pen Nanolithography on Subcellular Scales for the Templating of Functional Proteins and Cell Culture.* Small, 2008. **4**(10): p. 1785-1793.
10. Roth, E.A., et al., *Inkjet printing for high-throughput cell patterning.* Biomaterials, 2004. **25**(17): p. 3707-3715.
11. Odde, D.J. and M.J. Renn, *Laser-guided direct writing of living cells.* Biotechnology and Bioengineering, 2000. **67**(3): p. 312-318.
12. Nahmias, Y. and D.J. Odde, *Micropatterning of living cells by laser-guided direct writing: application to fabrication of hepatic endothelial sinusoid-like structures.* Nature Protocols, 2006. **1**(5): p. 2288-2296.
13. Kikuchi, Y., et al., *Arraying Heterotypic Single Cells on Photoactivatable Cell-Culturing Substrates.* Langmuir, 2008. **24**(22): p. 13084-13095.
14. Lee, K.N., et al., *Protein patterning by virtual mask photolithography using a micromirror array.* Journal of Micromechanics and Microengineering, 2003. **13**(1): p. 18-25.
15. Hoffmann, J.C. and J.L. West, *Three-dimensional photolithographic patterning of multiple bioactive ligands in poly(ethylene glycol) hydrogels.* Soft Matter, 2010. **6**(20): p. 5056-5063.
16. Pierschbacher, M.D. and E. Ruoslahti, *CELL ATTACHMENT ACTIVITY OF FIBRONECTIN CAN BE DUPLICATED BY SMALL SYNTHETIC FRAGMENTS OF THE MOLECULE.* Nature, 1984. **309**(5963): p. 30-33.
17. Kaneko, S., et al., *Photocontrol of cell adhesion on amino-bearing surfaces by reversible conjugation of poly(ethylene glycol) via a photocleavable linker.* Physical Chemistry Chemical Physics, 2011. **13**(9): p. 4051-4059.

Chapter 2 Literature Review*

*Some materials in this chapter were published in book chapters:

(1) Nan Cheng, Xudong Cao, and Henry T. Peng (2011). Chapter 2 Chitosan: A Promising Biomaterial for Tissue Engineering and Hemorrhage Control. In Arthur N. Ferguson and Amy G. O'Neil (Eds.), *Focus on Chitosan Research* (pp. 49-82). Hauppauge, NY: Nova Publisher.

(2) Catherine A. Goubko, Nan Cheng, and Xudong Cao (2011). Chapter 4 Photolabile Molecules as Light-Activated Switches to Control Biomolecular and Biomaterial Properties. In Karen J. Maes and Jaime M. Willems (Eds.), *Photochemistry: UV/VIS Spectroscopy, Photochemical Reactions and Photosynthesis* (pp. 175-202). Hauppauge, NY: Nova Publisher.

2.1 Introduction

In this chapter, the background knowledge related to this project is reviewed. First, the importance to study cell adhesion is reviewed. This sets the stage for reviews on studying cell adhesion. Finally, approaches to create heterogeneous surfaces on different material surfaces in order to control cell adhesion and the following cell processes are reviewed and discussed.

2.2 Cell adhesion

Cell adhesion on the extracellular matrix (ECM) proteins is a critical process for many cell processes and is also fundamental for studies to understand cell-cell and cell-material interactions. Cell adhesion and spreading are initiated immediately after cell contact with matrix proteins or an appropriate surface. Cell adhesion mechanisms can be categorized into two subtypes, occurring via either specific or nonspecific interactions, both of which are idealized descriptions of the adhesion process. Specific adhesion is usually mediated by the ligand-receptor interaction. The ligand and the receptor are two molecules that fit each other like a lock-key system. The two molecules are able to form the specific bond with each other, and the binding is usually an ionic bond, hydrogen bond or Van der Waals force. As a result, even a small change in the molecule conformation has a great influence on the strength of this bond. Many molecules residing on the cell membrane are referred to as receptors and can form specific strong binding with ECM proteins, carbohydrates, lectins, and transport proteins etc., which are usually referred to as ligands. In contrast, nonspecific adhesion involves Van der Waals forces and electrostatic forces. Usually, the binding in nonspecific adhesion is equally distributed over the contact area and the binding energy is much weaker than a specific adhesion.

For a specific adhesion to a surface, a cell must be transported from the bulk solution to the vicinity of the adhesion surface, and make contact with the immobilized ligand through the receptor on the cell when the two are close enough. The binding between the receptor and the complementary ligand can form a ligand-receptor domain and stretch the cell shape from a relaxed to a deformed shape. A current understanding of the specific cell

adhesion is based on the focal adhesion. Focal adhesions usually mean the specific sites of cell adhesion developed in cell culture, and these sites consist of assembled ECM receptors (usually integrins) that work as transmembrane components in a bidirectional manner between ECM components outside and actin filaments inside. They provide strong cell-substrate adhesion and also play an important role in signalling. One widely recognized model system of the focal adhesion is integrin-mediated adhesion based on *in vitro* studies of fibroblast, and the most studied model of integrin-mediated focal adhesions is the model built on fibronectin covered surfaces and cells. Rich fibronectins on the surface provide ligands for integrin expression on the cell membrane. The transmembrane integrins provide a strong ligand-receptor binding between the fibronectin presented on the surface and cells. At the same time, integrins induce cytoskeletons of the cells associated with them and cytoplasmic proteins bond to them. Proteins that have been discovered involving into mediating cell attachment and spreading in focal adhesions include fibronectin, chondronectin, ricin, laminin (LAM) and vitronectin [1, 2]. It is generally accepted that these proteins along with collagens and proteoglycans make up the ECM that fills the extracellular spaces between cells *in vivo* and *in vitro*.

Cell spreading onto a substrate is accompanied by a cytoskeleton rearrangement and it is critical for the survival, proliferation, differentiation and other cell behaviours of most normal mammalian cells. The phenomenon that the cell behaviours are dependent on the attachment to a surface is known as anchorage dependence. Studies have shown that many molecular processes in a cell are dependent on the cell adhesion and spreading. Transformation on cell is often seen if the cell loses anchorage-dependence to an appropriate surface [3-5]. The transformation of cells, accompanied with a morphological change, often results in a loss of the other normal constraint on cell proliferation such as decreased requirement for growth factors and a loss of capacity for growth arrest. *In vivo*, these changes are considered as a reason for tumor formation. When cells are not allowed to attach to a surface, the cells maintain a spherical shape. This sphere, compared with a spreading morphology of cell, has low permeability in the cell membrane. In contrast, the spreading cells exhibit a density-dependent inhibition of growth, and the cell numbers could remain constant for a period of time when cells reach a confluent monolayer. As an example for this

phenomenon, the study of 3T3 fibroblasts showed that, after a long time of cells maintained in cell suspension, the viability of cells decreases, and the cells are unable to initiate DNA synthesis and the synthesis of mRNA decline rapidly. Finally, the cells are all dead after 8-9 days in suspension [4, 5]. Another cell response to the attachment and spreading is cell differentiation. It is known that attached cells result in the activation of genes associated with growth and structure. But also, in some types of cells, the changes in the shape after cell attachment trigger the differentiation of the cell to another phenotype. For example, human epidermal keratinocytes will stop proliferating and undergo terminal differentiation when forced into a rounded morphology [6]. The second example to show the attachment affects cell differentiation is corneal epithelial cell. It maintains a fibroblastoid morphology and sensitive to fibroblast growth factor (FGF) in tissue culture polystyrene plate, and it maintains a cuboidal morphology and sensitive to epidermal growth factor (EGF) when it is cultured on collagen [7]. Further effect of cell adhesion is morphogenesis, spatial arrangement of cells and tissue formation. The formation of capillary tubes by vascular endothelial cells is an example of how the cell adhesion to the ECM controls the tubular network formation [8]. There are studies suggesting that the ECM dominates the process by controlling the cell shape and its sensitivity to soluble factors. Also, the chemical changes during cell attachment and the generation of tensile forces in the cytoskeleton play an important role in the signal transduction of the ECM binding [9, 10].

In summary, the ability of cell attachment and spreading on an appropriate matrix has profound implication for the cell. DNA, RNA, and protein synthesis are affected by suspension or attachment of these cells. The degree of cell attachment and spreading may affect the differentiation characteristics of a cell. ECM component may mediate different cells in different ways, including cell shape and responsiveness to growth factors. In addition, the insolubility of ECM components allows them to impact on mechanical stresses upon cell-ECM binding. Overall, cell adhesion and spreading can affect all aspects of cellular function from simple proliferation to tissue formation [11, 12]. Cell adhesion could be considered as the first step of cell behaviours and functions for anchor-dependence cells. From an engineering point of view, to mimic the ECM effects on cell fate and develop a engineered surface to explore the effects is a way to help us understand many cell process *in vivo* and

also develop biomaterials for tissue engineering to promote tissue regeneration and replace damaged tissues.

For a long time, scientists have realized that to study cell behaviours within complex multicellular tissues requires systematically studying cells within the context of specific model microenvironments. These models all mimic the *in vivo* cell-ECM matrix in certain extent. For cell biologists, these model systems helped understand fundamental cell biological mechanisms; for the researchers in regenerative medicine and tissue engineering, they can be considered as a remodelling of ECM and can be used to recapitulate some aspects of both the organization and multicellular complexity of tissues and gain insight into functions of the ECM with diverse tissues and organs [13]. Among all the cell behaviours, cell adhesion is the initial and most important step of cell response to ECMs or materials. It decides many subsequent cell processes such as cell proliferation, differentiation, migration, apoptosis and morphogenesis.

2.3 Substrate materials for the studies of cell attachment

To study cell adhesion *in vitro*, an appropriate surface needs to be developed at first in order to attach cells in a controlled manner. There are many methods developed to either modify bulk materials or two dimensional (2D) surfaces for studies of cell-cell or cell-material interactions [14]. Though cells in native tissue are embedded with a complex three dimensional (3D) microenvironment consisting of soluble molecules and non-soluble factors, and many researches are focusing on creating biocompatible scaffolds for this purpose, it is still important to study what happens on an engineered 2D surface, which will provide insights into many biological studies *in vitro*. Surface modification is an extensive tool being used to study cell-material interaction. Earlier works were concentrated on studying responses of proteins and cells to a chemically uniform surfaces and 2D surfaces with micro-topological and nano-topological features, while most recent works are focused on developing patterned surfaces and studying cell responses to asymmetric surfaces. Therefore, there are two different strategies employed in surface modification, i.e. topographical modification and chemical modification. Topographical modification usually involves in microscale features, such as wells, pillars, and grooves of various dimensions. Chemical

modification usually involves the introduction of different chemical cues into the system, such as ligands, functionality, and hydrophilicity.

With respect to the bulk material, the selection mainly depends on the research purpose. If implantation is the application, the materials' biocompatibility is very crucial. Also, materials' stability and degradation in the cellular environment are very important. On the other hand, if the purpose of the study is to investigate the fundamental phenomena and mechanisms in cell biology and cell-material interaction, the ease of fabrication is one factor that should be taken into consideration. Meanwhile, as a biological platform, it should also have the feasibility to modulate cell adhesive or cell non-adhesive molecules on the substrate *in vitro*.

2.3.1 Natural polymer

For cell adhesion studies *in vitro*, many materials have been used to satisfy either one or multiple requirements (simplicity, versatility and robustness) as substrates. With the improvement of microfabrication technology, it is possible to create precisely-controlled microstructures on polymer surfaces with desirable physical and mechanical properties. Polymers as base materials for biological studies have distinguished advantages. Many polymers are biodegradable and non-toxic to human body. They usually have a wide range of physical and chemical properties and could be modified to meet the requirements for different tissue environments. For example, to promote bone cell migration, proliferation, matrix deposition and mineralization, a variety of matrix proteins such as osteopontin, thrombospondin and bone sialoprotein are believed to play an important role. Thus, in order to treat bone damage and study bone-material interface, bone matrix proteins on the materials needs to be studied by either absorbed onto or covalently bonded to the surfaces [15]. Another example can be taken from neural tissue regeneration. To study and treat nervous system, the development of a graft of nerve to bridge the severed gap is an important step. To achieve successful regeneration, sprouting axonal growth without interference from the surrounding biological environment and a new connection of the axons with the distal is vital. This makes investigations to study the guidance of axonal growth *in vitro* on a suitable surface very important. The studies to create suitable guidance on polymer surfaces through

different fabrication techniques to mimic and study the axon-material interactions were done to serve this purpose [16, 17].

Natural polymers have been used in many cell and tissue-specific cell biological investigations. They normally refer to naturally occurring polymers and chemically modified derivatives of these polymers. Natural polymers as substrates for biological applications usually include cellulose, chitosan/chitin, collagen, hyaluronic acid (HA) and other polysaccharides. They are often biocompatible, biodegradable, and non-cytotoxic. Meanwhile, polysaccharides, as well as proteins, are very important components of ECMs and provide mechanical stability and structural integrity to tissues and organs. Therefore, using a natural material as a platform to mimic and investigate cell-matrix interactions *in vitro* is a good option to reveal the complexity and understand the mechanism of cell-ECM interactions *in vivo*.

2.3.1.1 Collagen

Collagen is a protein-based natural polymer and a major component of the ECM. It composes of polypeptide chains with a triple helix structure. The defining structure of collagen is that three parallel polypeptide strands in a left-handed polyproline II helix conformation with each other stagger to form a right handed triple helix by hydrogen bonds [18]. It provides structural support to connective tissues such as skin, tendons, bones, cartilages, and blood vessels [19-24]. It is shown to have the advantage of mimicking many features of the ECM and thus has the potential to direct cell migration, growth and organization during tissue regeneration. In a molecular perspective, collagen could be considered as polymers composed of many amino acids linked by amide bonds. Many cells have surface adhesion receptors that can recognize the triple helical structure of collagen, which is its advantage to use for cell adhesion. Its advantages also include high mechanical strength, good biocompatibility, low antigenicity and ease of chemical modifications. Collagen is therefore regarded by many researchers as an ideal scaffold or matrix for tissue engineering and cell biological studies. Collagen is mainly isolated from animal tissues. To date, 28 subtypes of collagens have been identified [18]. Among them, type I collagen is the most abundant and most studied for different biomedical applications. Despite many

advantages of collagen, the safety of collagen derived from animal tissues has raised immunological concerns, and techniques to develop recombinant and non-recombinant human collagens have been employed as a replacement of animal-origin collagen [25]. But the production of recombinant collagen is still a high-cost technique. Furthermore, compared to other natural-origin polymers, collagen is hard to process and the biodegradation is hard to control *in vitro* and *in vivo*. Crosslinking of collagen is necessary to control or extend degradation time and increase stability. Furthermore, as a protein-based polymer, the sterilization of collagen for any cell studies can be very difficult since many traditional sterilization methods could cause denaturation of the material and conformation changes to some extent.

Until today, there are many on-going biomedical investigations involving collagen, especially in the development of scaffolds and matrices for engineered tissues or drug delivery systems. There are also studies focused on the investigation of fundamental principles of cell-ECM interaction based on collagen in the past few decades. Although a large portion of research is still at the preliminary stage, collagen is still a promising ECM motif and believed to exhibit an unique capability to mimic biological activities due to its similar structure to the natural tissue scaffold in human body. Here, in Table 1, a summary of research efforts related to collagen in some relevant applications has been listed.

As seen in Table 1, collagen is used in a broad area of tissue engineering research. For example, different collagen-glycosaminoglycans (CGs) have been developed for dermal, peripheral nerve, bone and other tissues regenerations. It is considered as an ECM analog to promote regenerations. The microstructure, chemical composition, mechanical strength and the degradation rate of CG are considered as the key properties that should be controlled to meet the different requirement of regeneration. CG is also used in different *in vitro* studies of cell adhesion, motility and contraction. As shown in reference [26], the relationship of cell attachment and viability with CG microstructure was studied. During their study, they found that there was strong correlation between the pore size and cell viability. The viability of MC3T3 cells decreased with the increased mean pore size. It is believed that cell motility is one of the complex cell processes in human body and important for wound healing, metastatic tumor cell migration, stem cell study and tissue remodeling. Especially, as we

know, studies of cell motility on the surface lead to an improved understanding of this cell process. To study the cell motility on CG, Harley and coworkers [27] seeded NR6 fibroblast cells onto a CG scaffold with different pore sizes and then tracked the cell migration behaviors with a microscope. They elucidated the relationship of cell migration with the scaffold pore size and Young's modulus, which could be used as a reference parameter for scaffold development. In addition, there was also a study to show the influence of surface topography on the gene expression by seeding fibroblasts on both 2D and 3D CG surfaces [28]. Other collagen complex or derivatives investigated for biomedical applications include collagen/hydroxyapatite, laminin-collagen, and other [29-34] as shown in Table 1. Overall, collagen is a good candidate for biomedical applications due to its unique physical and chemical properties. But the fabrication of collagen is hard and less controllable compared to synthetic materials and also the cost is still high. Development of new techniques to produce collagen is a solution to increase its utility.

Table 1 Collagen and its derivatives for biomedical applications

Collagen type and structure	Cell type	Application	Active molecules	Ref.
Collagen I sponge	Bone mesenchymal stem cell	Tendon repair		[35, 36]
Recombinant collagen I sponge		Spinal instability treatment	Bone morphogenetic protein -2 (BMP-2)	[37]
Collagen sponge	Porcine third molar cell	Tooth repair		[38]
Collagen I/hydroxyapatite composites	Osteogenic cell	Bone repair		[30]
Collagen/hydroxyapatite composites	Osteosarcoma cell	Bone defect treatment	Nerve growth factor beta (NGF-β)	[31]
Collagen-glycosaminoglycan (CG) scaffold	Mouse clonal osteogenic cell	Cell attachment		[26]
CG scaffold	NR6 mouse fibroblast	Cell motility		[27]
CG matrix	Autologous keratinocyte	Skin regeneration		[39]
Collagen vitrigel membrane	Dendritic cell, keratinocyte and fibroblast	Reconstruction of human skin		[40]
Collagen I/III matrix		Peripheral nerve regeneration		[29, 32]
Polyglycolic acid tube with collagen sponge		Peripheral nerve regeneration		[33]
CG scaffold	Adult rat mesenchymal stem cells	Bone and cartilage regeneration		[41]
Collagen hydrogel	Marrow mesenchymal stem cell	Cartilage regeneration	BMP-2	[42]
Collagen nanofiber		Spinal cord injury (SCI) treatment	Neurotrophin-3 and chondroitinase	[43]
Collagen matrix		Vascularization	Vascular endothelial growth factor	[44]
Collagen vitrigel scaffold		Glomeruli regeneration / nephritic therapy	Glomerular ephithelial and mesangial cells	[45]
Laminin modified collagen scaffold		Peripheral nerve regeneration	Ciliary neurotrophic factor (CNTF)	[34]

2.3.1.2 Chitosan

Chitosan, a linear copolymer of 1,4 β-linked 2-acetamido-2-deoxy-D-glucopyranose and 2-amino-2-deoxy-D-glucopyranose, is an important polymer from polysaccharides for biomedical applications. Polysaccharides are usually the biopolymers constituted by the monomers of sugar rings. The sugar rings are linked by *O*-glycosidic bonds. Differences in molecular weight and chain shape result in different physical and chemical properties. Chitosan is one of widely used polysaccharides in biomedical fields and is deacetylated from chitin. Chitin is the second most abundant natural polymer in the world after cellulose, and it is found in the shell of crustaceans, the cuticles of insects and the cell walls of fungi [46]. Generally, chitosan refers to polymers of chitin with full or partial deacetylation degree. It is the only natural polycation because of the existence of plenty of primary amine groups from deacetylation. Usually, the typical commercial chitosan is at 70-95% of deacetylation degree [47].

Structure and functional groups

The existence of functional groups in chitosan could help create different desired derivatives with different biological properties. As seen in Figure 1, the specific function group $–NH_2$ at the C-2 position and non-specific -OH groups at the C-3 and C-6 positions are the important functional groups involving in most chemical modifications of chitosan to create proper chitosan derivatives for different biological applications. These chemical modifications include acylation, *N*-phthaloylation, tosylation, alkylation, Schiff base formation, reductive alkylation, *O*-carboxymethylation, *N*-carboxylalkylation, silylation and graft copolymerization. The amine group is a characteristic group of chitosan compared with the most abundant natural polymeric material, cellulose. It is the most active group on chitosan. As reported in the literatures, it is easy to be involved into many chemical reactions [48, 49]. In general, the potential of chitosan is mostly because of its biocompatibility, biodegradability, non-toxicity, and antibacterial activity [50]. Recently many studies showed that the porous structure, gelation properties, the existence of reactive functional groups and high affinity to *in vivo* macromolecules qualify chitosan and its derivatives promising biomaterials [51, 52]. Lysozyme is the primary enzyme responsible for *in vivo* degradation of

chitosan by hydrolysis of acetylated residues. Based on many studies, the degradation rate of chitosan is related to the degree of crystallinity and deacetylation. Basically, the higher degree of deacetylation (DD) chitosan has, the slower chitosan degradation it has in the body [53].

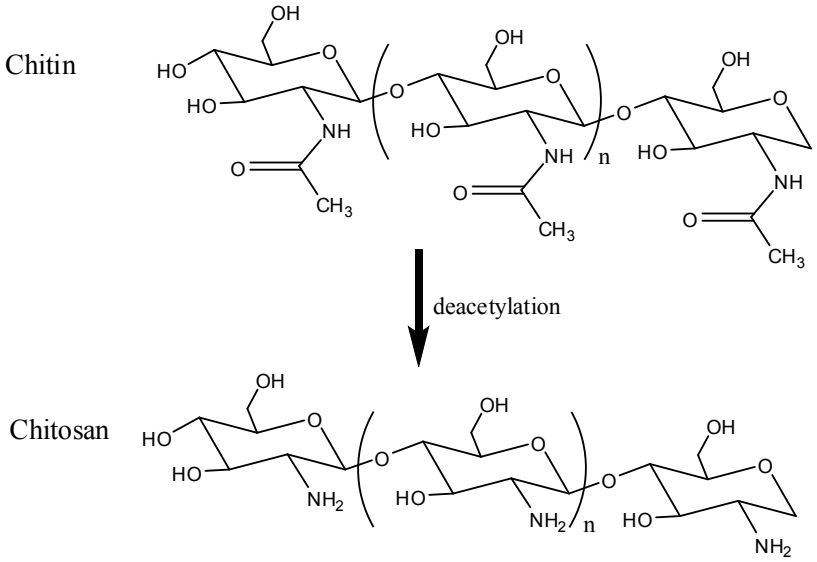

Figure 1 Chemical structures of chitin and chitosan

Biological applications of chitosan

As mentioned above, chitosan have cationic nature because of the existence of primary amines. This allows chitosan to form electrostatic interaction with negatively charged molecules like DNA and some proteins, which is useful in drug delivery system and protection of drug *in vivo*. Moreover, the large numbers of amine groups on chitosan make it pH-sensitive as a weak poly-base and this property held chitosan to be widely investigated as a delivery carrier. Another advantage is that chitosan can be combined with a variety of biomaterials such as alginate, collagen, hyaluronic acid, calcium phosphate and poly-L-lactic acid (PLLA) for potential use in drug delivery systems and tissue engineering scaffolds. At the same time, chitosan can be molded in various forms such as powder, paste, film, fiber, porous scaffold and others by the demand of specific applications. Table 2 intends to summarize some relevant applications of chitosan reported as research works in tissue engineering and other biomedical applications.

Surface modification of chitosan usually happens with primary amine groups on chitosan. By the introduction of different small molecules or macromolecules as the side chains of chitosan bulk, the optimization of different biochemical and biophysical parameters can be achieved. Depending on specific applications and target organs, these methods, such as increase of solubility in neutral pH, introduction of hydrophobic and hydrophilic molecules to render amphiphilicity, porous structure, and reduction of positive charges were applied for different purposes.

As seen in Table 2, chitosan can be combined with different materials and undergo different processes to achieve adequate scaffolds or matrix architectures, as well as suitable mechanical properties. However, these different properties of chitosan-based materials and processing techniques depend on the tissues to be regenerated. Meanwhile, different substrate models involving chitosan were established for *in vitro* cell biological studies.

The applications of chitosan were addressed according to different targeting organs. Chitosan is used extensively as a wound dressing and substitute of skin. The wound healing process can be divided into three different phases: inflammation, proliferation and scar maturation, involving certain arrangement of cell-cell interaction and ECM formation. It is believed that the healing relies on the contribution and collaboration of different cell types involved during the phases of proliferation, migration, matrix synthesis and contraction, and the mechanism is still roughly understood [54, 55]. Chitosan is found to have the capability to attract and activate macrophages and neurophils to initiate the healing process, limit scar formation and retraction, stimulate cell motility and increase *in vitro* angiogenesis, and also its intrinsic antibacterical activity [56, 57]. Considering these advantages, chitosan could provide good protection of wound and accelerate wound healing, and has been proposed as a wound dressing material and artificial skin. The early technology focused on the development of a bilayered skin substitute, the reduction of the immune reaction and the increase of cell adhesion [58]. In recent years, to overcome the weakness of a single structure, hybrid materials have been studied to promote dermal regeneration. Lim et al. developed a chitosan-PLGA-PEO fiber scaffold and the material displays a high hydrophilicity to maintain the water content and also exhibited good cell adhesion [59]. Guo et al. provided a chitosan-collagen/silicone membrane with a complex of vascular endothelial growth factor

(VEGF) encoded plasmid DNA and chitosan, and they used it to treat full-thickness burn wounds [60]. Their strategy combined the control release technique into the artificial skin substitute. The results showed the promising 70% of skin regeneration at 105 days and the improved expression of VEGF resulting in a high numbers of blood vessel formation during the regeneration. To build an *in vitro* model surface to investigate different methods to enhance necessary cell behaviors and understand the details of skin regeneration is an attractive area for many research groups. Here are two current research works as examples. Chitosan coated on PLLA was developed by Ding and coworkers [61] using plasma coupling technique to improve the material's solubility in neutral condition, and also to control cell attachment. Based on the results from the cell proliferation study and morphology investigation on the resulting surfaces with fibroblast and hepatocyte, the group illustrated the capability of their surface on the control of cell morphology and the potential application in understanding the mechanism of cell phase changes during cell growth and differentiation. Meanwhile, an argon treated chitosan exhibited excellent cell attachment, migration and proliferation of human skin-derived fibroblasts, which could help to accelerate wound healing processes [62].

Regarding to bone and cartilage regenerative materials, porous chitosan matrices and scaffolds are considered as potential candidates due to their proper biological and physical properties. Different strategies of bone regeneration involving chitosan have been demonstrated by researchers as listed in Table 2. Chitosan usually formed complexes with collagen to increase cell compatibility of the matrices and biostability. Some studies combined chitosan with the resembled glycosaminoglycans (GAGs), which are important constituents of bone or cartilage ECM, for bone regeneration [63-65]. Multi-component chitosan complexes have also been studied to mimic the bone microenvironment and help cell regeneration [66-69].The precise mechanism of bone regeneration is still unknown. But until now, it is known that certain cell types, such as osteoclasts and mesenchymal stem cells, are the main cells involved in the regeneration processes, and also some bioactive molecules, like bone morphogenetic proteins, kinases and growth factors. The question needed to solve is to understand the precise mechanisms of bone formation, the molecular level of these processes along with the interactions of these processes, and the key regenerative cells [70].

Cell adhesion as the first stage of other cell processes is the first subject needs to study. Taking a hydroxyapatite-coated carboxymethyl chitosan as an example, it is developed and used *in vitro* to understand bone regeneration. It is illustrated as a good model to promote cell attachment, proliferation and differentiation of MC3T3 osteoblasts and human bone marrow stem cells [71]. More examples were collected in Table 2. Thanks to its inherent cationicity and wide availability, chitosan has unique characteristic properties to be designed as bone regenerative surfaces or scaffolds.

Apart from the extensive studies in skin and bone regeneration, chitosan-based material has been used for peripheral nerve regeneration [72-77] and artificial liver [78, 79]. These studies involving chitosan and its derivatives for different tissue engineering applications are also the evidence to show their potential and efficiency for substitution of damaged native tissues or organs. Particularly for nerve repair, chitosan is an important material for peripheral nerve regeneration due to its good cytocompatibility and favorable immunogenicity. It has been studied by many scientists *in vitro* to understand or control neuronal cells [77, 80, 81]. In the early stage of the study, the focus was on the development of modified chitosan and chitosan complexes with other biopolymers for attachment, proliferation and differentiation of different neuronal cells. Nowadays many people started to use chitosan as a substrate or fabricate the fibrous chitosan matrix to control the orientation of cell growth and functions. Zhu et al. fabricated a laminin-blended chitosan to control axonal orientation *in vitro*. They used a dispensing-based rapid prototyping technique to create a 2D grid pattern and found dorsal root ganglion neurons grew preferentially on the laminin-blended chitosan patterns [82]. Pang et al. provided chitosan fibers for neuroepithelial stem cell growth. The survival, growth and differentiation were observed and the stem cell was capable to differentiate to neurons and glials on this chitosan fiber [83]. Another example is a growth factor immobilized chitosan matrix studied by Yang and coworkers [76]. The chitosan was crosslinked with nerve growth factor (NGF) by genipin. *In vitro* PC12 cell culture on this matrix indicated the bioactivity of immobilized NGF and the stimulation of neuronal differentiation of PC12 cells by the immobilized NGF. Furthermore, the degradation of chitosan resulted in a continuous release of NGF in a long term, which is also beneficial to nerve regeneration. Recently, a photocrosslinkable chitosan hydrogel was

used by Rickett et al. as a bioadhesive for nerve regeneration *in vitro* and *in vivo* [84]. The *in vitro* cell culture experiment showed the good cytocompatibility and non-toxicity of the chitosan, and the *in vivo* experiment additionally displayed a suitable mechanical property of this chitosan conduit as a nerve repair conduit. Moreover, solubility-improved carboxymethyl chitosan is also being applied for nerve regeneration. A crosslinked carboxymethyl chitosan film was synthesized and utilized in cell culture and *in vivo* implantation [85]. This crosslinked carboxymethyl chitosan has a very slow degradation preferable to long-term implantation. Schwann cell viability and regeneration of rat sciatic nerve defect were carried out on this film. Good biocompatibility and the improved myelination were observed. Most recently, a hybrid chitosan membrane [77] was fabricated and tested *in vitro* and *in vivo*. The *in vitro* study of N1E-115 neuroblastoma cells exhibited its good biocompatibility and the ability in supporting the cell survival and differentiation. At the same time, the *in vitro* functional recovery of rat sciatic nerve crush injury was evaluated and nerve fiber regeneration was assessed. It is concluded that the hybrid chitosan improved axonal growth and functional recovery. Another new kind of chitosan complex explored recently for nerve repair is the complex of biocompatible chitosan and conductive polypyrrole. As we know, action potential plays a central role in cell-cell communication in neurons. By introducing the conductive polymer into the chitosan, a precise platform of mimicking neuron behaviors and communication in order to understand the fundamental mechanism of neuron behaviors could be established. Two groups of researchers separately investigated the complex of chitosan and polypyrrole on its biodegradation [86] and its stimulation on Schwann cells [73] *in vitro*.

In summary, chitosan has great potential in a range of biomedical applications because of its unique physicochemical properties, and has been used in many different research studies related to tissue engineering, drug delivery and protein immobilization.

Table 2 Chitosan-based materials for different relevant tissue engineering applications

Chitosan/Chitosan derivatives, type	Cell type/animal model/human patient	Application	Active molecules	Ref.
Chitosan/chitin/fucoidan/alginate, hydrogel	Full-thickness skin defect on rat	Wound healing		[87]
Chitosan/ heparin, ointment	Full-thickness skin defect on rat	Wound healing		[88]
Galactosylated chitosan/alginate, scaffold	Hepatocytes and NIH3T3 fibroblast	Bioartificial liver		[78, 79]
Heparin-chitosan/alginate, scaffold	Human foreskin fibroblast	Control release of growth factor	Basic fibroblast growth factor(bFGF)	[89]
Chitosan/hydroxyapatite, scaffold		Bone regeneration	Dexamethasone and bFGF	[69]
Chitosan, membrane	Osteoblast and chondrocyte	Repairs of bone and cartilage defects		[90]
Chitosan/gelatin/hyaluronan with poly(lactide-co-glycotide) (PLGA) microsphere, scaffold	Chondrocytes (Rabbit)	Cartilage repair		[67]
Chitosan/gelatin/hyaluronan, scaffold	Auricular chondrocytes (Rabbit)	Cartilage repair	bFGF	[68]
Chitosan/gelatin/poly(L-Lysine), scaffold and membrane	Cortical and hippocampal neurons, glial cells and dorsal root ganglia	Repair of spinal cord injuries(SCIs)		[91]
Chitosan crosslinked with nerve growth factor(NGF) by genipin, scaffold	PC12 cell	Peripheral nerve regeneration	NGF	[76]
Chitosan, scaffold	Bone marrow stromal cell	SCI repair		[92]
Chitosan/polypyrrole, scaffold	Schwann cells	Peripheral nerve regeneration		[73]
Carboxymethyl chitosan, scaffold	Rat sciatic nerve injury model	Peripheral nerve regeneration	Glial cell-line derived neurotrophic factor and laminin	[75]
Chitosan/polyglycolic acid (PGA)	Sprague Dawley® (SD) rat, Sciatic nerve defected dog, and median nerve defected human patient	Treatment for long-term delayed injuries of peripheral nerve		[72]

Table 2 Chitosan-based materials for different relevant tissue engineering applications (continued)

Chitosan, membrane	N1E-115 neural cell, and nerve sciatic crush injured Wistar rat	Peripheral nerve reconstruction and functional recovery		[77]
Chitosan, bilayered tube with out-layer of film and inner-layer of nano/microfiber	SD rat	Peripheral nerve regeneration	Laminin peptide sequences	[74]
Chitosan, scaffold	Primary porcine tenocyte	Tendon repair		[51]
Chitosan/collagen, hydrogel	Human marrow-derived stem cell	Bone repair		[93]
Chitosan/ calcium phosphate cement, scaffold	Mesenchymal stem cell (MSC)	Bone regeneration		[94]
Chitosan/polybutylene succinate, scaffold	Bone marrow-derived mesenchymal progenitor cell (BMC9)	Cartilage regeneration		[95]
Chitosan-PLGA-poly ethylene oxide, nanofiber, with PLGA, microfiber	Dermal sheath cell	Artificial skin		[59]
Photocrosslinkable chitosan, hydrogel	Human hepatoblastoma cell (HepG2) and NIH/3T3 fibroblast	Optimization of cell function and liver tissue engineering		[96]
Chitosan/poly-L-lactic acid (PLLA), film	Mouse fibroblast (L929) and human hepatocyte (L02)	Cell morphology control		[61]
Chitosan, membrane and sponge	3T3 fibroblast	Wound dressing		[97]
Photocrosslinkable chitosan, hydrogel	Bleeding mouse tail	Wound dressing		[98]
Chitosan/hyaluronan, scaffold	Fibroblast (Rabbit)	Ligament repair		[99]
Chitosan/collagen, scaffold	Human periodontal ligament cell, and athymic mouse	Ligament repair	Human transforming growth factor beta 1 (hTGF-β1)	[100]
Chitosan/gelatin, scaffold	Chondrocyte (Rabbit)	Cartilage regeneration	Plasmid DNA encoding TGF- β1	[66]

2.3.1.3 Other natural polymers

Other natural-derived polymers, such as alginate, gelatin and hyaluronic acid, are also important candidates for different biological applications.

Alginate is a natural anionic polymer from brown seaweed and consists of random sequences of (1→4) linked β-D-mannuronic acid and α-L-guluronic acid (Figure 2 (a)). It has the advantages of biocompatibility, low toxicity, and specially gelation by addition of divalent cations such as Ca^{2+} [101]. Due to its anionic property, alginate is inherently mammalian cell non-adhesive. To create cell adhesive alginate derivatives, some cell-adhesive peptides have been incorporated into alginate. RGD (Arg-Gly-Asp), DGEA (Asp-Gly-Glu-Ala) and YIGSR (Tyr-Ile-Gly-Ser-Arg) peptide sequences have been reported for the development of cell adhesive alginates. MC3T3-E1 preosteoblasts and C2C12 myoblasts have been exploited on RGD modified alginates [102, 103]. YIGSR modified alginate has been used to promote neural cell adhesion [104]. Most recently, for controlling cell adhesion, an alginate gel has been controlled in a microfluidic device by a light-triggered release of caged calcium and it was used for 3D cell culture and co-culture [105]. Specifically, MC3T3-E1 and human umbilical vein endothelial cell (HUVEC) were co-cultured in the microfluidic device through the photo-sensitive alginate gel. It provided an opportunity to integrate the control of 3D cell culture microenvironment into microfluidic systems. Briefly, alginate is anionic and has no cell receptors. It is an ideal blank platform to quantify cell adhesion with different cell adhesive peptides and surface concentrations of a specific peptide. Except for cell adhesion studies , alginate has been widely used to drug delivery system and also tissue regeneration for bone, cartilage and blood vessel [101].

Hyaluronic acid (HA) is an anionic polysaccharide and an essential component of the ECM. It is a polymer of D-glucuronic acid and D-*N*-acetylglucosamine (Figure 2 (b)) and widely studied in tissue engineering and cell-cell/material interaction studies. Like chitosan, it is feasible to be fabricated into different physical forms, hydrogels, electrospun fibers, membranes and porous scaffolds. Like alginate, it is a natural anti-adhesive polymer due to its anions. These characteristic physical and chemical properties made HA a popular biopolymer used to examine the interaction between cell-material with different physical

parameters, and manipulate cell behaviours. Taking fibronectin modified HA as an example, it has been applied to investigate the effect of matrix elasticity. From the study of human dermal fibroblasts on it, researchers found that the cells showed a more organized actin cytoskeleton on a stiffer fibronectin-HA hydrogel [106]. This is a typical example to display how the stiffness of a matrix affect cell adhesion and how cells response to different surface mechanical properties. Another popular application of HA derivatives is on the control of cell behaviours, especially stem cells. Burdick group [107, 108] reported a photocrosslinked HA hydrogel and its influence on stem cell behaviours. They found the hydrogel seeded with mesenchymal stem cells (MSCs) could induce chondrogenesis and improve the production of cartilage matrix proteins. It can be considered as an illustration to show how the surface cues on a material affect cell behaviours. Another research group showed the response of human embryonic stem cells (hECSs) to a 3D hydrogel environment. The cells behave differently, compared with MSCs. hECSs intended to keep their undifferentiated morphology on HA hydrogel but maintain their capacity to differentiate and continue proliferation [109]. Besides homogenous HA hydrogels, heterogeneous HA hydrogels with designed and varied surface properties has been developed for biological applications. It has potential in directing cell growth, morphogenesis of different organs, and high-throughput screening of useful proteins and drugs. A photocrosslinkable HA hydrogel was demonstrated to have the capability to selectively uncrosslink under the spatial controlled UV light. hMSCs were seeded on this selectively uncrosslinked HA hydrogel and it was found that they prefer to attach to unexposed regions with crosslinking structures [110, 111]. This development may be useful to study cell behaviour within a controllable microenvironment that mimics *in vivo* reality of cell microenvironment.

Gelatin is obtained from alkaline or acidic pretreated and thermal denatured collagen. It has high carboxylic acid content [112] and usually used to form complexes with other biopolymers like chitosan [113] and poly(caprolactone) (PCL) [114]. For example, gelatin was coated onto PCL nanofibers to improve cell adhesion and provide support to the proliferation [114]. Recently, chitosan/gelatin polyelectrolyte (PEC) has been studied for its cytocompatibility with different neural cells and proven as a more promising candidate as a

nerve implanted material, to chitosan/gelatin/PLLA [91]. There are also other applications of chitosan/gelatin PEC as cartilage repair candidates reported [66-68].

(a)

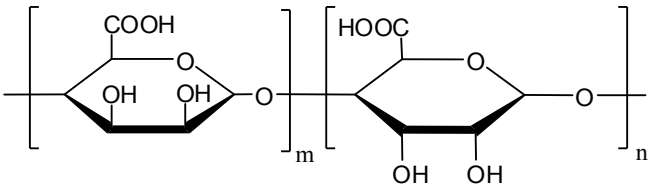

(b)

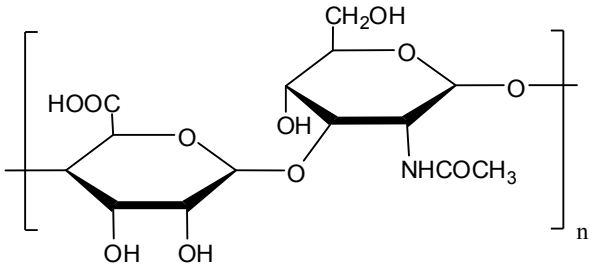

Figure 2 Chemical structures of alginate, (a), and hyaluronic acid, (b)

2.3.2 Self-assembled monolayers (SAMs) on gold

Noble metal surfaces as a group of materials for biomedical application have been used over 100 years. In the early stages, they were used implantable materials for bone fracture fixation. They have good inertness and enough mechanical strength, compared with polymers. But usually they don't have biodegradability. Thus, a lot of techniques have been developed to provide the metal and its alloys surface biofunctionality and bioactivity to be more suitable for body implantations [115]. The *in vitro* applications of metal and its alloys are usually on the studies of different cell phenomena.

2.3.2.1 Self-assembled monolayer (SAM) on a metal surface

SAMs on metal surfaces, especially gold surfaces, are a well-known and widely used technique to provide metal surface functionality and bioactivity.

In the 1980's, scientists discovered that alkanethiols spontaneously formed a crystalline-like monolayer on gold surfaces, and called them self-assembled monolayers (SAMs) [116]. The discovery quickly opened a new area of study. It makes it feasible and simple to create desired surface functionality on gold substrates by simply immersing gold substrates into dilute solutions of various alkanethiols. SAMs offer a unique combination of inert gold surface with different organic molecules. The mechanism of SAM formation has been studied for years and researchers have found that the alkanethiol chains form a tilted approximately 30° with the surface on a typical SAM [117, 118]. With the variation of chemistry on the alkanethiol chains, the exact structures of each individual SAM are still under investigations. Actually, the phenomena of self-assembly commonly exist in nature. The protein folding, DNA hybridization and transcription, and the formation of cell membranes all have self-assembly involved. The forces for these natural assemblies are hydrogen bonding, electrostatic interactions, hydrophobic interactions and Van der Waals forces. With regards to the mechanism of alkanethiols assembled on gold, the driving forces include the strong interaction between sulphur and gold, hydrophobic interaction and Van der Waals force. As found, the sulphur and gold formed a semi-covalent bond, which has half binding strength of carbon-carbon covalent binding. The mechanism of S-Au binding could be suggested as an oxidative addition and a reductive elimination of the hydrogen. The eliminated hydrogen may form molecular hydrogen but it has not been observed or verified yet [119-121]. In addition, the interactions of methylene carbons on alkane chains help lower the overall surface energy and order the molecular chains [118]. A schematic alkanethiol on gold is shown in Figure 3. The sulphur interacted with gold is considered as the head group. The alkyl chains are high ordered and tilted around 30° to the surface. Importantly, the various functional groups on the top of the surface are considered as tail groups and provide a platform where desired groups can be applied to produce surfaces with different chemistry and serve different purposes. By simply varying the tail group, the surface can be customized to have different physical and chemical properties, including hydrophilic or hydrophobic, protein resistant or protein adhesive, and allow or rejec chemical bindings. In this project, we utilized the ease to control surface functionality on SAM for further biomolecule immobilization.

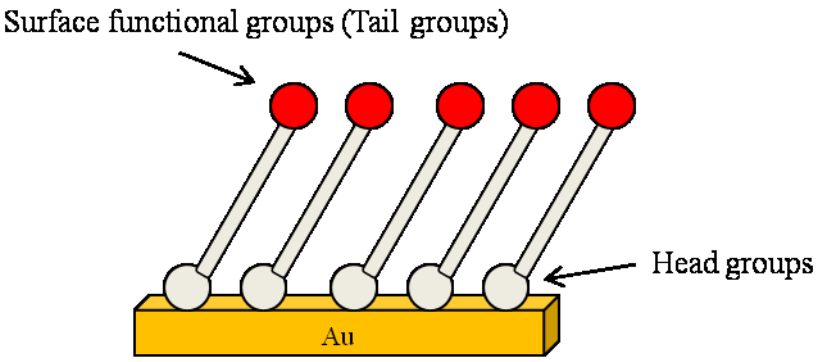

Figure 3 Schematic diagram of thiol-gold SAM

The preparation of SAM is very simple and can be done by just placing the clean gold substrate into a low concentration of alkanethiol ethanol solution. The initial formation of a monolayer is very fast and the initially formed monolayer is not well-organized. Over time, the self-assembled molecules move and become more ordered. Reported assembly times vary, but typically are 12 h to 2 days based on different reports [122]. The research showed that the well-organized monolayer highly depends on the purity of the alkanethiols. Even a low percentage of impurity in self-assembled molecules, alkanethiols, has a obvious influence on the formation, and may result in a disordered monolayer, or a monolayer with disordered regions [123, 124]. Some details about SAMs have been revealed later by different researchers [125-128]. They found that the complex or bulky tail groups can disrupt the closely packed arrangement of the alkane chains and result in a less ordered self-assembled layer. Further, the mixed SAM from a solution of two or more alkanethiols could be formed and controlled. It is shown that the mole ratio of alkanethiols on SAM was related to the mole ratio of alkanethiols in the solution, but there was competition between different alkanethiols and it resulted in different ratios of alkanethiols between in the solution and the surface.

The major advantage of SAM is that it can be prepared in a laboratory using a very simple method. As described above, the substrate just needs to be dipped in the required dilute solution for a specified time, washed thoroughly with the same solvent and then dried [121]. The strong chemisorption between substrate and self-assembled molecule with various functional groups provides an approach for studies and applications in many areas [125, 129, 130]. The examples include surface wetting, non-fouling property, electrochemistry, surface

passivation, protein binding, DNA assembly, corrosion resistance, biological arrays, cell interactions, and molecular electronics.

The biological application of SAMs is usually on the development of biosensors and understanding of cell-cell/material interactions [131]. These applications are mainly due to its simpleness to immobilize biomolecules and the mimic of complex cell microenvironment.

2.3.2.2 Cell studies on SAMs of alkanethiol-gold

The initial attachment of living cells could be greatly aided by the pre-modification of either the deposited cells or the platforms. The modification of the platform can be accomplished by physical or chemical means. One of the most popular methods to promote cell attachment on a surface is using self-assembled monolayers on gold with distinct terminal functional groups for specific protein and cell adsorption or immobilization. Cell studies have already been carried out on different kinds of SAM surfaces.

The use of SAMs as a surface model for *in vitro* cell studies has some important advantages. The major one is just as described above: easy formation of ordered and stable monolayers. The similarity of the monolayer to cell membrane is another important advantage, which makes it suitable for biomolecule immobilization. Furthermore, the flexibility to design the tail group on a SAM can meet different requirements for biological applications. Also, for any *in vitro* investigations, only a small amount of biomolecules is needed on a SAM. Additionally, many surface techniques are available for a molecular level of investigation, such as atomic force microscopy (AFM) and scanning tunnelling microscopy (STM).

Here, in Table 3, some significant cell studies on SAMs have been listed from the vast research efforts undertaken on them in biological areas and reported over the past three decades.

Table 3 Some selected cell studies on SAMs of alkanethiol-gold

Self-assembled molecule/Substrate	Bioactive molecules/cell type	Potential application	Ref.
Mixed thiols: mannitol-terminated alkanethiol and hexadecanethiol		Non-fouling surface and cell patterning	[132]
Carboxyl- and methyl-terminated alkanethiols	Horse heart cytochrome c	Electron-transfer on protein bonded SAMs	[133]
Thiopeptide	Lipid: dimyristoylphosphatidylethanolamine (DMPE)	Bilayer model surface	[134]
Hydroxyl-, methyl-, amine- and carboxyl-terminated alkanethiols	Fibronectin / myoblast	Modulation of protein adsorption and cell adhesion	[135]
Mixed thiols: hexadecanethiol and tri(ethylene glycol)-terminated alkanethiol	Fibronectin / endothelial cell	Control of cell attachment	[136]
Carboxyl- and methyl-terminated alkanethiols	Primary human osteroblast	Kinetics of cell attachment and cell proliferation	[137]
Oligo(ethylene glycol)-terminated alkanethiol	Benzophenone and RGD-contained peptide / fibroblast	Regulation of cell adhesion and cell patterning	[138]
Oligo(ethylene glycol)-terminated alkanethiol and hydroquinone-terminated alkanethiol	A substrate for c-Src (AclYGEFKKKC-NH_2)	Peptide chip to evaluate protein kinase activity	[139]
Tri(ethylene glycol)-terminated alkanethiol and hydroquinone-terminated alkanethiol	Peptides (GRGDS and PHSRN) / baby hamster kidney cell and 3T3 Swiss fibroblast	Investigation of peptides on cell adhesion and mechanism	[140]
Photocleavable alkanethiols with bioactive segments	Peptide (GRGDS)	Protein patterning of Cell-cell signalling	[141]
Photocleavable hydroquinone-terminated alkanethiol	Cyclopentadiene-tagged ligand	Protein patterning for biospecific interactions	[142]
Aminothiophenol and benzenethiol		Carbon tube immobilization	[143]
Hexa(ethylene glycol)-terminated alkanethiol	Rabbit IgG and goat anti-rabbit IgG	Biological nanoarray	[144]

Table 3 Some selected cell studies on SAMs of alkanethiol-gold (Continued)

Initiator-terminated alkanethiol	Fibronectin and fetal bovine serum (FBS) / NIH/3T3 fibroblast	Surface initiated atomic transfer radical polymerization (SI-ATRP) and non-fouling surface	[145]
Hydroxyl-, methyl- and tetra(ethylene glycol)-terminated alkanethiol	Helicobacter pylori (H. pylori)	Bacterial behaviours on the effect of different surface functionality	[146]
Initiator-terminated alkanethiol	Preosteoblastic cell	SI-ATRP, phosphate mineralization and bone cell growth on a model surface	[147]
Mixed thiols: acetylenic $Co_2(CO)_6$– and tri(ethylene glycol)-terminated alkanethiols	Fibronectin and GRGDS peptide / CHO cell and Hela cell	Click chemistry and electrochemical control on cell adhesion	[148]
RGD peptide-terminated alkanethiol	RGD peptide / NIH/3T3 fibroblast	Dynamic control of cell adhesion and detachment	[149]
Initiator-terminated alkanethiol	Bovine serum albumin (BSA)	Chiral polymer brush formation and protein adsorption	[150]
tetra(ethylene glycol)-, hydroquinone-, quinine-, ferrocene-, and ferrocenium-terminated alkanethiol	Human mesenchymal stem cell (hMSC)	Screening the surface chemistry effects on stem cell differentiation	[151]
tri(ethylene glycol)-terminated alkanethiol	Poly(D-lysine) / embryonic cortical neuron	The effect of nano-patterns on neuronal growth	[152]
DNA oligoneucleotide-PEG- and tri(ethylene glycol)-terminated alkanethiol, and dithiolaromatic triethyleneglycol	Breast cancer marker, oestrogen receptor-α	DNA arrays and detection of breast cancer marker	[153]

In the early studies of SAMs for biological applications, to understand protein adsorption and cell behaviour on a surface with various functional groups attracted researchers' attention. Different chain length of alkanethiols with different tail groups, such as hydroxyl, methyl, carboxyl, and amine were studied for their effect on cell attachment and cell morphology [135, 137]. For example, the proliferation of myoblast cells was investigated on hydroxyl, methyl, amine and carboxyl covered SAMs by Garcia and coworkers [135]. Very recently, people used different functionalized SAMs to determine bacterial behaviours with different surface chemistry, which could be beneficial to create bioarrays for bacteria detection [146]. At the meantime, different oligo(ethylene glycol)s (EGs) were studied to provide efficient non-fouling surfaces [132, 136, 144]. As we know, most biological systems recognize foreign objects through physical and chemical properties and molecular confirmation. PEG is recognized and extensively used in many biological applications because of its capacity to resist protein and cell from binding to the substrate. Moreover, PEG is found to have no toxicity. Thus, PEG coating on an inert solid surface is a continuous research focus to control protein adsorption and cell adhesion for biosensors, high-throughput screening, and cell biology. Alkanethiol-SAM terminated with oligomers of ethylene glycols was the primary SAMs developed to resist the adsorption of model proteins and cells. Mrksich et al. studied the endothelial cell on a patterned SAM with methyl and tri(ethylene glycol), and found that fibronectin just attached to methyl covered regions, as well as the cells [136]. Polymer brush synthesized on SAMs was another popular topic being studied. It can be introduced onto SAM through an initiator-alkanethiol and SI-ATRP. It is an alternative approach to produce PEG covered surface with protein resistant property or other polymeric properties. Some researchers reported this approach with several different applications. Ma et al. successfully synthesized PEG brushed SAM and tested its protein and cell resistance with fibronectin, FBS and fibroblast [145]. Lobbicke et al. used it for bone cell study. They produced a SAM surface with poly(methacrylic acid) (PMAA) and poly(dimethyaminothyl methacrylate) (PDM-AEMA) brush by SI-ATRP. The pH responsivity of the polymer brush could help its mineralization with calcium phosphate and then preosteoblastic cell proliferation [147].

To mimic cell microenvironment and other related cell behaviors, different stimuli were applied on SAMs to create heterogeneous functionality or alter physical and chemical properties on SAMs. Mrksich and his colleagues did a lot of work on controlling surface properties of SAMs with different methods including micro-printing and photochemistry. The first example from their group was to create line patterning of oligo(ethylene glycol)- and methyl-terminated alkanethiols for cell patterning in 1997 by micro-printing technique [154]. They successfully patterned oligo(ethylene glycol)s and methyls on transparent gold and silver. The second example was a monolayer with photocleavable hydroquinone developed in 2004. The light could selectively remove the photocleavable molecule and expose hydroquinone, which could undergo oxidization to benzoquinone for ligand immobilization [142]. Additionally, they also developed a peptide chip on the SAM for the evaluation of protein activity by developing a monolayer presenting benzoquinone groups and the Diels-Alder reaction between diene modified peptides and quinine groups on the SAM helped the selective immobilization of the peptides [139]. Other groups such as Herbert et al. have also conducted patterning studies with oligopeptides to manipulate cell adhesion and migration with fibroblasts [138]. In recent years, different potential bioarrays with mixed self-assembled molecules were reported. Different stimuli were introduced into the systems. Electrical potential was introduced as a stimulus and converted the surface chemistry by dicobalt hexacarbonyl terminated alkanethiol. The adhesion of CHO and Hela cells was controlled on this SAM [148]. Still utilizing electrical potential, a new approach to develop DNA sensor was reported by Henry et al. A breast cancer marker was applied as a model to demonstrate its potential in theranostics and pharmacogenomics. In addition, chiral effect of molecules on protein adsorption has been studied on SAM. L/D-valine branched polyacryloyl brush was studied by Sun and his coworkers [150].

Generally, SAM on gold is a good candidate for biological applications because of its distinguishing properties on varying tail groups and its well-ordered single molecule layer. As seen in Table 3, it has been used on cell behaviour studies about adhesion, proliferation, differentiation and migration, screening of surface chemistry effects on cells, creation of protein and cell resistant surfaces, DNA sensors, and other biological areas where a precise control on surface chemistry was required. However, SAM has certain limitation during

these biomedical applications. The chemical stability of some SAMs is not very good as monolayer can be chemically oxidized during the investigations. It is not compatible with some image acquisition techniques since it is not transparent. Some hydrophobic SAMs accumulate organic contaminants easily due to their high surface energy. But, still, SAM is a promising model surface to study for these applications mentioned above. When a stimulus was introduced during the development of SAMs, a more complex platform is able to generate for better mimic of cells with their microenvironment.

2.3.3 SAMs of organosilane

SAMs of organosilane on glass or silicon wafers can be used to modify surface properties. They are also important substrates for cell adhesion studies *in vitro* and have been successfully developed to obtain control over the molecule composition and surface functionality. Organosilanes can form a close-packed single molecule layer on glass or silicon wafers due to the hydrophobic and Van der Waals interactions among the alkyl chains of the organosilane molecules. They have the particular advantage to investigate the influence of surface properties on cell adhesion and the following behaviours by varying surface chemistry [155]. For example, Faucheux et al. utilized organosilanes on glass with the terminal groups of methyl, bromine, vinyl, amine, PEG and hydroxyl to explore and understand their influence on the adhesion, growth and functions of human fibroblast [155]. In addition to the investigation of surface chemistry and topography on protein absorption and cell adhesion, the SAM of organosilanes is also a promising surface to precisely control cell attachment. It has been shown that deep UV irradiation can alternate SAMs of organosilane by a photocleavage mechanism for further modification and surface patterning [156]. Photolithography can be employed on SAMs of organosilane to generate patterning. The study from Kira et al. can be taken as an example. They developed a SAM of organosilane with perfluroalkyl groups on glass, and used it to control protein adsorption and growth of PC12 and HeLa cells [157]. Around the same time, Das et al. used a SAM of organosilane with amine groups to coculture nerve and muscle cells on it and mimic neuromuscular junctions [158]. Most recently Yamamoto and his colleagues reported a method based on organosilanes on glass slides to create an *in-situ* control on an *in vitro* neuronal circuit to mimic *in vivo* architecture and functions of neural circuits. They achieved

the control by locally modifying culture surface *in-situ* with a laser, and then the neurites were guided by these *in situ* changes on culture surfaces [159]. The SAM of organosilane is recognized as an important surface fabrication technique to control cell adhesion for the development of biochips.

2.3.4 Other methods on solid substrates for cell studies

2.3.4.1 Soft lithography

Except polymers and SAMs, there are still other strategies used on a solid surface for cell adhesion, particularly a precise control on cell adhesion. Soft lithography is one of the commonly used techniques to control chemical structure on a solid surface for cell-substrate interactions. It refers to a number of techniques with the common feature that at some stage of the process a soft material is used to create the chemical structures. Microcontact printing (μCP) is the most studied in this family. The technique was originally developed for microelectronics applications and later was used for cell adhesion studies, particularly for the production of surfaces for cell patterning. Due to its simplicity and flexibility, there have been numerous applications of cell adhesion studies, especially cell patterning studies, published based on it. The process can be explained as follows: an elastomeric stamp was prepared by casting on a microstructured master surface and hardened; a solution with biomolecules to be printed was inked on the stamp and then transferred to a substrate by the stamp, usually a noble metal surface or glass; after the removal of the stamp, the biomolecule was patterned on the designed substrate. In some cases, a second molecule solution was backfilled on the substrate to increase the contrast with patterned regions. The topographic masters of stamps are often created by photolithography and other mechanical methods. Poly(dimethylsiloxane) (PDMS) is the most widely used stamp material. After oxygen or air plasma, PDMS stamps are usually favourable to absorb the ink on their surfaces and then ready to a substrate. Based on different applications, many different molecular solutions could be used as inks for μCP and transferred to a substrate [160, 161]. The simple example of μCP to create direct patterning for cell adhesion is based on the physisorption of cell adhesive molecules on the surfaces. Many different ECM proteins and peptide sequences have been successfully printed for cell adhesion. For cell patterning studies, fibronectin,

LAM and cell adhesive peptide sequences have been used as the inks to direct cell adhesion. Csucs et al. were able to print a RGD sequence contained macromolecule and backfill the rest of the surface with a PEG derivative to create an alternative RGD and PEG covered TCPS or glass for fibroblasts' adhesion and patterning [162, 163]. Altomare et al. recently created a fibronectin strip pattern on a film of L-lactide/trimethylene carbonate copolymer and then used it for directing muscle cell growth [164]. Furthermore, LAM was successfully patterned on a silicon wafer and the precise position of neuronal cells was controlled by these LAM patterns on the wafer. Neuronal networks could be formed by this method *in vitro* [165]. In addition, the technique could also be used to patterning specific antibodies for bacteria detection and patterning [166]. At the same time, μCP has been reported to combine with SAM techniques for cell adhesion. Conventionally a hydrophobic alkanethiol was printed on a gold substrate to form a patterned SAM, and then the remaining regions on the surface was usually rendered cell non-adhesive with PEGs [167]. Another method involving both μCP and SAM was also adapted for cell adhesion studies. In detail, an amine-reactive SAM was used as a substrate; μCP was applied to pattern cell adhesive protein first and the rest regions were blocked by amine-terminated PEG to create cell non-adhesion on these regions [168]. Generally, μCP is a simple and cost-effective method for surface patterning and can be applied to numerous kinds of surfaces. But some limitation still hinders its applications in biological fields. The major limitation is that it is challenging for μCP to create complex and precise patterns in a nano-scale and to pattern three or more biomolecules on one substrate [161]. The practical pattern size of a regular PDMS can be small to 1 μm and this limits the resolution of the pattern and subsequently cell studies about nano-scale effect on cell behaviours. Meanwhile, three or more biomolecules are impossible to be patterned using μCP by PDMS stamp and a special stamp needs to provide for chemical patterning of multiple biomolecules [169]. Other challenges include the lack to create a biomolecule gradient and a precise geometry [161].

2.3.4.2 Photolithography

Other than soft lithography, another popular method on a solid substrate particular for cell adhesion and patterning is photolithography. It was also originally developed for microelectronic applications and then adapted to biological fields for cell studies. The

general procedure is that a photoresist (UV-sensitive polymer) layer is spin-coated to a wafer and baked to dry; this polymer-coated wafer is placed under UV irradiation with close contact to a photomask to remove the photoresist layer or alter its properties on irradiated regions; after irradiation, biomolecules can be deposited to the irradiated surface and then be lifted-off with the remaining photoresist layer on certain regions by an organic solvent. In some cases, biomolecules were deposited evenly on top of the photoresist layer before irradiation and then were selectively removed with the photoresist layer after irradiation. For cell studies, as soft lithography, photolithography is usually used for cell patterning to develop cell assay-related platforms [161]. For example, Revzin et al. utilized photolithography for the patterning of PEG hydrogel on a glass slide, followed by collagen deposition to control cell adhesion, and they observed cells attachment and growth in their patterned microwells on glass. They suggested the technique can be applied to manufacture high-density arrays for cell-cell or cell-surface interactions [170]. Another example could be taken from the study of Albrecht et al. [171]. They described a method to precisely control cell position and develop a hydrated 3D cellular microenvironment using photolithography and poly(ethylene glycol) diacrylate (PEGDA). The cells enable to be encapsulated into specific PEGDA hydrogel regions on a solid surface. In a word, photolithography is a high-throughout strategy to create precise cell adhesion for *in vitro* cell arrays. But, as with soft lithography, it is very challenging to control immobilized biomolecules density for cell studies and it usually involves harsh organic solvents in the process, which is harmful for bioactivity of biomolecules and further cells [161].

As mentioned above, soft lithography and photolithography are all important strategies for cell adhesion studies, particular for precise control of cell adhesion, on a solid surface. The substrate materials of the two strategies can be silicon wafers, glass, polystyrene, polymeric hydrogels, noble metals etc. Therefore, they help to introduce different materials into cell adhesion studies. Besides these two strategies discussed, there are still other methods used to control surface features for cell adhesion. For example, Fan et al. used etching on a silicon to create different roughness and nanoscale topographical structure for neural cells [172] The studies showed the significant dependence of neural cell adhesion and viability on the silicon surface roughness. Recently, Nikkhah et al. utilized silicon chip and

etching technique to build up a micro-array and it was used for co-culture of human breast cancer and breast cells. They found the heterotrophic cell interaction in the co-culture and suggested that this silicon chip has potential to be used in other co-culture studies and cell-based biosensing devices.

2.4 Photochemistry applied in biological applications

To dynamically control the surface chemistry or the immobilization of biomolecules on a material, light is considered as an ideal external stimulus since it can be manipulated spatially and temporally in microscale, even nanoscale. Therefore, photolabile molecules are often employed as a switch controlled by light in biological applications. Photolabile molecules incorporated on biomaterials and SAMs introduce a dynamic control to the materials.

2.4.1 Photolabile molecule

The photolabile molecules could be categorized into two kinds: photoaffinity molecules and photocleavable molecules. It depends on whether a formation or cleavage of chemical bond happens after light irradiation. For photoaffinity molecules, a bond forms during the molecule and a desired molecule varied with the application; for photocleavable molecules, a covalent bond breaks and the molecule is removed from the bulk material [173].

2.4.1.1 Photoaffinity molecules

Figure 4 lists the major photoaffinity molecules used for biomedical applications. Benzophenone is a common photo initiator in photochemistry and used for a lot of screening studies [174-176]. It was first reported for cell adhesion studies on by Herbert et al. to study cell behaviours on a micropatterned SAM [138]. Through photoimmobilization of a cell-adhesive peptide, the location, the number and the shape of cells were controlled. Later, Ruiz et al. [177] reported modified polyurethane with benzophenone to control cell attachment on a polymer and mimic the cell membrane. Moreover, Bessone et al. [178] reported a fabrication method of a microfluidic device with alternative hydrophobic and hydrophilic patterns of microchannels involving benzophenone. Another popular photoaffinity molecule,

aryl azide, has been reported to immobilize dextran, a similar protein and cell resistant polymer as PEG, on poly(ethylene terephohalate) surface as a versatile development of surface modification [179]. Other applications of aryl azide includes biolabelling [180], protein mapping [181] and gene mapping [182]. The last example is diazirine. Diazirine as a photocrosslinker was studied to capture glycoprotein interactions [183], used in genetic bacteria [184] and immobilization of biomolecules on polymer surfaces [185], and used as a probe for protein-DNA interactions [186].

2.4.1.2 Photocleavable molecules (photocages)

Photocleavable molecule, also called photocages, form the other class of photolabile molecules widely used in biological applications. As shown in Figure 4, it usually includes *o*-nitrobenzyl, benzoin, *o*-cinnamoyl, *m*-nitrophenol and coumarinylmethyl [173].

Among all the photocaging studies, *o*-nitrobenzyl and its derivatives are the most frequently used photocages [187-192]. The photolysis and photocleavage mechanism of *o*-nitrobenzyl is that hydrogen transfers from the benzyl position to the nitro functional group during photo irradiation, and the transfer is achieved by the elimination of *o*-nitrosobenzaldehyde from the bicyclic intermediate which is generated during the process, as shown in Figure 5.

a. Photoaffinity molecules

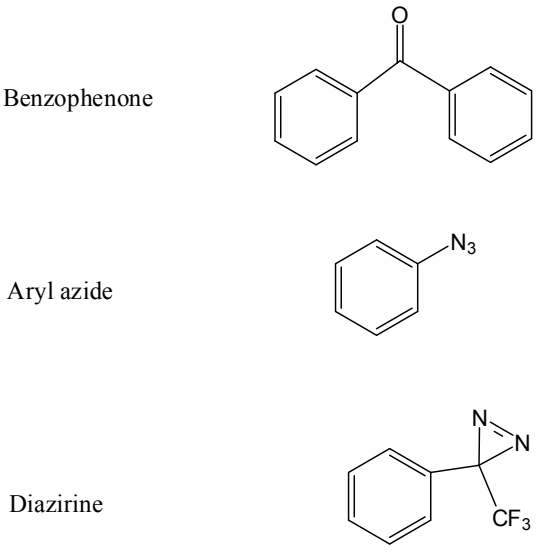

b. Photocleavable molecules

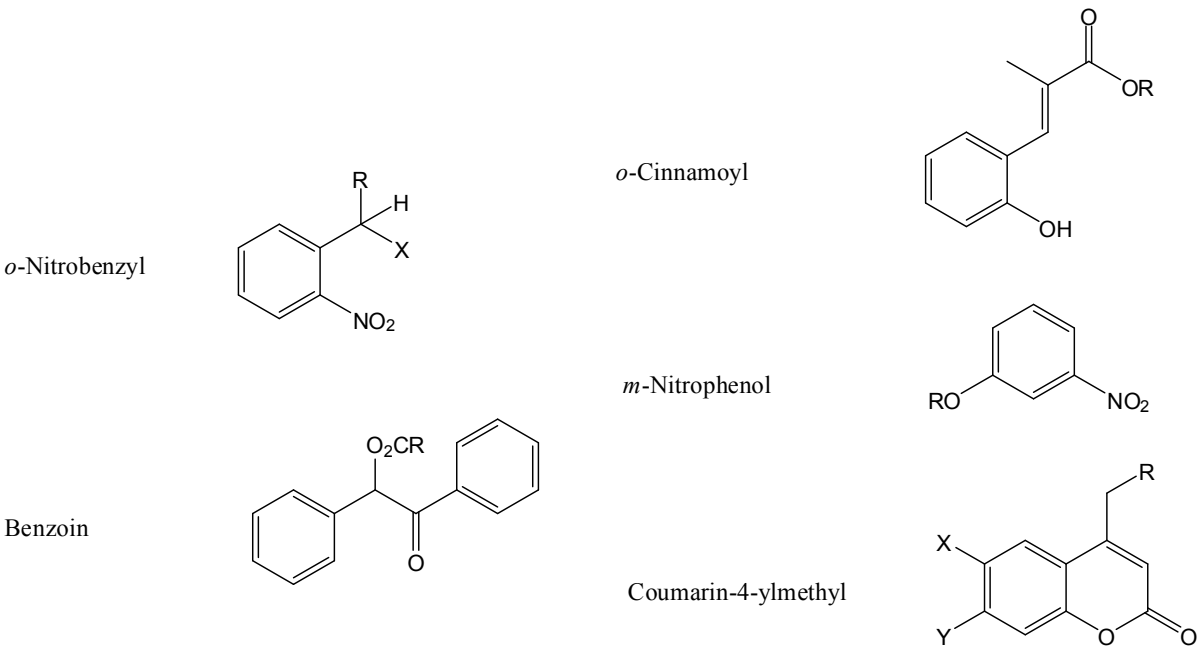

Figure 4 Major photoaffinity and photocleavable molecules

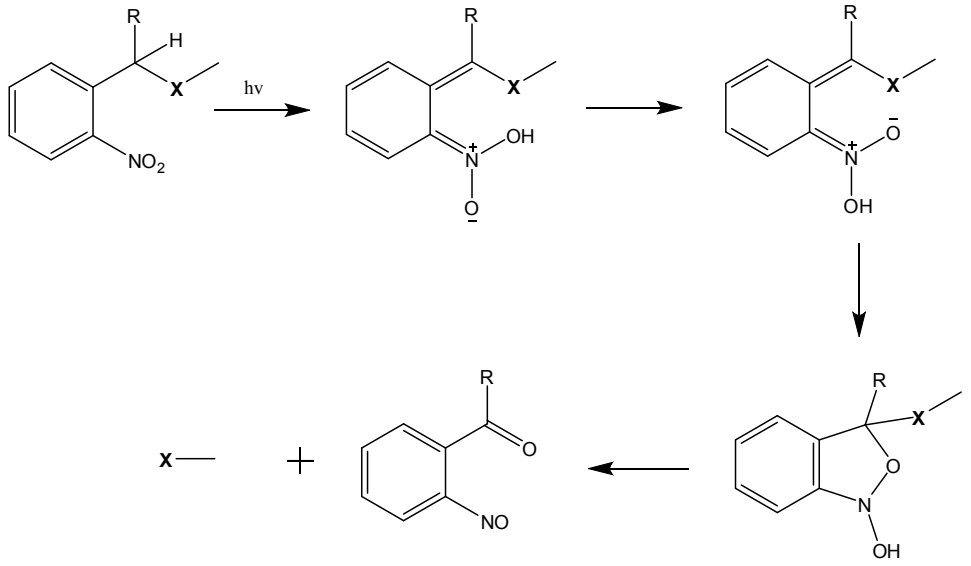

Figure 5 Photolysis of a nitrobenzyl derivative. X is the cage-protected group.

2.4.2 Biological applications of photocages

Here, biological applications of photocages and its derivatives could be divided into two parts for discussion: the photocage on polymeric materials to create scaffolds or films mainly for *in vivo* applications and on solid surfaces for *in vitro* studies of labelling, screening and fundamental cell biology.

2.4.2.1 Photocages on solid surfaces [193]

Cage compound modified solid surfaces hold great promise for various biotechnological and biomedical applications. It could be used as a platform for drug and biomarker discovery, mapping protein-protein interaction, DNA screening, and analysis of cellular processes [194, 195]. For such purposes, one of the strategies is to develop a functional substrate that has the capability to respond to an external stimulus. Light as external stimulus, combined with photocages, has the great advantages of the high resolution, both spatial and temporal control, and also no residue, which may cause some unexpected side effects on the development of microarray chips.

A popular application of photocleavable surface is used for DNA screening and *in situ* synthesis. DNA probe arrays are useful tools in biomedical research and diagnostics

because of their ability to simultaneously address large numbers of genes [187]. The photocleavable molecules in these designs are used to temporarily protect the terminal groups of nucleotide monomers, which are often assembled on glass or metal surfaces and block the DNA polymerase reaction after the incorporation of each nucleotide. Irradiation and the use of appropriate photomasks allow the release of terminal groups and the control of the sequence and the size. The significant advantage of using photochemistry is that no chemical reagent and no purification are required. The fabrication of photosensitive DNA microarrays usually aims to increase the rate and efficiency of photo deprotection. Seo et al. [187] reported a successful DNA sequencing approach based on sequencing by synthesis on a solid surface using photocleavable fluorescent nucleotides in 2004. They attached the azido-labeled DNA onto an alkyne-modified glass. A series of nucleotide analogues have different fluorescent dyes attached through an *o*-nitrobenzyl linker. The results showed that the near-UV irradiation led to the efficient release of the fluorophore and demonstrated the feasibility of performing the DNA polymerase reaction on the solid surface. Their development of DNA sequencing has the potential use on the whole genome sequencing and pharmacogenetics. So far, limited success with photochemical approaches has been reported but several cage compounds have been studied and shown the fast efficient photo deprotection of hydroxyl group for DNA microarray synthesis [196], like coumarin family [197], indoline and quinoline. Fodor et al. reported a successful array of 1024 peptides using a nitrobenzyl derivative protective group. Its ability to produce high-density oligonucleotide arrays (GenChip®probe arrays) has been utilized in DNA sequencing technology [198].

The basic challenge on the fabrication of protein and cell microarrays is the protein labelling with high resolution on the substrate. To achieve this, high density of individual and isolated reactive protein sites are required. Light, as a versatile trigger, can induce photoreaction instantaneously on the surfaces and control the immobilization without chemical reagents [199, 200]. Several studies have already been conducted to provide the feasibility to apply different photocleavable molecules on different solid surfaces and demonstrate their advantages. Basically, the caged molecule area was attached to a solid substrate and was irradiated through a mask or by laser lithography. Deprotection happened selectively on the regions exposed to the light and free functional groups were generated to

react with a second molecule, usually a biomolecule. Irradiation with different strategies could lead to the synthesis of a desired set of products on one surface [200]. It offers significant advantages for sensing applications, including reduced operation time, parallel detection of multiple targets and tiny amounts of sample requirement. Sundberg et al. [201] fabricated a heterogeneous surface with two different antibodies on a solid substrate in 1996. In their study, a nitrobenzyl derivative, nitroveratryloxycarbonyl (NVOC), was used as the caging agent. They immobilized a caged biotin analogue to the glass surfaces first and exposed it to UV light through a photolithographic mask to yield deprotected biotin regions for streptavidin binding, and biotinylated macromolecules were linked through biotin-streptavidin-biotin bridging. Finally they achieved two different biotinylated antibodies immobilized at different regions on a planar substrate. Alonso et al. [202] created a photosensitive silica also based on NVOC chemistry. Further, a typical protein repellent tetra(ethylene glycol) was used to assemble on silica surface with a NVOC terminal group. By UV irradiation, they could achieve highly selective deprotection of amine groups and site-specific immobilization of tris-nitrilotriacetic acid (tris-NTA) for His-tagged protein attachment and biotin for streptavidin attachment. In their system, oligoethylene glycol was introduced to the substrate, which helped to decrease the non-specific binding between the substrate and proteins. Lee et al. [203] developed a maskless photolithography process to control protein patterns with NVOC molecules. They fabricated a two dimensional micromirror array, where they used a digital micromirror as a virtual photomask to create biotin pattern. Most recently Grunwald et al.[204] applied photocleavable surfaces to capture and recognize virus. They created a photoactivable tris-NTA by a nitrobenzyl linker. The photoactivable tris-NTAs were self-inactivated by His-tagged proteins. Irradiation could activate the affinity by cleaving a tethered intramolecular ligand arming a multivalent chelator head. In their study, different strategies were applied to create site-specific protein pattern, including mask patterning, laser lithography, and successive activation of different areas using *in situ* laser scanning lithography. Furthermore, they also demonstrated the capability of their system to capture virus specific very low-density lipoprotein receptors, which made it a highly flexible platform for detection and analysis of clinically relevant virus particles. Until now, many different photocleavable solid systems have been developed and most of them are used nitrobenzyl groups to control protein specific binding to the solid

support [205-209]. To control the size of a pattern and avoid non-specific binding of proteins is still a big challenge for protein patterning technique based on photochemistry.

It is a critical step to control cell adhesion on a cell-culturing substrate for the development of cell microarrays. Using light as a stimulus and developing functional substrates that could response to light irradiation in order to switch surface properties is a powerful way to fabricate them. Research has already been done to create cell patterns either on glass surface, silicon or SAMs [189, 190]. For example, Dillmore et al. [142] provided a method to pattern ligands and cells on a SAM of alkanethiol-gold by using a nitrobenzyl derivate. Their method began with a NVOC-hydroquinone contained monolayer on gold. After successful synthesis, irradiation exposed the hydroquinone and the following oxidization of hydroquinone provided a site for the immobilization of cell adhesive peptide. Finally the designed surface could generate circular cell attachment corresponding to the photomask applied (Figure 6). Park et al. [210] also developed a protein and cell pattern on a thiolated gold SAM surface by nitrobenzyl derivates. Their strategy was to immobilize various cell adhesive peptides containing the ketone group and generate cell patterns. They showed the sequential immobilization of two fluorescent dyes in a pattern and also the immobilization of ligands in gradients to demonstrate the capability to immobilize different biomolecules.

Besides the studies mentioned above, there are studies of photocleavable substrates to serve other purposes such as protein purification [194] and microfluidic devices [178]. Recent research done by Jang et al. is a good example to develop a microfluidic system with single-cell attached inside. It could be a device for single-cell analysis to overcome any misleading of cell behaviours by averaging a large group of cells. They modified microchannels inside a surface with a nonfouling polymer, 2-methyacryloyloxyethyl phosphorylcholine (MPC), by a nitrobenzyl derivative. By UV irradiation, MPC was selectively removed with the photocage in the microchannel. The size of the exposed regions could be controlled by a photomask and it desired for a single endothelial cell attached.

A solid support with photocleavable molecules is a good platform to develop different microarrays for DNA analysis and diagnostics, protein-protein interaction and cell

process studies, drug screening and other biomedical applications. A solid flat support could minimize the topographical influence on the development of microarray chips and also it could tolerate many harsh operations or reaction conditions like organic solvents and high temperature, which are usually a problem for biomaterials.

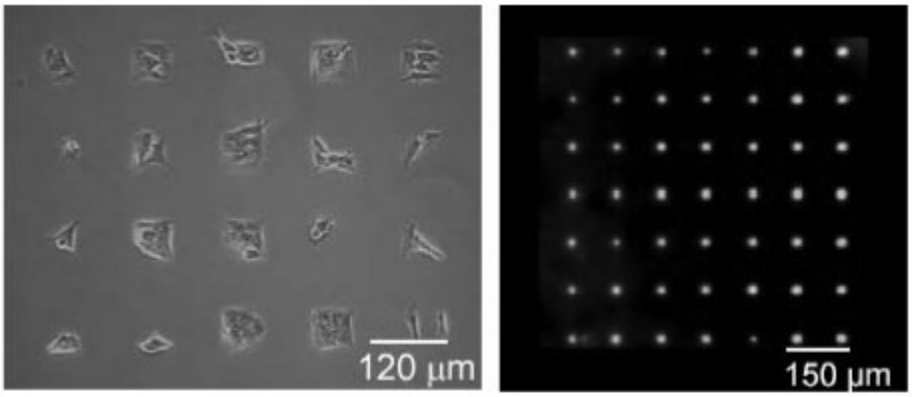

Figure 6 Swiss 3T3 fibroblasts cells selective attached on a SAM through photocleavable molecule. Reprinted from Ref. [142]. Copyright © 2004 American Chemical Society.

2.4.2.2 Photocages on polymer scaffolds and films

To incorporate photocages into polymers is a new strategy to prepare a desired material with heterogeneous properties for tissue engineering.

Some researchers utilized the photocages to switch wettability of polymers for potential biological applications. For example, Brown et al. [211] synthesized a polymer brush from a nitrobenzyl modified methacrylate (MAA) monomer by SI-ATRP. The UV irradiation can remove the nitrobenzyl from the bulk bone of the resulting PMAA and the surface exhibited a hydrophilic property instead of a hydrophobic property provided by the nitrobenzyl groups. The condensation of water droplet on the irradiated surface with a photomask provided the evidence on the capability of their strategy (Figure 7). Except the wettability, the photocage has also been used to control sol-gel transition temperature. A triblock polymer was developed by Woodcock and coworkers [212]. The existence of hydrophobic nitrobenzyls lowered the transition temperature and the cleavage of nitrobenzyl groups by light triggered the gel-sol transition at a constant temperature. Except applications

above, control release of prodrug, DNA and protein by light is also popular application for photocleavable nitrobenzyl groups incorporating polymers [188].

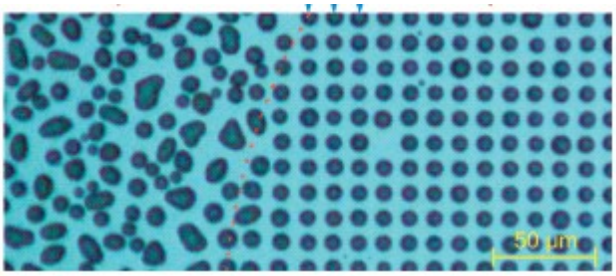

Figure 7 A water condensation image on a photo-patterned polymer surface. Reprinted from Ref. [211]. Copyright © 2009 American Chemical Society.

The application of photocages to switch a polymeric surface (2D) or scaffold (3D) into protein/cell-adhesive or protein/cell non-adhesive in order to control cell adhesion and growth is an important application for these molecules.

Burdick group [213] reported a copolymer with photocleavable side groups for cell adhesion. The copolymer is consisted of photocleavable 2-nitrobenzyl acrylate and (hydroxyethyl)methacrylate) (NBA-co-HEMA) and exhibits a light-sensitive property under UV irradiation. This polymeric film swelled and showed stress-induced wrinkling patterns when there was UV exposure on its surface. The cells attached and behaved very differently on their fibronectin-coated polymer films with various exposure times. On this film, there were cells attached without UV exposure but the cell spreading was not good. After 15 min of exposure, there is little cell attachment. With longer exposure (90 min), more cells were attached and the cells spread very well. The control of substrate mechanic, topography and chemistry simultaneously was achieved, which are all the parameters to influence cell behaviours.

A 3D scaffold that supports cellular growth and behaviour is required by engineering full tissues. Recently several groups have attempted to achieve cell patterning in a 3D structure. Except the works just mentioned in the previous paragraph, there are several research focusing on either control of ligand presentation or control of degradation in a polymer scaffold [214]. The incorporation of photocleavable molecules is one choice to

realize these controls. For example, Shoichet and her lab [215, 216] used agarose as the bulk material and incorporate it with a nitrobenzyl- or coumarin-modified cysteine by grafting. The matrix showed a light-responsive property. With selectively exposure of this matrix to UV light, controllable presentation of the functional molecule, sulfhydryl, and the following ligand immobilization was achieved, which enable to orient cell growth, particularly neuronal cell growth and axonal growth. To improve the control over 3D, especially the depth of patterns, they expanded to using confocal and two-photon microscopy to control the patterning in all three dimensions. The recent studies showed they improved their system to pattern multiple growth factors and realized the successful control on migration of neural precursor cell into 3D hydrogel channels generated by immobilization of cell-adhesive sequence RGD in the channels [217, 218].

Recently, Kloxin et al. reported another strategy to utilize nitrobenzyl [219]. They used a nitrobenzyl group as a crossliker between PEG and acrylate, and the polymerization of acrylate formed a crosslinked PEG-polyacrylate with the photocleavable molecule. Upon UV irradiation, the rearrangement of nitrobenzyl groups caused the break of crosslinking and made the hydrogel uncrosslinked (photodegradable). The controllable photodegradation of the hydrogel encapsulating cells created regions that were permissive to cell migration inside the hydrogel. Most recently, their group incorporated the photoaffinity and photocleavage into one 3D hydrogel. They successfully patterned two different adhesive peptide sequences (RGD and PHSRN) and, at the same time, released the entrapped cells in the hydrogels. The physical and chemical properties of their crosslinked hydrogel could be controlled independently and simultaneously [220].

Overall, the introduction of photoaffinity and photocleavable molecules provides us a way to import a non-invasive stimulus, light, into systems and realize real-time control or heterogeneity of physical or chemical properties of materials. Particularly for biological applications, it helps create model surfaces for many *in vitro* biological studies and the development of cell arrays for diagnosis, screening and probing; it also helps mimic the complexity of full tissues for tissue engineering and implantations.

2.5 Conclusion

In my project, we combined the photocleavable molecules, nitrobenzyl derivatives, with two different kinds of surfaces, SAM of alkanethiol-gold and chitosan. The SAM is based on a flat solid surface and good to utilize as a model surface for *in vitro* biological applications, such as fundamental cell biological and biochips. Chitosan, as a biocompatible and biodegradable polysaccharide, is a good candidate for different *in vivo* biological studies and potential tissue engineering applications. As mentioned above, nitrobenzyl groups introduced the light as a stimulus into the system and help control the ligand presentation. The cell attachment could be controlled by the heterogeneous presentation of ligands on our selected materials.

2.6 References

1. Burridge, K. and M. ChrzanowskaWodnicka, *Focal adhesions, contractility, and signaling.* Annual Review of Cell and Developmental Biology, 1996. **12**: p. 463-518.
2. Cukierman, E., et al., *Taking cell-matrix adhesions to the third dimension.* Science, 2001. **294**(5547): p. 1708-1712.
3. Martin A. Hjortso, J.W.R., ed. *Cell adhesion: fundamentals and biotechnological applications*. Bioprocess technology 1995, Marcel Dekker: New York. 273.
4. Benecke, B.J., A. Benzeev, and S. Penman, *CONTROL OF MESSENGER-RNA PRODUCTION, TRANSLATION AND TURNOVER IN SUSPENDED AND REATTACHED ANCHORAGE-DEPENDENT FIBROBLASTS.* Cell, 1978. **14**(4): p. 931-939.
5. Folkman, J. and A. Moscona, *ROLE OF CELL-SHAPE IN GROWTH-CONTROL.* Nature, 1978. **273**(5661): p. 345-349.
6. Watt, F.M., P.W. Jordan, and C.H. Oneill, *CELL-SHAPE CONTROLS TERMINAL DIFFERENTIATION OF HUMAN EPIDERMAL-KERATINOCYTES.* Proceedings of the National Academy of Sciences of the United States of America, 1988. **85**(15): p. 5576-5580.
7. Miller, F.R., D. McEachern, and B.E. Miller, *GROWTH-REGULATION OF MOUSE MAMMARY-TUMOR CELLS IN COLLAGEN GEL CULTURES BY DIFFUSIBLE FACTORS PRODUCED BY NORMAL MAMMARY-GLAND EPITHELIUM AND STROMAL FIBROBLASTS.* Cancer Research, 1989. **49**(21): p. 6091-6097.
8. Akaogi, K., et al., *Specific accumulation of tumor-derived adhesion factor in tumor blood vessels and in capillary tube-like structures of cultured vascular endothelial cells.* Proceedings of the National Academy of Sciences of the United States of America, 1996. **93**(16): p. 8384-8389.
9. Buck, C.A. and A.F. Horwitz, *CELL-SURFACE RECEPTORS FOR EXTRACELLULAR-MATRIX MOLECULES.* Annual Review of Cell Biology, 1987. **3**: p. 179-205.
10. Ingber, D.E. and J. Folkman, *HOW DOES EXTRACELLULAR-MATRIX CONTROL CAPILLARY MORPHOGENESIS.* Cell, 1989. **58**(5): p. 803-805.
11. Joshi, H.C., et al., *TENSION AND COMPRESSION IN THE CYTOSKELETON OF PC-12 NEURITES.* Journal of Cell Biology, 1985. **101**(3): p. 697-705.

12. Dennerll, T.J., et al., *TENSION AND COMPRESSION IN THE CYTOSKELETON OF PC-12 NEURITES II - QUANTITATIVE MEASUREMENTS.* Journal of Cell Biology, 1988. **107**(2): p. 665-674.
13. Lutolf, M.P. and J.A. Hubbell, *Synthetic biomaterials as instructive extracellular microenvironments for morphogenesis in tissue engineering.* Nature Biotechnology, 2005. **23**(1): p. 47-55.
14. Dillow, A.K. and M. Tirrell, *Targeted cellular adhesion at biomaterial interfaces.* Current Opinion in Solid State & Materials Science, 1998. **3**(3): p. 252-259.
15. Lebaron, R.G. and K.A. Athanasiou, *Extracellular matrix cell adhesion peptides: Functional applications in orthopedic materials.* Tissue Engineering, 2000. **6**(2): p. 85-103.
16. Fields, R.D., et al., *NERVE REGENERATION THROUGH ARTIFICIAL TUBULAR IMPLANTS.* Progress in Neurobiology, 1989. **33**(2): p. 87-&.
17. Shin, H., S. Jo, and A.G. Mikos, *Biomimetic materials for tissue engineering.* Biomaterials, 2003. **24**(24): p. 4353-4364.
18. Shoulders, M.D. and R.T. Raines, *Collagen Structure and Stability*, in *Annual Review of Biochemistry*. 2009. p. 929-958.
19. Eyre, D.R., *COLLAGEN - MOLECULAR DIVERSITY IN THE BODYS PROTEIN SCAFFOLD.* Science, 1980. **207**(4437): p. 1315-1322.
20. Ramshaw, J.A.M., J.A. Werkmeister, and V. Glattauer, *Collagen-based biomaterials*, in *Biotechnology and Genetic Engineering Reviews, Vol 13*. 1996. p. 335-382.
21. Chajra, H., et al., *Collagen-based biomaterials and cartilage engineering. Application to osteochondral defects.* Bio-Medical Materials and Engineering, 2008. **18**: p. S33-S45.
22. Chevallay, B. and D. Herbage, *Collagen-based biomaterials as 3D scaffold for cell cultures: applications for tissue engineering and gene therapy.* Medical & Biological Engineering & Computing, 2000. **38**(2): p. 211-218.
23. Zheng, W.F., W. Zhang, and X.Y. Jiang, *Biomimetic Collagen Nanofibrous Materials for Bone Tissue Engineering.* Advanced Engineering Materials, 2010. **12**(9): p. B451-B466.
24. Kew, S.J., et al., *Regeneration and repair of tendon and ligament tissue using collagen fibre biomaterials.* Acta Biomaterialia, 2011. **7**(9): p. 3237-3247.
25. Leonard, M.P., et al., *Endoscopic subureteral collagen injection: Are immunological concerns justified?* Journal of Urology, 1998. **160**(3): p. 1012-1016.
26. O'Brien, F.J., et al., *The effect of pore size on cell adhesion in collagen-GAG scaffolds.* Biomaterials, 2005. **26**(4): p. 433-441.
27. Harley, B.A.C., et al., *Microarchitecture of three-dimensional scaffolds influences cell migration behavior via junction interactions.* Biophysical Journal, 2008. **95**(8): p. 4013-4024.
28. Jaworski, J. and C.M. Klapperich, *Fibroblast remodeling activity at two- and three-dimensional collagen-glycosaminoglycan interfaces.* Biomaterials, 2006. **27**(23): p. 4212-4220.
29. Keilhoff, G., et al., *Bio-compatibility of type I/III collagen matrix for peripheral nerve reconstruction.* Biomaterials, 2003. **24**(16): p. 2779-2787.
30. Wahl, D.A. and J.T. Czernuszka, *Collagen-hydroxyapatite composites for hard tissue repair.* European Cells & Materials, 2006. **11**: p. 43-56.
31. Letic-Gavrilovic, A., A. Piattelli, and K. Abe, *Nerve growth factor beta(NGF beta) delivery via a collagen/hydroxyapatite (Col/HAp) composite and its effects on new bone growth.* Journal of Materials Science-Materials in Medicine, 2003. **14**(2): p. 95-102.
32. Harley, B.A., et al., *Optimal degradation rate for collagen chambers used for regeneration of peripheral nerves over long gaps.* Cells Tissues Organs, 2004. **176**(1-3): p. 153-165.
33. Inada, Y., et al., *Regeneration of peripheral nerve gaps with a polyglycolic acid-collagen tube.* Neurosurgery, 2004. **55**(3): p. 640-646.

34. Cao, J.I., et al., *The use of laminin modified linear ordered collagen scaffolds loaded with laminin-binding ciliary neurotrophic factor for sciatic nerve regeneration in rats.* Biomaterials, 2011. **32**(16): p. 3939-3948.
35. Awad, H.A., et al., *Repair of patellar tendon injuries using a cell-collagen composite.* Journal of Orthopaedic Research, 2003. **21**(3): p. 420-431.
36. Juncosa-Melvin, N., et al., *Mechanical stimulation increases collagen type I and collagen 1219 type III gene expression of stem cell-collagen sponge constructs for patellar tendon repair.* Tissue Engineering, 2007. **13**(6): p. 1219-1226.
37. Yang, C.L., et al., *The application of recombinant human collagen in tissue engineering.* Biodrugs, 2004. **18**(2): p. 103-119.
38. Sumita, Y., et al., *Performance of collagen sponge as a 3-D scaffold for tooth-tissue engineering.* Biomaterials, 2006. **27**(17): p. 3238-3248.
39. Compton, C.C., et al., *Organized skin structure is regenerated in vivo from collagen-GAG matrices seeded with autologous keratinocytes.* Journal of Investigative Dermatology, 1998. **110**(6): p. 908-916.
40. Uchino, T., T. Takezawa, and Y. Ikarashi, *Reconstruction of three-dimensional human skin model composed of dendritic cells, keratinocytes and fibroblasts utilizing a handy scaffold of collagen vitrigel membrane.* Toxicology in Vitro, 2009. **23**(2): p. 333-337.
41. Farrell, E., et al., *A collagen-glycosaminoglycan scaffold supports adult rat mesenchymal stem cell differentiation along osteogenic and chondrogenic routes.* Tissue Engineering, 2006. **12**(3): p. 459-468.
42. Mimura, T., et al., *Spatiotemporal control of proliferation and differentiation of bone marrow-derived mesenchymal stem cells recruited using collagen hydrogel for repair of articular cartilage defects.* Journal of Biomedical Materials Research Part B-Applied Biomaterials, 2011. **98B**(2): p. 360-368.
43. Liu, T., et al., *Sustained release of neurotrophin-3 and chondroitinase ABC from electrospun collagen nanofiber scaffold for spinal cord injury repair.* Journal of Biomedical Materials Research Part A, 2012. **100A**(1): p. 236-242.
44. Koch, S., et al., *Enhancing angiogenesis in collagen matrices by covalent incorporation of VEGF.* Journal of Materials Science-Materials in Medicine, 2006. **17**(8): p. 735-741.
45. Wang, P.C. and T. Takezawa, *Reconstruction of renal glomerular tissue using collagen vitrigel scaffold.* Journal of Bioscience and Bioengineering, 2005. **99**(6): p. 529-540.
46. Silva, S.S., J.F. Mano, and R.L. Reis, *Potential applications of natural origin polymer-based systems in soft tissue regeneration.* Critical Reviews in Biotechnology, 2010. **30**(3): p. 200-221.
47. Chen, C.H. and Y.F. Dai, *Effect of chitosan on interfacial polymerization of aniline.* Carbohydrate Polymers, 2011. **84**(2): p. 840-843.
48. Kim, I.Y., et al., *Chitosan and its derivatives for tissue engineering applications.* Biotechnology Advances, 2008. **26**(1): p. 1-21.
49. Sashiwa, H. and S.I. Aiba, *Chemically modified chitin and chitosan as biomaterials.* Progress in Polymer Science, 2004. **29**(9): p. 887-908.
50. No, H.K., et al., *Antibacterial activity of chitosans and chitosan oligomers with different molecular weights.* International Journal of Food Microbiology, 2002. **74**(1-2): p. 65-72.
51. Bagnaninchi, P.O., et al., *Chitosan microchannel scaffolds for tendon tissue engineering characterized using optical coherence tomography.* Tissue Engineering, 2007. **13**(2): p. 323-331.
52. CÃ¡rdenas, G., et al., *Chitosan composite films. Biomedical applications.* Journal of Materials Science: Materials in Medicine, 2008. **19**(6): p. 2397-2405.

53. Zhang, H. and S.H. Neau, *In vitro degradation of chitosan by a commercial enzyme preparation: effect of molecular weight and degree of deacetylation.* Biomaterials, 2001. **22**(12): p. 1653-1658.
54. Martin, P., *Wound healing - Aiming for perfect skin regeneration.* Science, 1997. **276**(5309): p. 75-81.
55. Blanpain, C., *STEM CELLS Skin regeneration and repair.* Nature, 2010. **464**(7289): p. 686-687.
56. Mori, T., et al., *Mechanism of macrophage activation by chitin derivatives.* Journal of Veterinary Medical Science, 2005. **67**(1): p. 51-56.
57. Muzzarelli, R.A.A., *Chitins and chitosans for the repair of wounded skin, nerve, cartilage and bone.* Carbohydrate Polymers, 2009. **76**(2): p. 167-182.
58. Schulz, J.T., R.G. Tompkins, and J.F. Burke, *Artificial skin.* Annual Review of Medicine, 2000. **51**: p. 231-244.
59. Lim, H.J., et al., *Hybrid Scaffolds Composed of Chitosan-PLGA-PEO Nanofibers and PLGA Microfibers for Artificial Skin.* Tissue Engineering and Regenerative Medicine, 2011. **8**(4): p. 108-115.
60. Guo, R., et al., *The healing of full-thickness burns treated by using plasmid DNA encoding VEGF-165 activated collagen-chitosan dermal equivalents.* Biomaterials, 2011. **32**(4): p. 1019-1031.
61. Ding, Z., et al., *Immobilization of chitosan onto poly-L-lactic acid film surface by plasma graft polymerization to control the morphology of fibroblast and liver cells.* Biomaterials, 2004. **25**(6): p. 1059-1067.
62. Zhu, X., et al., *Effect of argon-plasma treatment on proliferation of human-skin-derived fibroblast on chitosan membrane in vitro.* Journal of Biomedical Materials Research Part A, 2005. **73A**(3): p. 264-274.
63. Wu, Y.N., et al., *Cartilaginous ECM component-modification of the micro-bead culture system for chondrogenic differentiation of mesenchymal stem cells.* Biomaterials, 2007. **28**(28): p. 4056-4067.
64. Abarrategi, A., et al., *Chitosan scaffolds for osteochondral tissue regeneration.* Journal of Biomedical Materials Research Part A, 2010. **95A**(4): p. 1132-1141.
65. Hoemann, C.D., et al., *Tissue engineering of cartilage using an injectable and adhesive chitosan-based cell-delivery vehicle.* Osteoarthritis and Cartilage, 2005. **13**(4): p. 318-329.
66. Guo, T., et al., *Porous chitosan-gelatin scaffold containing plasmid DNA encoding transforming growth factor-beta 1 for chondrocytes proliferation.* Biomaterials, 2006. **27**(7): p. 1095-1103.
67. Tan, H.P., et al., *Gelatin/chitosan/hyaluronan scaffold integrated with PLGA microspheres for cartilage tissue engineering.* Acta Biomaterialia, 2009. **5**(1): p. 328-337.
68. Tan, H.P., et al., *Gelatin/chitosan/hyaluronan ternary complex scaffold containing basic fibroblast growth factor for cartilage tissue engineering.* Journal of Materials Science-Materials in Medicine, 2007. **18**(10): p. 1961-1968.
69. Tigli, R.S., et al., *In Vitro Release of Dexamethasone or bFGF from Chitosan/Hydroxyapatite Scaffolds.* Journal of Biomaterials Science-Polymer Edition, 2009. **20**(13): p. 1899-1914.
70. Deschaseaux, F., L. Sensebe, and D. Heymann, *Mechanisms of bone repair and regeneration.* Trends in Molecular Medicine, 2009. **15**(9): p. 417-429.
71. Budiraharjo, R., K.G. Neoh, and E.T. Kang, *Hydroxyapatite-coated carboxymethyl chitosan scaffolds for promoting osteoblast and stem cell differentiation.* Journal of Colloid and Interface Science, 2012. **366**(1): p. 224-232.

72. Jiao, H.S., et al., *Chitosan/polyglycolic acid nerve grafts for axon regeneration from prolonged axotomized neurons to chronically denervated segments.* Biomaterials, 2009. **30**(28): p. 5004-5018.
73. Huang, J.H., et al., *Electrical regulation of Schwann cells using conductive polypyrrole/chitosan polymers.* Journal of Biomedical Materials Research Part A, 2010. **93A**(1): p. 164-174.
74. Wang, W., et al., *Enhanced nerve regeneration through a bilayered chitosan tube: The effect of introduction of glycine spacer into the CYIGSK sequence.* Journal of Biomedical Materials Research Part A, 2008. **85A**(4): p. 919-928.
75. Patel, M., et al., *GDNF blended chitosan nerve guides: An in vivo study.* Journal of Biomedical Materials Research Part A, 2009. **90A**(1): p. 154-165.
76. Yang, Y.M., et al., *Nerve conduits based on immobilization of nerve growth factor onto modified chitosan by using genipin as a crosslinking agent.* European Journal of Pharmaceutics and Biopharmaceutics, 2011. **79**(3): p. 519-525.
77. Amado, S., et al., *Use of hybrid chitosan membranes and N1E-115 cells for promoting nerve regeneration in an axonotmesis rat model.* Biomaterials, 2008. **29**(33): p. 4409-4419.
78. Seo, S.J., et al., *Alginate/galactosylated chitosan/heparin scaffold as a new synthetic extracellular matrix for hepatocytes.* Tissue Engineering, 2006. **12**(1): p. 33-44.
79. Seo, S.J., et al., *Enhanced liver functions of hepatocytes cocultured with NIH 3T3 in the alginate/galactosylated chitosan scaffold.* Biomaterials, 2006. **27**(8): p. 1487-1495.
80. Bian, Y.Z., et al., *Evaluation of poly(3-hydroxybutyrate-co-3-hydroxyhexanoate) conduits for peripheral nerve regeneration.* Biomaterials, 2009. **30**(2): p. 217-225.
81. Zheng, Z.H., et al., *In vitro biocompatibility of three chitosan/polycation composite materials for nerve regeneration.* Neural Regeneration Research, 2008. **3**(8): p. 837-842.
82. Zhu, N., et al., *Effects of laminin blended with chitosan on axon guidance on patterned substrates.* Biofabrication, 2011. **2**(4): p. 8.
83. Fang, P., et al., *Survival and Differentiation of Neuroepithelial Stem Cells on Chitosan Bicomponent Fibers.* Chinese Journal of Physiology, 2010. **53**(4): p. 208-214.
84. Rickett, T.A., et al., *Rapidly Photo-Cross-Linkable Chitosan Hydrogel for Peripheral Neurosurgeries.* Biomacromolecules, 2011. **12**(1): p. 57-65.
85. Wang, G., et al., *Preparation of cross-linked carboxymethyl chitosan for repairing sciatic nerve injury in rats.* Biotechnology Letters, 2010. **32**(1): p. 59-66.
86. Wan, Y., et al., *Biodegradability of conducting chitosan-g-polycaprolactone/polypyrrole conduits.* Polymer Degradation and Stability, 2010. **95**(10): p. 1994-2002.
87. Murakami, K., et al., *Hydrogel blends of chitin/chitosan, fucoidan and alginate as healing-impaired wound dressings.* Biomaterials, 2010. **31**(1): p. 83-90.
88. Kweon, D.K., S.B. Song, and Y.Y. Park, *Preparation of water-soluble chitosan/heparin complex and its application as wound healing accelerator.* Biomaterials, 2003. **24**(9): p. 1595-1601.
89. Ho, Y.C., et al., *Heparin-functionalized chitosan-alginate scaffolds for controlled release of growth factor.* International Journal of Pharmaceutics, 2009. **376**(1-2): p. 69-75.
90. Lahiji, A., et al., *Chitosan supports the expression of extracellular matrix proteins in human osteoblasts and chondrocytes.* Journal of Biomedical Materials Research, 2000. **51**(4): p. 586-595.
91. Martin-Lopez, E., et al., *Chitosan, Gelatin and Poly(L-Lysine) Polyelectrolyte-Based Scaffolds and Films for Neural Tissue Engineering.* Journal of Biomaterials Science-Polymer Edition, 2012. **23**(1-4): p. 207-232.
92. Chen, X., et al., *Bone marrow stromal cells-loaded chitosan conduits promote repair of complete transection injury in rat spinal cord.* Journal of Materials Science-Materials in Medicine, 2011. **22**(10): p. 2347-2356.

93. Wang, L.M. and J.P. Stegemann, *Thermogelling chitosan and collagen composite hydrogels initiated with beta-glycerophosphate for bone tissue engineering.* Biomaterials, 2010. **31**(14): p. 3976-3985.
94. Moreau, J.L. and H.H.K. Xu, *Mesenchymal stem cell proliferation and differentiation on an injectable calcium phosphate - Chitosan composite scaffold.* Biomaterials, 2009. **30**(14): p. 2675-2682.
95. Oliveira, J.T., et al., *Assessment of the Suitability of Chitosan/PolyButylene Succinate Scaffolds Seeded with Mouse Mesenchymal Progenitor Cells for a Cartilage Tissue Engineering Approach.* Tissue Engineering Part A, 2008. **14**(10): p. 1651-1661.
96. Fukuda, J., et al., *Micromolding of photocrosslinkable chitosan hydrogel for spheroid microarray and co-cultures.* Biomaterials, 2006. **27**(30): p. 5259-5267.
97. Mi, F.L., et al., *Fabrication and characterization of a sponge-like asymmetric chitosan membrane as a wound dressing.* Biomaterials, 2001. **22**(2): p. 165-173.
98. Ishihara, M., et al., *Photocrosslinkable chitosan as a dressing for wound occlusion and accelerator in healing process.* Biomaterials, 2002. **23**(3): p. 833-840.
99. Funakoshi, T., et al., *Novel chitosan-based hyaluronan hybrid polymer fibers as a scaffold in ligament tissue engineering.* Journal of Biomedical Materials Research Part A, 2005. **74A**(3): p. 338-346.
100. Zhang, Y.F., et al., *Novel chitosan/collagen scaffold containing transforming growth factor-beta 1 DNA for periodontal tissue engineering.* Biochemical and Biophysical Research Communications, 2006. **344**(1): p. 362-369.
101. Lee, K.Y. and D.J. Mooney, *Alginate: Properties and biomedical applications.* Progress in Polymer Science (Oxford), 2012. **37**(1): p. 106-126.
102. Rowley, J.A., G. Madlambayan, and D.J. Mooney, *Alginate hydrogels as synthetic extracellular matrix materials.* Biomaterials, 1999. **20**(1): p. 45-53.
103. Alsberg, E., et al., *Cell-interactive alginate hydrogels for bone tissue engineering.* Journal of Dental Research, 2001. **80**(11): p. 2025-2029.
104. Dhoot, N.O., et al., *Peptide-modified alginate surfaces as a growth permissive substrate for neurite outgrowth.* Journal of Biomedical Materials Research - Part A, 2004. **71**(2): p. 191-200.
105. Chueh, B.H., et al., *Patterning alginate hydrogels using light-directed release of caged calcium in a microfluidic device.* Biomedical Microdevices, 2010. **12**(1): p. 145-151.
106. Ghosh, K., et al., *Cell adaptation to a physiologically relevant ECM mimic with different viscoelastic properties.* Biomaterials, 2007. **28**(4): p. 671-679.
107. Erickson, I.E., et al., *Differential Maturation and Structure-Function Relationships in Mesenchymal Stem Cell- and Chondrocyte-Seeded Hydrogels.* Tissue Engineering Part A, 2009. **15**(5): p. 1041-1052.
108. Chung, C. and J.A. Burdick, *Influence of Three-Dimensional Hyaluronic Acid Microenvironments on Mesenchymal Stem Cell Chondrogenesis.* Tissue Engineering Part A, 2009. **15**(2): p. 243-254.
109. Gerecht, S., et al., *Hyaluronic acid hydrogen for controlled self-renewal and differentiation of human embryonic stem cells.* Proceedings of the National Academy of Sciences of the United States of America, 2007. **104**(27): p. 11298-11303.
110. Khetan, S. and J.A. Burdick, *Patterning hydrogels in three dimensions towards controlling cellular interactions.* Soft Matter, 2011. **7**(3): p. 830-838.
111. Khetan, S. and J.A. Burdick, *Patterning network structure to spatially control cellular remodeling and stem cell fate within 3-dimensional hydrogels.* Biomaterials, 2010. **31**(32): p. 8228-8234.
112. Kuijpers, A.J., et al., *Cross-linking and characterisation of gelatin matrices for biomedical applications.* Journal of Biomaterials Science-Polymer Edition, 2000. **11**(3): p. 225-243.

113. Chiono, V., et al., *Genipin-crosslinked chitosan/gelatin blends for biomedical applications.* Journal of Materials Science-Materials in Medicine, 2008. **19**(2): p. 889-898.
114. Guarino, V., et al., *hMSC interaction with PCL and PCL/gelatin platforms: A comparative study on films and electrospun membranes.* Journal of Bioactive and Compatible Polymers, 2011. **26**(2): p. 144-160.
115. Fazel-Rezai, R., ed. *Biomedical Engineering - From Theory to Applications*. 2011, InTech: Rijeka. 411-412.
116. Nuzzo, R.G. and D.L. Allara, *ADSORPTION OF BIFUNCTIONAL ORGANIC DISULFIDES ON GOLD SURFACES.* Journal of the American Chemical Society, 1983. **105**(13): p. 4481-4483.
117. Dubois, L.H., B.R. Zegarski, and R.G. Nuzzo, *MOLECULAR ORDERING OF ORGANOSULFUR COMPOUNDS ON AU(111) AND AU(100) - ADSORPTION FROM SOLUTION AND IN ULTRAHIGH-VACUUM.* Journal of Chemical Physics, 1993. **98**(1): p. 678-688.
118. Bain, C.D., et al., *FORMATION OF MONOLAYER FILMS BY THE SPONTANEOUS ASSEMBLY OF ORGANIC THIOLS FROM SOLUTION ONTO GOLD.* Journal of the American Chemical Society, 1989. **111**(1): p. 321-335.
119. Ulman, A., *Formation and structure of self-assembled monolayers.* Chemical Reviews, 1996. **96**(4): p. 1533-1554.
120. Sellers, H., et al., *STRUCTURE AND BINDING OF ALKANETHIOLATES ON GOLD AND SILVER SURFACES - IMPLICATIONS FOR SELF-ASSEMBLED MONOLAYERS.* Journal of the American Chemical Society, 1993. **115**(21): p. 9389-9401.
121. Senaratne, W., L. Andruzzi, and C.K. Ober, *Self-assembled monolayers and polymer brushes in biotechnology: Current applications and future perspectives*. Biomacromolecules, 2005. **6**(5): p. 2427-2448.
122. Schwartz, D.K., *Mechanisms and kinetics of self-assembled monolayer formation.* Annual Review of Physical Chemistry, 2001. **52**: p. 107-137.
123. Kang, J. and P.A. Rowntree, *Gold film surface preparation for self-assembled monolayer studies.* Langmuir, 2007. **23**(2): p. 509-516.
124. Strong, L. and G.M. Whitesides, *STRUCTURES OF SELF-ASSEMBLED MONOLAYER FILMS OF ORGANOSULFUR COMPOUNDS ADSORBED ON GOLD SINGLE-CRYSTALS - ELECTRON-DIFFRACTION STUDIES.* Langmuir, 1988. **4**(3): p. 546-558.
125. Love, J.C., et al., *Self-assembled monolayers of thiolates on metals as a form of nanotechnology.* Chemical Reviews, 2005. **105**(4): p. 1103-1169.
126. Collard, D.M. and M.A. Fox, *USE OF ELECTROACTIVE THIOLS TO STUDY THE FORMATION AND EXCHANGE OF ALKANETHIOL MONOLAYERS ON GOLD.* Langmuir, 1991. **7**(6): p. 1192-1197.
127. Liedberg, B. and P. Tengvall, *MOLECULAR GRADIENTS OF OMEGA-SUBSTITUTED ALKANETHIOLS ON GOLD - PREPARATION AND CHARACTERIZATION.* Langmuir, 1995. **11**(10): p. 3821-3827.
128. Ulman, A., et al., *MIXED ALKANETHIOL MONOLAYERS ON GOLD SURFACES - WETTING AND STABILITY STUDIES.* Advances in Colloid and Interface Science, 1992. **39**: p. 175-224.
129. Delamarche, E., et al., *Golden interfaces: The surface of self-assembled monolayers.* Advanced Materials, 1996. **8**(9): p. 719-&.
130. Gooding, J.J., et al., *Self-assembled monolayers into the 21(st) century: Recent advances and applications.* Electroanalysis, 2003. **15**(2): p. 81-96.
131. Chaki, N.K. and K. Vijayamohanan, *Self-assembled monolayers as a tunable platform for biosensor applications.* Biosensors & Bioelectronics, 2002. **17**(1-2): p. 1-12.

132. Luk, Y.Y., M. Kato, and M. Mrksich, *Self-assembled monolayers of alkanethiolates presenting mannitol groups are inert to protein adsorption and cell attachment.* Langmuir, 2000. **16**(24): p. 9604-9608.
133. Arnold, S., et al., *Investigation of the electrode reaction of cytochrome c through mixed self-assembled monolayers of alkanethiols on gold(111) surfaces.* Journal of Electroanalytical Chemistry, 1997. **438**(1-2): p. 91-97.
134. Bunjes, N., et al., *Thiopeptide-supported lipid layers on solid substrates.* Langmuir, 1997. **13**(23): p. 6188-6194.
135. Lan, M.A., et al., *Myoblast proliferation and differentiation on fibronectin-coated self assembled monolayers presenting different surface chemistries.* Biomaterials, 2005. **26**(22): p. 4523-4531.
136. Mrksich, M., et al., *Controlling cell attachment on contoured surfaces with self-assembled monolayers of alkanethiolates on gold.* Proceedings of the National Academy of Sciences of the United States of America, 1996. **93**(20): p. 10775-10778.
137. Scotchford, C.A., et al., *Growth of human osteoblast-like cells on alkanethiol on gold self-assembled monolayers: The effect of surface chemistry.* Journal of Biomedical Materials Research, 1998. **41**(3): p. 431-442.
138. Herbert, C.B., et al., *Micropatterning gradients and controlling surface densities of photoactivatable biomolecules on self-assembled monolayers of oligo(ethylene glycol) alkanethiolates.* Chemistry & Biology, 1997. **4**(10): p. 731-737.
139. Houseman, B.T., et al., *Peptide chips for the quantitative evaluation of protein kinase activity.* Nature Biotechnology, 2002. **20**(3): p. 270-274.
140. Feng, Y.Z. and M. Mrksich, *The synergy peptide PHSRN and the adhesion peptide RGD mediate cell adhesion through a common mechanism.* Biochemistry, 2004. **43**(50): p. 15811-15821.
141. Ryan, D., et al., *Patterning multiple aligned self-assembled monolayers using light.* Langmuir, 2004. **20**(21): p. 9080-9088.
142. Dillmore, W.S., M.N. Yousaf, and M. Mrksich, *A photochemical method for patterning the immobilization of ligands and cells to self-assembled monolayers.* Langmuir, 2004. **20**(17): p. 7223-7231.
143. Nishino, T., S. Kanata, and C. Hirata, *Immobilization of Carbon Nanotubes on Au(111) via Self-assembled Monolayers.* Chemistry Letters, 2011. **40**(11): p. 1217-1219.
144. Bruckbauer, A., et al., *An addressable antibody nanoarray produced on a nanostructured surface.* Journal of the American Chemical Society, 2004. **126**(21): p. 6508-6509.
145. Ma, H.W., et al., *"Non-fouling" oligo(ethylene glycol)-functionalized polymer brushes synthesized by surface-initiated atom transfer radical polymerization.* Advanced Materials, 2004. **16**(4): p. 338-+.
146. Parreira, P., et al., *Effect of surface chemistry on bacterial adhesion, viability, and morphology.* Journal of Biomedical Materials Research Part A, 2011. **99A**(3): p. 344-353.
147. Lobbicke, R., et al., *Polymer Brush Controlled Bioinspired Calcium Phosphate Mineralization and Bone Cell Growth.* Biomacromolecules, 2011. **12**(10): p. 3753-3760.
148. Choi, I., et al., *On-Demand Electrochemical Activation of the Click Reaction on Self-Assembled Monolayers on Gold Presenting Masked Acetylene Groups.* Journal of the American Chemical Society, 2011. **133**(42): p. 16718-16721.
149. Yoon, S.H. and M.R.K. Mofrad, *Cell adhesion and detachment on gold surfaces modified with a thiol-functionalized RGD peptide.* Biomaterials, 2011. **32**(30): p. 7286-7296.
150. Wang, X., H. Gan, and T.L. Sun, *Chiral Design for Polymeric Biointerface: The Influence of Surface Chirality on Protein Adsorption.* Advanced Functional Materials, 2011. **21**(17): p. 3276-3281.

151. Luo, W. and M.N. Yousaf, *Developing a self-assembled monolayer microarray to study stem cell differentiation.* Journal of Colloid and Interface Science, 2011. **360**(2): p. 325-330.
152. Staii, C., et al., *Distance Dependence of Neuronal Growth on Nanopatterned Gold Surfaces.* Langmuir, 2011. **27**(1): p. 233-239.
153. Henry, O.Y.F., J.L.A. Sanchez, and C.K. O'Sullivan, *Bipodal PEGylated alkanethiol for the enhanced electrochemical detection of genetic markers involved in breast cancer.* Biosensors & Bioelectronics, 2010. **26**(4): p. 1500-1506.
154. Mrksich, M., et al., *Using microcontact printing to pattern the attachment of mammalian cells to self-assembled monolayers of alkanethiolates on transparent films of gold and silver.* Experimental Cell Research, 1997. **235**(2): p. 305-313.
155. Faucheux, N., et al., *Self-assembled monolayers with different terminating groups as model substrates for cell adhesion studies.* Biomaterials, 2004. **25**(14): p. 2721-2730.
156. Dulcey, C.S., et al., *DEEP UV PHOTOCHEMISTRY OF CHEMISORBED MONOLAYERS - PATTERNED COPLANAR MOLECULAR ASSEMBLIES.* Science, 1991. **252**(5005): p. 551-554.
157. Kira, A., et al., *Micropatterning of perfluoroalkyl self-assembled monolayers for arraying proteins and cells on chips.* Applied Surface Science, 2009. **255**(17): p. 7647-7651.
158. Das, M., et al., *Embryonic motoneuron-skeletal muscle co-culture in a defined system.* Neuroscience, 2007. **146**(2): p. 481-488.
159. Yamamoto, H., et al., *In-situ guidance of individual neuronal processes by wet femtosecond-laser processing of self-assembled monolayers.* Applied Physics Letters, 2011. **99**(16): p. 3.
160. Whitesides, G.M., et al., *Soft lithography in biology and biochemistry.* Annual Review of Biomedical Engineering, 2001. **3**: p. 335-373.
161. Falconnet, D., et al., *Surface engineering approaches to micropattern surfaces for cell-based assays.* Biomaterials, 2006. **27**(16): p. 3044-3063.
162. Csucs, G., et al., *Microcontact printing of novel co-polymers in combination with proteins for cell-biological applications.* Biomaterials, 2003. **24**(10): p. 1713-1720.
163. Kane, R.S., et al., *Patterning proteins and cells using soft lithography.* Biomaterials, 1999. **20**(23-24): p. 2363-2376.
164. Altomare, L., et al., *Microcontact printing of fibronectin on a biodegradable polymeric surface for skeletal muscle cell orientation.* International Journal of Artificial Organs, 2010. **33**(8): p. 535-543.
165. Lauer, L., C. Klein, and A. Offenhausser, *Spot compliant neuronal networks by structure optimized micro-contact printing.* Biomaterials, 2001. **22**(13): p. 1925-1932.
166. St John, P.M., et al., *Diffraction-based cell detection using a microcontact printed antibody grating.* Analytical Chemistry, 1998. **70**(6): p. 1108-1111.
167. Chen, C.S., et al., *Geometric control of cell life and death.* Science, 1997. **276**(5317): p. 1425-1428.
168. Rozkiewicz, D.I., et al., *Covalent microcontact printing of proteins for cell patterning.* Chemistry-a European Journal, 2006. **12**(24): p. 6290-6297.
169. Bernard, A., et al., *Microcontact printing of proteins.* Advanced Materials, 2000. **12**(14): p. 1067-1070.
170. Revzin, A., R.G. Tompkins, and M. Toner, *Surface engineering with poly(ethylene glycol) photolithography to create high-density cell arrays on glass.* Langmuir, 2003. **19**(23): p. 9855-9862.
171. Albrecht, D.R., et al., *Photo- and electropatterning of hydrogel-encapsulated living cell arrays.* Lab on a Chip, 2005. **5**(1): p. 111-118.
172. Fan, Y.W., et al., *Culture of neural cells on silicon wafers with nano-scale surface topograph.* Journal of Neuroscience Methods, 2002. **120**(1): p. 17-23.

173. Dorman, G. and G.D. Prestwich, *Using photolabile ligands in drug discovery and development.* Trends in Biotechnology, 2000. **18**(2): p. 64-77.
174. Shi, H.B., M. Uttamchandani, and S.Q. Yao, *Applying Small Molecule Microarrays and Resulting Affinity Probe Cocktails for Proteome Profiling of Mammalian Cell Lysates.* Chemistry-an Asian Journal, 2011. **6**(10): p. 2803-2815.
175. Sun, L., et al., *Diversity Oriented Design of Various Benzophenone Derivatives and Their in Vitro Antifungal and Antibacterial Activities.* Molecules, 2011. **16**(11): p. 9739-9754.
176. Fink, J., et al., *Comparative study and improvement of current cell micro-patterning techniques.* Lab on a Chip, 2007. **7**(6): p. 672-680.
177. Ruiz, L., et al., *Phosphorylcholine-containing polyurethanes for the control of protein adsorption and cell attachment via photoimmobilized laminin oligopeptides.* Journal of Biomaterials Science-Polymer Edition, 1999. **10**(9): p. 931-955.
178. Besson, E., et al., *A novel and simplified procedure for patterning hydrophobic and hydrophilic SAMs for microfluidic devices by using UV photolithography.* Langmuir, 2006. **22**(20): p. 8346-8352.
179. Bhat, V.T., N.R. James, and A. Jayakrishnan, *A photochemical method for immobilization of azidated dextran onto aminated poly(ethylene terephthalate) surfaces.* Polymer International, 2008. **57**(1): p. 124-132.
180. Dorman, G., *Photoaffinity labeling in biological signal transduction.* Bioorganic Chemistry of Biological Signal Transduction, 2001. **211**: p. 169-225.
181. Baruah, H., et al., *An engineered aryl azide ligase for site-specific mapping of protein-protein interactions through photo-cross-linking.* Angewandte Chemie-International Edition, 2008. **47**(37): p. 7018-7021.
182. Geselowitz, D.A. and R.D. Neumann, *QUANTITATION OF TRIPLE-HELIX FORMATION USING A PHOTO-CROSS-LINKABLE ARYL AZIDE BIOTIN OLIGONUCLEOTIDE CONJUGATE.* Bioconjugate Chemistry, 1995. **6**(4): p. 502-506.
183. Tanaka, Y. and J.J. Kohler, *Photoactivatable Crosslinking sugars for capturing glycoprotein interactions.* Journal of the American Chemical Society, 2008. **130**(11): p. 3278-+.
184. Tippmann, E.M., et al., *A genetically encoded diazirine photocrosslinker in Escherichia coli.* Chembiochem, 2007. **8**(18): p. 2210-2214.
185. Dankbar, D.M. and G. Gauglitz, *A study on photolinkers used for biomolecule attachment to polymer surfaces.* Analytical and Bioanalytical Chemistry, 2006. **386**(7-8): p. 1967-1974.
186. Shigdel, U.K., J.L. Zhang, and C. He, *Diazirine-based DNA photo-cross-linking probes for the study of protein-DNA interactions.* Angewandte Chemie-International Edition, 2008. **47**(1): p. 90-93.
187. Seo, T.S., et al., *Photocleavable fluorescent nucleotides for DNA sequencing on a chip constructed by site-specific coupling chemistry.* Proceedings of the National Academy of Sciences of the United States of America, 2004. **101**(15): p. 5488-5493.
188. Kim, M.S. and S.L. Diamond, *Photocleavage of o-nitrobenzyl ether derivatives for rapid biomedical release applications.* Bioorganic & Medicinal Chemistry Letters, 2006. **16**(15): p. 4007-4010.
189. Chen, S.Y. and L.M. Smith, *Photopatterned Thiol Surfaces for Biomolecule Immobilization.* Langmuir, 2009. **25**(20): p. 12275-12282.
190. Nakayama, H., et al., *Silane coupling agent bearing a photoremovable succinimidyl carbonate for patterning amines on glass and silicon surfaces with controlled surface densities.* Colloids and Surfaces B-Biointerfaces, 2010. **76**(1): p. 88-97.
191. Han, X.J., et al., *Supported bilayer lipid membrane arrays on photopatterned self-assembled monolavers.* Chemistry-a European Journal, 2007. **13**(28): p. 7957-7964.

192. Shin, G.J., et al., *Svnthesis and micropatterning properties of a novel base-soluble, positive-working, photosensitive polyirnide having an o-nitrobenzyl ether group.* Journal of Polymer Science Part a-Polymer Chemistry, 2007. **45**(5): p. 776-788.
193. Willems, K.J.M.a.J.M., ed. *Photochemistry: UV/VIS Spectroscopy, Photochemical Reactions and Photosynthesis*. Chemical Engineering Methods and Technology. 2011, Nova Science Publishers. 175-202.
194. Lim, M. and K.J. Rothschild, *Photocleavage-based affinity purification and printing of cell-free expressed proteins: Application to proteome microarrays.* Analytical Biochemistry, 2008. **383**(1): p. 103-115.
195. Nakanishi, J., et al., *Spatiotemporal control of cell adhesion on a self-assembled monolayer having a photocleavable protecting group.* Analytica Chimica Acta, 2006. **578**(1): p. 100-104.
196. Afroz, F., et al., *Photo-removable protecting groups for in situ DNA microarray synthesis.* Clinical Chemistry, 2004. **50**(10): p. 1936-1939.
197. Furuta, T., et al., *Phototriggers for nucleobases with improved photochemical properties.* Organic Letters, 2007. **9**(23): p. 4717-4720.
198. Chee, M., et al., *Accessing genetic information with high-density DNA arrays.* Science, 1996. **274**(5287): p. 610-614.
199. Mrksich, M., *Using self-assembled monolayers to model the extracellular matrix.* Acta Biomaterialia, 2009. **5**(3): p. 832-841.
200. Pelliccioli, A.P. and J. Wirz, *Photoremovable protecting groups: reaction mechanisms and applications.* Photochemical & Photobiological Sciences, 2002. **1**(7): p. 441-458.
201. Sundberg, S.A., et al., *SPATIALLY-ADDRESSABLE IMMOBILIZATION OF MACROMOLECULES ON SOLID SUPPORTS.* Journal of the American Chemical Society, 1995. **117**(49): p. 12050-12057.
202. Alonso, J.M., et al., *Photopatterned surfaces for site-specific and functional immobilization of proteins.* Langmuir, 2008. **24**(2): p. 448-457.
203. Lee, K.N., et al., *Photochemical selective surface modification using micromirror array for biochip fabrication*, in *Micromachining and Microfabrication Process Technology Vii*, J.M. Karam and J. Yasaitis, Editors. 2001. p. 352-359.
204. Grunwald, C., et al., *In situ assembly of macromolecular complexes triggered by light.* Proceedings of the National Academy of Sciences of the United States of America. **107**(14): p. 6146-6151.
205. Mancini, R.J., et al., *Synthesis of a photo-caged aminooxy alkane thiol.* Org Biomol Chem, 2009. **7**(23): p. 4954-9.
206. Veiseh, M., M.H. Zareie, and M.Q. Zhang, *Highly selective protein patterning on gold-silicon substrates for biosensor applications.* Langmuir, 2002. **18**(17): p. 6671-6678.
207. Banala, S., A. Arnold, and K. Johnsson, *Caged substrates for protein labeling and immobilization.* Chembiochem, 2008. **9**(1): p. 38-41.
208. Nakagawa, M. and K. Ichimura, *Photopatterning of self-assembled monolayers to generate aniline moieties.* Colloids and Surfaces a-Physicochemical and Engineering Aspects, 2002. **204**(1-3): p. 1-7.
209. Ito, Y., et al., *Photo-reactive polyvinylalcohol for photo-immobilized microarray.* Biomaterials, 2005. **26**(2): p. 211-216.
210. Park, S. and M.N. Yousaf, *An interfacial oxime reaction to immobilize ligands and cells in patterns and gradients to photoactive surfaces.* Langmuir, 2008. **24**(12): p. 6201-6207.
211. Brown, A.A., O. Azzaroni, and W.T.S. Huck, *Photoresponsive Polymer Brushes for Hydrophilic Patterning.* Langmuir, 2009. **25**(3): p. 1744-1749.
212. Woodcock, J.W., et al., *Dually responsive aqueous gels from thermo- and light-sensitive hydrophilic ABA triblock copolymers.* Soft Matter, 2010. **6**(14): p. 3325-3336.

213. Ramanan, V.V., et al., *Photocleavable side groups to spatially alter hydrogel properties and cellular interactions.* Journal of Materials Chemistry, 2010. **20**(40): p. 8920-8926.
214. Katz, J.S. and J.A. Burdick, *Light-Responsive Biomaterials: Development and Applications.* Macromolecular Bioscience, 2010. **10**(4): p. 339-348.
215. Luo, Y. and M.S. Shoichet, *Light-activated immobilization of biomolecules to agarose hydrogels for controlled cellular response.* Biomacromolecules, 2004. **5**(6): p. 2315-2323.
216. Wylie, R.G. and M.S. Shoichet, *Two-photon micropatterning of amines within an agarose hydrogel.* Journal of Materials Chemistry, 2008. **18**(23): p. 2716-2721.
217. Wylie, R.G., et al., *Spatially controlled simultaneous patterning of multiple growth factors in three-dimensional hydrogels.* Nature Materials, 2011. **10**(10): p. 799-806.
218. Wylie, R.G. and M.S. Shoichet, *Three-Dimensional Spatial Patterning of Proteins in Hydrogels.* Biomacromolecules, 2011. **12**(10): p. 3789-3796.
219. Kloxin, A.M., et al., *Photodegradable Hydrogels for Dynamic Tuning of Physical and Chemical Properties.* Science, 2009. **324**(5923): p. 59-63.
220. DeForest, C.A. and K.S. Anseth, *Cytocompatible click-based hydrogels with dynamically tunable properties through orthogonal photoconjugation and photocleavage reactions.* Nature Chemistry, 2011. **3**(12): p. 925-931.

Chapter 3 Photoactive SAM Surface for Control of Cell Attachment

Nan Cheng and Xudong Cao

Journal of Colloid and Interface Science

2010, 348(1), 71-79

3.1 Abstract

A new approach to control cell attachment using photochemistry and self-assembled monolayers (SAMs) has been developed. Poly(ethylene glycol) (PEG) was introduced onto a gold SAM surface to initially create a cell repulsive surface via a photo-cleavable o-nitrobenzyl functional group. This cell repulsive surface was subsequently rendered cell adhesive by exposure to UV-irradiation which cleaved the photoactive o-nitrobenzyl group, followed by immobilization of cell adhesive peptides to the irradiated regions. Water contact angle measurements, atomic force microscopy (AFM) and X-ray photoelectron spectroscopy (XPS) were used to confirm the photoreactions and to characterize surface properties. To study cell attachment on the prepared surfaces, NIH/3T3 fibroblast cells were used. The cell culture results demonstrated that PEG covered SAMs had the ability to repel cells and that the surface became cell-adhesive after UV irradiation to cleave cell non-adhesive PEG from the exposed surface via photo-labile o-nitrobenzyl groups, followed by immobilization of cell adhesive RGD peptides. In this study, we show that cell attachment can be controlled on photocleavable PEG-gold SAMs by UV exposure. We also show that the resulting surface is effective to control cell attachment for up to 5 days in culture.

3.2 Introduction

To understand the effect of the extracellular microenvironment on cell behavior is a fundamentally important topic in cell biology because it benefits the development of many other research areas in biology and biotechnology, including screening of drug candidate libraries, regenerative medicine, biosensors, and fundamental investigations into cell-cell interactions and communications [1]. To this end, control of cell attachment on substrate materials is a preliminary step of crucial importance [2, 3]. It uses not only mechanical interactions [4-6], but also chemical signals, such as the interactions of cell surface receptors with their specific cell adhesive molecules in the extracellular matrix (ECM) to regulate cell adhesion. To date, surface patterning is routinely used to immobilize proteins in order to pattern cells for cell behavior studies; in fact many studies have presented successful strategies to control the position of cell attachment on different surfaces. These methods include photolithography, micro-contact printing (μCP), microfluidics and photochemistry [3, 7]. However, among these methods, photochemistry method is perhaps the most promising technique to study biological systems as other methods suffer, to various degrees, drawbacks when applied to biological systems. For example, photolithography requires expensive equipment and clean rooms for manufacturing, which are often not available to an average biology laboratory. Furthermore, the use of harsh solvents in the process can hinder the use of biomolecules which are often easily denatured [8]. In comparison, the primary advantage of using photochemistry is that it can provide both spatial and temporal control over cleavage of photo-labile molecules or biologically active molecules [9, 10]. O-nitrobenzyl derivatives are the most commonly used and well studied photo-labile caging groups, and they can react with and protect (i.e. cage) many functional groups, such as amine [11], carboxyl [12], hydroxyl [13] and thiol [14] groups that can be subsequently released (i.e. uncage) for further reactions when exposed to UV light in a well controlled manner. In fact, o-nitrobenzyl derivatives have been reported to offer precise control of patterning sizes on the micro-scales and even nano-scale [11, 15]. While photo-cleavage of o-nitrobenzyl groups and subsequent immobilization of cell binding molecules have been well studied to control cell attachments by other researchers [15], the introduction of cell repulsive molecules such as PEG to reduce surface non-specific binding in combination with cell adhesive molecules to better define the

surface cell adhesive properties has not been reported. Here we present a method to create a surface which can control cell attachment using photochemistry and SAMs. The design of our surface is as follows: the basic substrate was a self-assembled monolayer of alkanethiols on gold. This alkanethiol SAM permitted the control of interfacial structures and properties, and presented well-defined surface properties based on alkanethiols, the terminal functional groups on the SAM surface. The resulting SAM surface was first modified with PEG to render it protein and cell resistant. By subsequently removing the cell repulsive PEG using photo activation followed by cell adhesive peptide immobilization, cell adhesive surfaces were created. This was achieved by using o-nitrobenzyl derivatives as photo-labile cages to protect the thiol functional groups that, upon photo-uncaging, reacted with the cell adhesive peptide, Arg-Gly-Asp (RGD). In this study, we report our preparation and characterization of the photoactive SAM surface. We show that a photoactive SAM surface can be used effectively to control cell adhesion.

3.3 Experimental

3.3.1 Materials

All chemicals were purchased from Sigma-Aldrich (St. Louis, MO) and used as received unless otherwise indicated. Deioinized distilled water was obtained from Milli-RO 10 Plus and Milli-Q UF Plus system (Bedford, MA) with a 18MΩ resistance.

3.3.2 Gold coated glass slide preparation

Gold coated glass slides prepared by thermo-evaporation method were purchased from the Arrandee™ Company, Germany. The slides were 11×11 mm in size with a 2.5 ± 1.5 nm thickness chromium underlayer and a 250 ± 50 nm gold coating as the upper layer. Immediately before use, the gold slide surfaces were cleaned, in sequence, by piranha solution (3:1 (v/v) of 98% H_2SO_4 and 30% H_2O_2, *caution: piranha solution is a very corrosive solution and appropriate safety precautions should be utilized, including the use of acid-resistant gloves and adequate shielding*), Milli-Q water, anhydrous ethanol

(Commercial Alcohols, Toronto, ON), and finally dried under clean nitrogen flow at room temperature.

3.3.3 Surface modification

Layer-by-layer surface modification on the gold slides was performed in sequence as describe below. The schematic of the surface modification is shown in Figure 1.

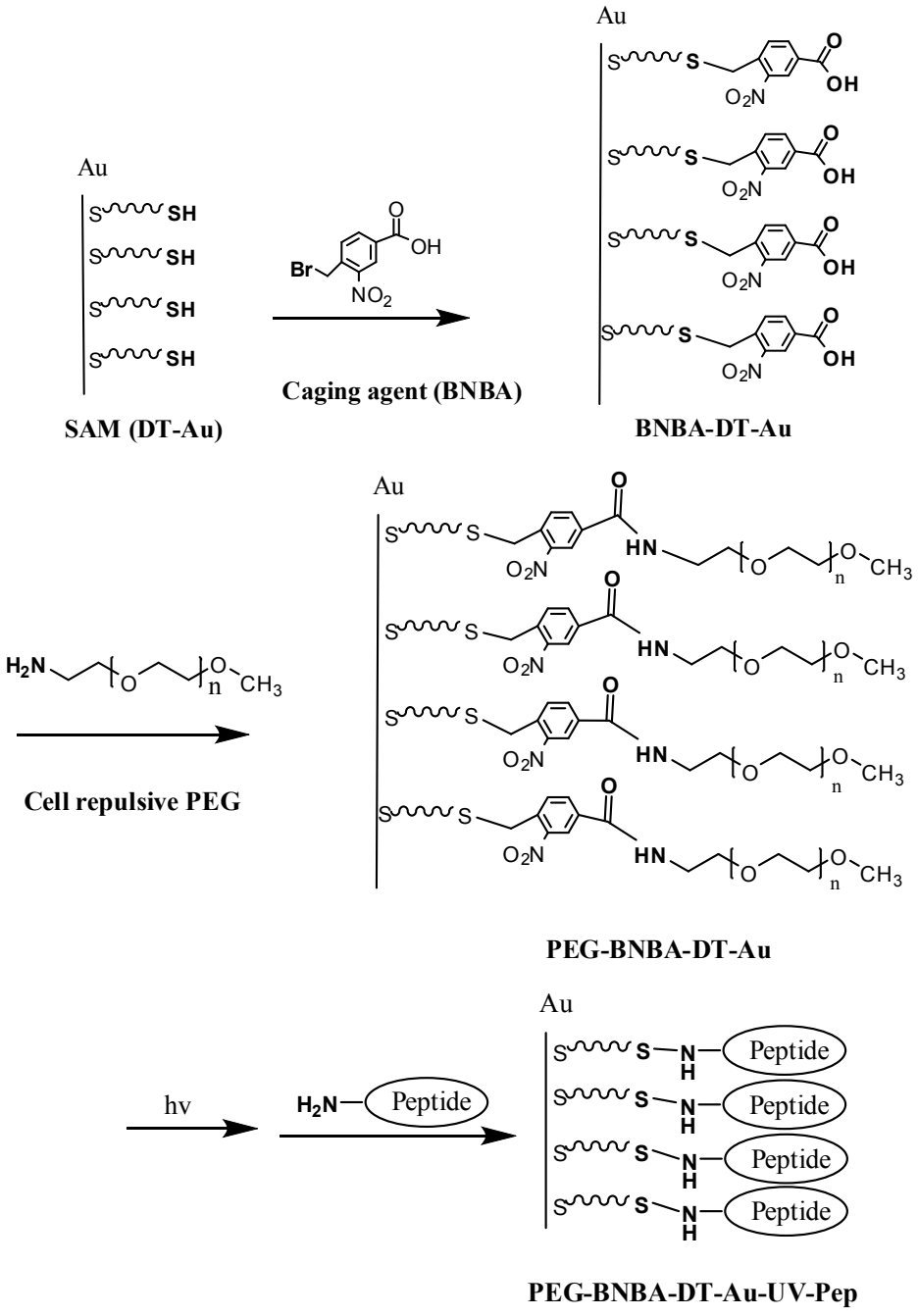

Figure 1 Schematic representation of PEG immobilization, photo activation and peptide immobilization

3.3.3.1 Preparation of 1,8-octanedithiol-gold SAM (DT-Au SAM)

To prepare the SAM layer, clean gold slides were immersed and kept in anhydrous ethanol with 1mM 1,8-octanedithiol (DT) at room temperature for 24 hours, extensively rinsed with both anhydrous ethanol and Milli-Q water, and then dried under clean nitrogen flow. The obtained SAM coated samples, referred to as DT-Au herein, were stored under anhydrous ethanol for future use. This step introduced thiol functional groups to the gold SAM surface.

3.3.3.2 Preparation of 4-bromomethyl-3-nitrobenzoic acid (BNBA)-DT-Au surface

The prepared DT-Au slides were immersed in 2mM BNBA ethanol solution for 24 hours to modify the surface with BNBA. The resulting surfaces were rinsed with anhydrous ethanol, and dried under clean nitrogen flow. The prepared samples were stored in anhydrous ethanol in the dark until needed. This step served to cage the thiol functional groups on the SAM surface using photo-labile BNBA. Due to the photo reactivity of the BNBA modified surface, care should be taken to store surfaces in the dark and handled under subdued light hereinafter.

3.3.3.3 Preparation of PEG-BNBA-DT-Au surface

The BNBA-DT-Au slides prepared in the previous step were submerged in a mixture of 5mM N-hydroxysuccinimide (NHS) (Pierce, Rockford, IL) and 5 mM 1-ethyl-3-(3-dimethylaminopropyl) carbodiiminde (EDC) (Pierce, Rockford, IL) for 30 min. Methoxypolyethylene glycol amine 5000 (PEG) powder was then directly added to the reaction mixture (final concentration = 10 mg/ml) to react for 24h at 4℃ under constant agitation. Upon completion of the reaction, the resulting slides were rinsed sequentially with anhydrous ethanol and Milli-Q water. The obtained slides were stored in anhydrous ethanol in the dark for future use. This step served to introduce cell non-adhesive PEG to the SAM surface via photoactive BNBA, thus rendering the whole SAM surface cell non-adhesive.

3.3.3.4 Photoactivation of PEG-BNBA-DT-Au surfaces (PEG-BNBA-DT-Au-UV)

UV irradiation from a 365 nm Longwave UV Lamp (Black-Ray B-100 Longwave UV lamp, 100 W, UVP, Upland, CA) was used to cleave the photoactive caging group BNBA from the SAM surface. This step removed the cell non-adhesive PEG from the SAM surface and released the caged thiol group for further modifications. Specifically, the PEG-BNBA-DT-Au glass slides were irradiated ~5 cm from the light source while submerged under a thin layer of PBS (pH 7.4) solution for 5 min. The irradiated surfaces were then rinsed sequentially with Milli-Q water, anhydrous ethanol, and finally Milli-Q water.

3.3.3.5 Binding of RGD peptide to the photoactivated PEG-BNBA-DT-Au surfaces (PEG-BNBA-DT-Au-UV-RGD)

To render the surface cell adhesive, the peptide sequence, RGD, was immobilized via the photo-uncaged thiol functional groups. Briefly, 10ml RGD solution (1mg/ml) in PBS (pH 7.4) and 24 mg Sulfo-SMCC (Pierce, Rockford, IL) were reacted for 30 min at room temperature under constant agitation to activate the amine groups on the RGD for reaction with the photo-uncaged thiol groups on the SAM surface. Subsequently the maleimide-activated RGD peptide was applied on the surface of PEG-BNBA-DT-Au-UV overnight at 4℃, followed by rinses with Milli-Q water to remove any physically adsorbed RGD peptides. The resulting surfaces were stored at 4℃ in PBS for future use.

3.3.4 *In vitro* cell attachment studies

To test the relative cell adhesiveness of the different SAM surfaces, NIH/3T3 fibroblasts were used as model adherent cells. The cells were routinely maintained in medium containing Dulbecco's Modified Eagle's Medium (DMEM) (Invitrogen) supplemented with 10% fetal bovine serum (FBS) (Invitrogen), 100 U/mL Penicillin (Invitrogen), and 0.1 mg/mL Streptomycin (Invitrogen), and kept in T-75 flasks at 37˚C in a humidified environment containing 5% CO_2. Prior to cell seeding on the experimental surfaces, cells were trypsinized, centrifuged into a pellet, re-suspended in culture medium and counted using a hemocytometer.

CellTracker™ Red (Invitrogen) was used to label the fibroblasts according to the vendor's protocol for better visualization of the cells in this study. Briefly, 10 mM stock solution of the dye in DMSO was prepared and was subsequently dissolved in DMEM to produce a 2.5 μM working solution. One milliliter of the working solution was added to the wells containing the fibroblasts in 12-well plates (BD Falcon) and allowed to incubate for 45 minutes at 37ºC. The staining solution was then replaced with pre-warmed fresh media and allowed to incubate for another 30 minutes at 37ºC. Cells were then washed in PBS (pH 7.4) followed by incubation in fresh media. The stained cells were subsequently seeded onto the experimental surfaces at a density of 5×10^3 cells/cm^2. Cells were observed using fluorescence microscope (Olympus IX81) every 24 h, and observations were documented using Image-Pro Plus software (Media Cybernetics, Silver Spring, MD).

3.3.5 Water contact angle measurements

Water contact angle (WCA) of surface modified gold slides and bare gold slides were obtained using the sessile drop method with a VCA Optima XE system (AST product, Billerica, MA). The surfaces of Au, DT-Au, BNBA-DT-Au and PEG-BNBA-DT-Au were tested immediately after surface modifications. Five random (and different) spots on each slide were analyzed and two slides for each sample were tested. To study the relationship between the photolysis efficiency and exposure times, the WCAs of PEG-BNBA-DT-Au surfaces subjected to different exposure times ranging from 0s to 1200s were measured and recorded. For all WCA measurements, both advancing and receding angles were taken and recorded.

3.3.6 X-ray photoelectron spectroscopy (XPS)

To investigate the properties of the different surfaces prepared in this study, high-resolution X-ray photoelectron spectra were recorded on an AXIS Ultra high performance XPS (Kratos, Chestnut Ridge, NY) with monochromatic AlKα source at 140 W with a fixed take-off angle of 90°. The intensity of the binding energy and atomic concentrations were determined by numerical integration of the relative peak areas using the atomic sensitivity factor specified by the manufacturer.

3.3.7 AFM imaging

To study the layer-by-layer modifications and surface topography changes before and after UV illumination, AFM imaging was implemented using Veeco Multimode AFM Nanoscope V (Veeco Instruments, Santa Barbara, CA). All images were collected in tapping mode in air at room temperature using a low-force Si scanning probe. Multiple different testing areas on each sample surface were analyzed. Surface roughness was quantified with the roughness function in the Nanoscope software.

3.4 Results and Discussion

In this study, we developed a new approach to control cell attachment using a photoactive SAM. SAMs on gold with thiols are good candidates to immobilize biomolecules such as antibodies, proteins, and peptides due to the strong and selective interaction of thiol groups with gold surface. Thiol based SAMs have been shown to have high vertical affinity to the gold surface and high lateral mobility allowing the lateral packing of molecules to be stabilized by intermolecular Van der Waals forces [16]. As a result, thiol-gold SAMs with different functionalities have been well documented. However, most of these studies aiming to pattern either proteins or cells require some mechanical means, such as micro-contact printing and microfluidic channels, and these fabrication methods are not simple and often achieve low precision. PEG is an important and widely used molecule to prevent non-specific binding of proteins and other biomolecules on surfaces. Numerous surface treatment methods to produce PEG interfaces for protein resistance have been reported, including PEG grafting[17], adsorptive chemistries[18], direct SAM formation of PEG segments and plasma surface treatment[17]. Here we used chemical linkage to introduce PEG molecules to the SAM surface to create efficient and stable protein and cell resistance [19]. The photoactive bifunctional linker, BNBA, acted as a switch that, upon UV irradiation, was cleaved from the SAM surface thereby removing the cell repulsive PEG from the surface and exposing originally protected thiol groups for further cell adhesive peptide immobilization. This eventually switched the SAM surface from cell repulsive to cell adhesive. In addition, we hypothesized that the increased hydrophilicity of the cleaved leaving group – due to the presence of the hydrophilic PEG segments – would facilitate the

removal of the photolysis by-products from the irradiated surface in the aqueous solution, minimizing further side reactions with the deprotected surfaces. This could be advantageous to overcome the side reaction issues which have been well documented for the photo-uncaging reactions of o-nitrobenzyl groups in the literature[20].

3.4.1 PEG immobilization

The PEG modified gold surface was obtained using layer-by-layer reactions on a bare gold surface, as shown in Figure 1. Au, DT-Au, BNBA-DT-Au, BNBA-DT-Au-UV, PEG-BNBA-DT-Au and PEG-BNBA-DT-Au-UV represent surfaces of bare gold, dithiol-gold, caging agent BNBA modified dithiol-gold surface before and after UV activation, and PEG modified BNBA-DT-Au before and after UV activation, respectively. DT-Au is an alkanedithiol SAM for protein attachment and has been extensively studied [21, 22]. The reaction between thiol groups and BNBA is a spontaneous reaction, which has been reported by others [23]. The reaction between BNBA and PEG is a typical reaction between the primary amine group on PEG and the carboxylic acid group on BNBA by EDC reaction.

Water contact angle measurements were used to characterize the resulting surfaces after layer-by-layer reactions that resulted in changes in hydrophilicities of the surfaces in each step. By measuring the water contact angles of the surfaces, the reaction in each step was indirectly verified. Advancing and receding contact angles for each sample are shown in Figure 2. It is evident that the advancing contact angle (ACA) for gold was 45.4 ± 3.6˚and the ACA increased to 90.1 ± 5.0˚ after reacting with DT. This increase in ACA is likely due to the hydrophobicity of alkane chains and thiol functional groups on the surface, suggesting the successful formation of a DT-Au SAM. Similarly, after the introduction of the bifunctional o-nitrobenzyl derivative (i.e. BNBA) to the DT-Au SAM surface, the ACA of the resulting surface changed to 70.2 ± 3.3˚. This is most likely due to reactions between the BNBA and the thiol groups on the DT-Au SAM surface. As a result, this reaction introduced hydrophilic carboxyl groups which decreased the WCA even though the BNBA aromatic ring is hydrophobic. As expected, when PEG was introduced to the surface, the ACA of PEG-BNBA-DT-Au further decreased to 57.5 ± 1.1˚. This is consistent with the hydrophilic characteristic of PEG, which is known for its ability to form hydrogen bonds with water

through oxygen ether[24]. The WCA measurements, both advancing and receding angles, are consistent with the layer-by-layer reaction steps as outlined in Figure 1. In addition, the WCAs for Au, DT-Au and PEG-BNBA-DT-Au are all in good agreement with previously reported values [25, 26]

In comparing the advancing WCA of the bare Au surface (45.4 ± 3.6°) with that of the PEG-BNBA-DT-Au (57.5 ± 1.1°), it is interesting to note that the surface became more hydrophobic when the surface was modified with PEG whereas a study by Benhabbour et al. [27] showed that a bare gold surface became more hydrophilic when it was coated with PEG. This discrepancy can be mostly attributed to the following reasons: 1) in the study by Benhabbour et al., the researchers used highly branched PEG molecules with hydroxyl (–OH) terminal groups; in comparison, the current study employs linear PEG molecules with methoxy ($–OCH_3$) terminal groups. These differences in the PEG molecules will most likely result in a more complete PEG surface coverage in the former study (highly branched vs. linear PEG) and more a hydrophilic surface presenting functional groups on the surface than the latter (-OH vs. $–OCH_3$). Ultimately, this could predictably result in a lower WCA from the PEG modified surface (30-42° vs. 57.5 ± 1.1°) in the study by Benhabbour et al.; 2) in addition, the study by Benhabbour et al. [27] reported a higher bare gold WCA (70 ± 3°) than the current study (45.4 ± 3.6°). While a wide range of bare gold surface WCAs have been reported in the literature [26, 28, 29] and both values are well within the reported value range, it is believed that the difference in the two WCAs of the bare gold surfaces is due to differences in operational conditions and ambient environments.

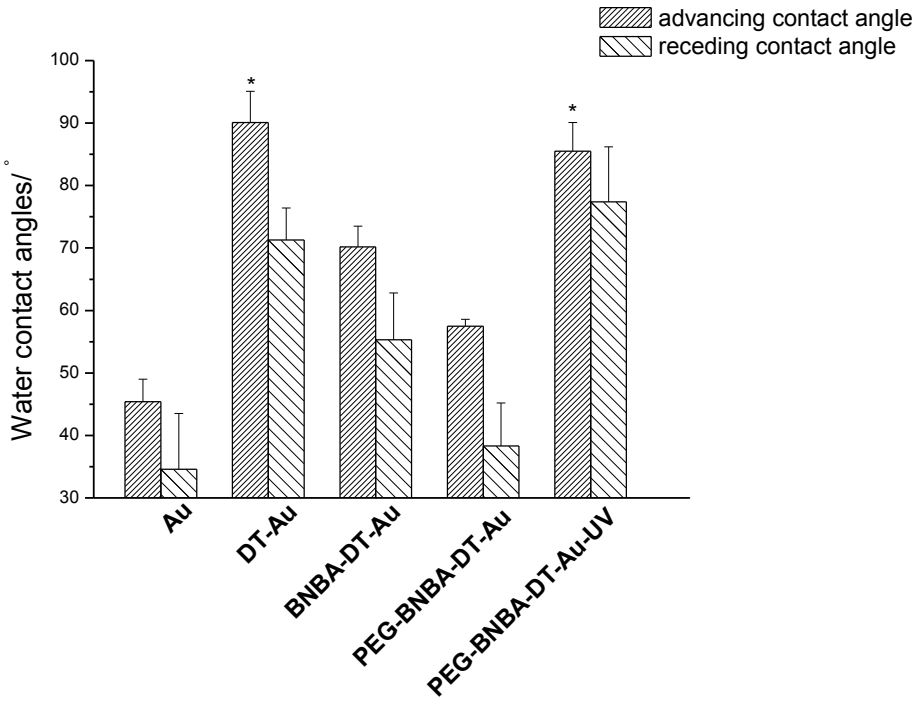

Figure 2 Advancing and receding water contact angles of different surfaces. Error bar = standard deviation, n=10. *DT-Au and PEG-BNBA-DT-Au-UV are not significantly different at p = 0.05 significance level.

To further characterize our surfaces, tapping mode AFM was employed to follow the morphology changes of the surface at each step. AFM images obtained for different samples are shown in Figure 3A. It is evident that the morphologies of Au and DT-Au surfaces were significantly different, suggesting the success of SAM formation (more AFM data can be seen in Supplementary Data). In comparison with the DT-Au surface morphology, the different BNBA-DT-Au surface morphology can be attributed to the introduction of BNBA on top of the thiol group functionalized surface. The morphology of the PEG-BNBA-DT-Au surface (Figure 3A (d)) was distinctively different from those of both BNBA-DT-Au and DT-Au. It is clear that PEG growth took place at the boundaries between the grains as well as on the grains, which is consistent with results reported by Haviland et al. [19]. Surface roughness, presented in an increasing order, is as follows: DT-Au, BNBA-DT-Au, and PEG-BNBA-DT-Au. This order is consistent with the order in which the surfaces were created in

a layer-by-layer configuration, suggesting that the more steps involved preparing a surface, the rougher the resulting surface. It is interesting to note the exception that the surface roughness decreased from the pure Au surface to the DT-Au SAM surface. This is likely due to the transition from an original Au surface to a highly ordered dithiol layer as a result of the formation of a gold-thiol SAM.

A.

a) Au

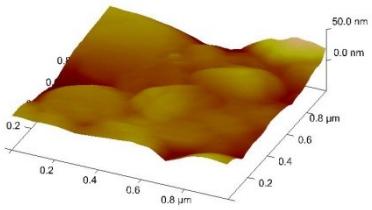

b) DT-Au

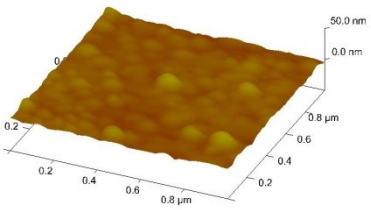

c) BNBA-DT-Au

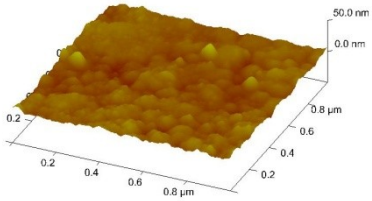

d) PEG-BNBA-DT-Au

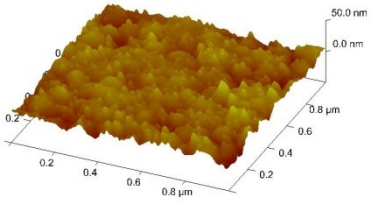

e) BNBA-DT-Au-UV

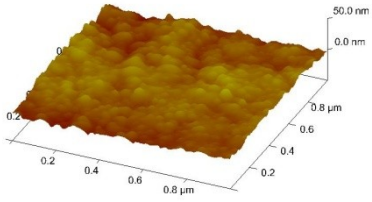

f) PEG-BNBA-DT-Au-UV

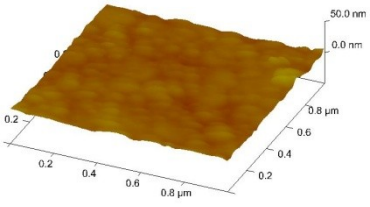

B.

	Au	DT-Au	BNBA-DT-Au	PEG-BNBA-DT-Au	BNBA-DT-Au-UV	PEG-BNBA-DT-Au-UV
R_q	2.70	2.34	3.30	4.28	3.44	2.10
R_a	2.16	1.64	2.57	3.23	2.57	1.59

Figure 3 A. AFM images of Au a), DT-Au b), BNBA-DT-Au c), PEG-BNBA-DT-Au d), and BNBA-DT-Au-UV e), PEG-BNBA-DT-Au-UV f); B. Roughness of different surfaces.

The layer-by-layer fabrication process was also monitored by XPS. As shown in Figure 4 a), the formation of SAMs was confirmed by S2p spectra. As has been previously reported [30, 31], the dithiol functional groups on Au showed two different binding energy peaks on S2p spectra. The doublet peak at 162.1 eV represented the binding energy of thiolate composition (Au-S), and the doublet peak at 163.6 eV was assigned to the binding energy of free thiol (C-SH). In S2p spectrum, the energy separation is due to the components of $S2p_{3/2}$ and $S2p_{1/2}$. In assigning the S2p peaks, the $S2p_{3/2}$ and $S2p_{1/2}$ peaks were fitted with a fixed binding energy difference of ~ 1.18 eV, a spin-orbit splitting, and a peak intensity ratio of about 2:1. For an example of C-SH peak, due to the signals from both $S2p_{3/2}$ and $S2p_{1/2}$, the peak is a doublet and can be fitted into two peaks: 163.6 eV and 164.8 eV. Likewise, the same peak assignment criteria were applied for the doublet peak of Au-S at 162.1 eV. The same peak assignment criteria were used by other published studies [32-34]. The successful formation of different samples was confirmed by the spectra of C1s, N1s and O1s on different surfaces. As shown in Figure 4b), there were no evident C1s, N 1s and O1s peaks on the Au surface spectrum; however, when dithiols were introduced to the gold surface to form the DT-Au SAM, significant C1s peak appeared around 285 eV, but there were still no nitrogen or oxygen peaks on the DT-Au spectra; N1s and O1s peaks appeared when the caging agent BNBA (containing nitrogen and oxygen) was introduced to the surfaces, as shown on the BNBA-DT-Au spectra in Fig. 4b. During PEG immobilization to the surface, there were no new elements introduced to the surface. However, the relatively

small nitrogen peak and the changes in the carbon and oxygen peaks in comparison with that of the BNBA-DT-Au surface suggest a large number of C and O atoms were added to the surface thus, attributing to the smaller nitrogen peak for PEG-BNBA-DT-Au. This additional evidence confirms the successful PEG linkage to the caged surface. The inset of Figure 4b) shows the C1s spectra of the BNBA-DT-Au surface. The component peaks arising from the 1s orbital of C-C/C-H, C-N, C-S and O=C-O were assigned by convention and the energy scale shifted accordingly. The C-C/C-H peak was assigned to a binding energy of ~ 285.9 eV. The remaining C1s peaks were assigned to higher energy levels. Taking the C-O peak as an example, because of the electronegative oxygen atom which draws electron density from the carbon atom and subsequently reduces the shielding of the nuclear charge, the binding energy of the electrons around it is increased, and as a result its peak shifted to higher binding energy. Similar shifts have also be observed with C-N and C-S [30, 31, 35]. The multiple overlapping peaks in the C1s spectra are the additional evidence to confirm the layer-by-layer process.

A closer look at the spectra in Fig 4b reveals several unexpected peaks. They include C1s and O1s peaks in Au and O1s peak in DT-Au spectra. We believe that the existence of C1s and O1S peaks in Au is due to quick adsorption of organic impurities on the pure gold surface from the ambient environment. The O1s peak on DT-Au could be inherited indirectly from the impurity contaminated pure gold surface. In addition, an unexpected peak at ~500 eV in PEG-BNBA-DT-Au spectrum is likely a Na Auger peak, and similar assignment has been reported in other studies [36-38]. A Na Auger peak is caused by the energy of the electron ejected from the atoms due to the filling of Na K shell by an electron from L shell coupled with the ejection of an electron from L shell. Based on the presence of a Na Auger peak, we believe there was an adventitious contamination from the environment.

To further characterize the surface properties, a surface thickness calculation was carried out based on XPS data using the Thickogram method [39] at a 45˚ take-off angle. The attenuation lengths of different samples in the calculation were estimated by kinetic energy, density and electrons according to a previous study [40]. As shown in Table 1, the thickness of DT-Au was calculated to be 1.07 ± 0.14 nm which is consistent with a previous report [31]; the thickness of BNBA-DT-Au was estimated to be 3.21 ± 0.15 nm; the thickness of

PEG-BNBA-DT-Au was 3.86 ± 0.54 nm. Therefore, it can be concluded that the thickness increased with increasing number of chemical reactions on the surface as expected.

a)

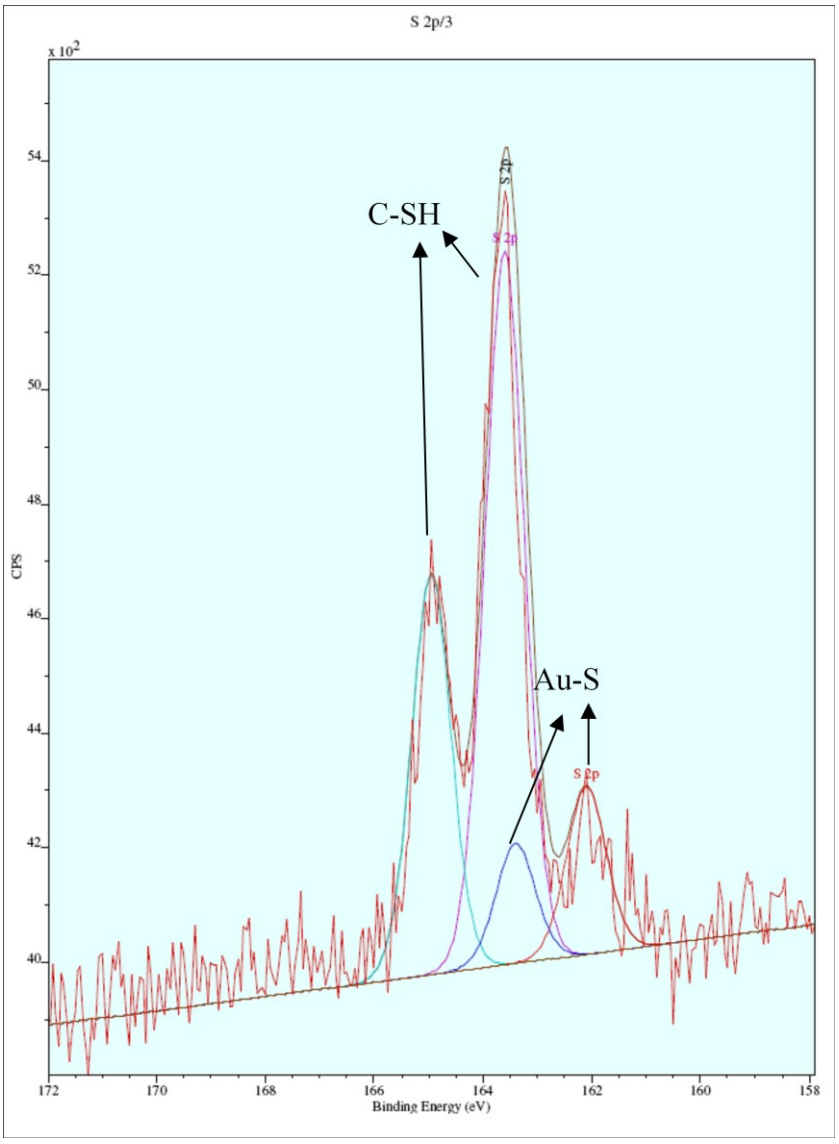

b)

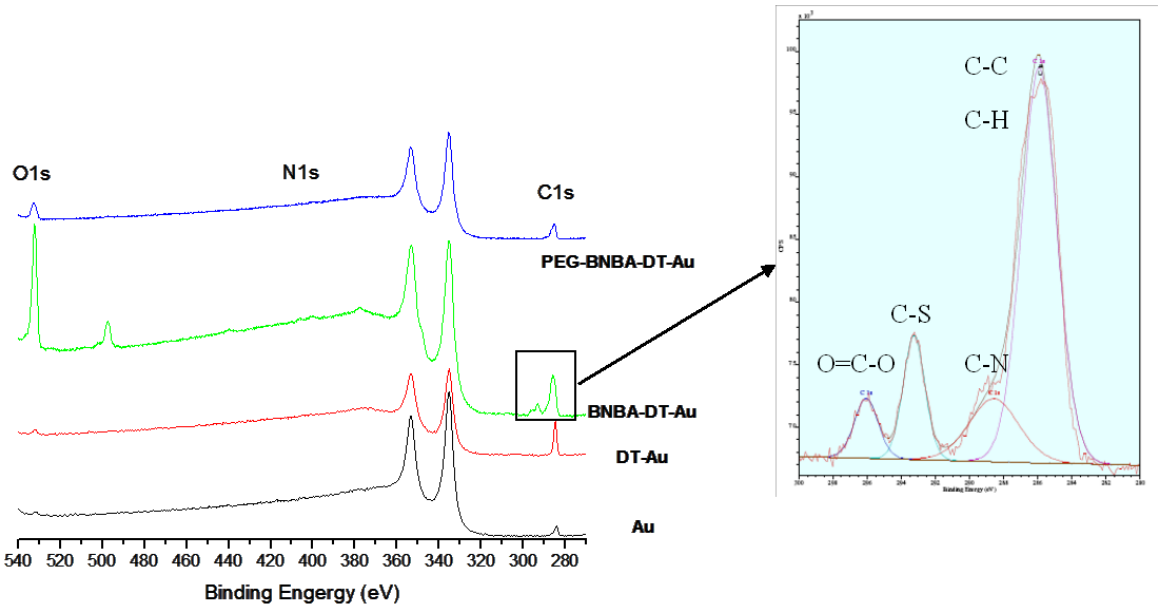

Figure 4 X-ray photoelectron spectra of different samples: a) S 2p spectrum of DT-Au, and b) summary spectra of C 1s, N 1s and O 1s on different samples, inset: C 1s spectrum of BNBA-DT-Au

Table 1 Thickness of Different Samples on Gold Surfaces Based on XPS

Sample	Thickness/nm
DT-Au	1.07±0.14
BNBA-DT-Au	3.21±0.15
PEG-BNBA-DT-Au	3.86±0.54

3.4.2 Photoactivation

The mechanism for the deprotection reaction involving the o-nitrobenzyl group has been studied in the literature and is hypothesized to be as follows: hydrogen transfers from the benzyl position to the nitro functional group during photo irradiation, and the transfer is achieved by the elimination of o-nitrosobenzaldehyde from the bicyclic intermediate which is generated during the process [41, 42]. As shown in Figure 2, the change of water contact angles (both advancing and receding) on PEG-BNBA-DT-Au surface after UV activation strongly suggests the successful cleavage of PEG from the surface via the o-nitrobenzyl leaving group. After photoactivation, the PEG-BNBA-DT-Au-UV surface was deprotected to resume a thiol covered surface. Therefore, the water contact angles of PEG-BNBA-DT-Au-UV (85.5 ± 4.6˚ for advancing water contact angle and 77.4 ± 4.8˚ for receding water contact angle) were expected to be similar to that of the thiol terminated surface, DT-Au (90.1 ± 5.0˚ for advancing water contact angle and 71.3 ± 5.1˚ for receding water contact angle). In fact, water contact angles for the two surfaces were not found to be significantly different ($p > 0.05$). The switching of PEG-BNBA-DT-Au surface from hydrophilic to hydrophobic after UV activation (i.e. PEG-BNBA-DT-Au-UV) was the first evidence to demonstrate the success of the uncaging process. In addition, as shown in Figure 3A, high resolution AFM images of the samples both before and after UV exposure (i.e. PEG-BNBA-DT-Au vs. PEG-BNBA-DT-Au-UV or BNBA-DT-Au vs. BNBA-DT-Au-UV) showed dramatically different molecular packing that resulted in different surface morphologies, and further confirmed that the photo reactions took place on the respective surfaces. However, the PEG-BNBA-DT-Au and BNBA-DT-Au surfaces also behaved differently when exposed to UV. The roughness of the PEG-BNBA-DT-Au surface dropped significantly after photo activation, from 4.28 to 2.10 for R_q and from 3.23 to 1.59 for R_a, whereas that of the BNBA-DT-Au surface showed little changes, as suggested in Fig 3B. These differences are most likely because of the removal of the PEG molecules via the cleaved o-nitrobenzyl from the PEG-BNBA-DT-Au surface. The different behaviors of the BNBA-DT-Au and PEG-BNBA-DT-Au surfaces after photo activation also suggest another probable benefit to introducing PEG molecules onto the surface: in addition to providing a highly hydrophilic and protein/cell repulsive surface to control cell attachment, the hydrophilic PEG segments likely

improved the uncaging of thiols by facilitating the removal of the highly reactive nitroso and aldehyde containing by-products from the uncaged thiol surface to the aqueous solution after the photo activation. This could significantly reduce the surface concentrations of the active photo by-products which are known to react with thiols rendering the overall photo uncaging of thiol groups less effective[43]. In comparison, the highly reactive nitroso and aldehyde containing by-products from the BNBA-DT-Au surface would likely show a more hydrophobic characteristic due to their benzyl ring structure. Thus, instead of readily entering the aqueous solution, it could accumulate on the uncaged surface during photoactivation. These locally concentrated reactive by-products therefore would likely quench the newly generated thiols on the surface, as has been documented by other researchers[44, 45]. This observation is also in good agreement with our surface roughness data. As shown in Figure 3B, in comparison with the roughness of the smooth DT-Au surface, the roughness of the BNBA-DT-Au surface did not change or slightly increased (Ra remained the same at 2.57 but Rq increased from 3.30 to 3.40) after the photo activation while that of the PEG-BNBA-DT-Au reduced significantly (Rq reduced from 4.28 to 2.10 and Ra reduced from 3.23 to 1.59, respectively). This strongly suggests that the introduction of the PEG molecule made the nitrobenzyl cage a better leaving group.

To determine time-dependent characteristics of the PEG-BNBA-DT-Au surface after UV exposure, time-dependent WCA measurements were taken at different UV exposure time durations as described in previous studies [46, 47]. As shown in Figure 5, the initial advancing water contact angle at t = 0 s was 57.5˚ and a sharp increase in both advancing and receding contact angles was observed between 0 s to 120 s. Beyond the 120 s exposure, the measured WCAs leveled off to values of advancing /receding of $90^{o}/68^{o}$. It is therefore concluded that the exposure time should be longer than 120 s.

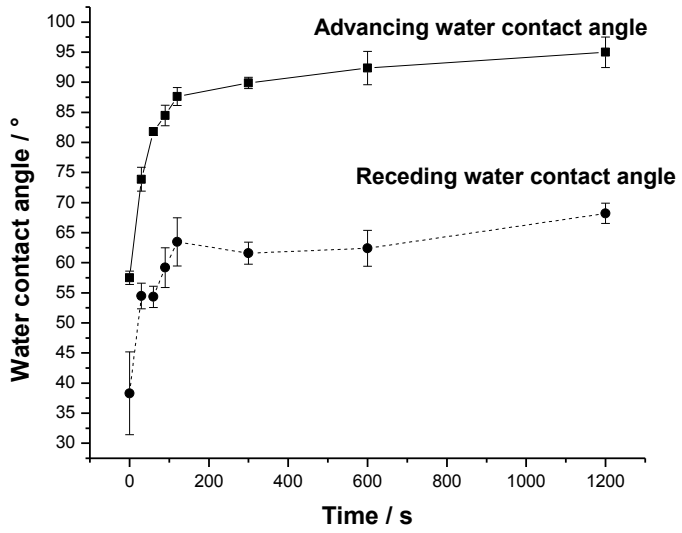

Figure 5 Increase in WCAs vs. exposure times for PEG-BNBA-DT-Au under UV activation. Error bar = Standard deviation, n = 5.

3.4.3 Cell attachment

To test cell attachment to the photoactive SAM surfaces, NIH/3T3 fibroblast cells were seeded on the surfaces of interest. The studied surfaces were exposed to UV followed by reactions with the cell adhesive peptide RGD[48]. The reaction took place between maleimide-activated RGD and the uncaged thiol groups on the surface after UV activation. We observed cells seeded on different surfaces for 4 days with cells seeded on a tissue culture plate as a positive control. Figure 6A is the fluorescence image of cells on different surfaces after seeding. It shows that the different surfaces had different cell adhesive capacities. Specifically, there were almost no cells on either BNBA-DT-Au or PEG-BNBA-DT-Au surfaces after 4days of culture, and the cells on these surfaces did not seem to proliferate as demonstrated in Figure 6B. As expected, both the BNBA-DT-Au-UV-RGD and PEG-BNBA-DT-Au-UV-RGD surfaces had higher cell counts than BNBA-DT-Au and PEG-BNBA-DT-Au over the time points investigated. Significantly, the PEG-BNBA-DT-Au-UV-RGD surface consistently had higher cell counts than the BNBA-DT-Au-UV-RGD surface. Figure 6B summarizes the quantitative results based on the cell culture studies from Day 1 day to Day 4. As shown in Figure 6B, cell density on PEG-BNBA-DT-Au-UV-RGD

was close to that on DT-Au-RGD, which is consistent with the surface characterization results. As expected, both the BNBA-DT-Au and the PEG-BNBA-DT-Au surfaces showed the lowest cell density among all surfaces. After UV activation and RGD immobilization, cell repulsive PEG segments were cleaved away from the surface, and cell adhesive RGD peptides were chemically linked to the surface. This switched a cell non-permissive surface to cell permissive. It is worthwhile to note that while the BNBA-DT-Au-UV-RGD surface allowed cell attachment and cell proliferation, the cell counts were consistently lower than those of PEG-BNBA-DT-Au-UV-RGD. This difference could be attributed to our theory that the PEG modified cage is a better leaving group for the photo uncaging reaction. Therefore the PEG modified cage leaving group ultimately resulted in a more effective and thiol-richer surface for the uncaged PEG-BNBA-DT-Au surface compared to the BNBA-DT-Au surface. In addition, after 5 days of culture, the intensity of the fluorescent day in each cell decreased dramatically and it was unable to support further investigations.

A.

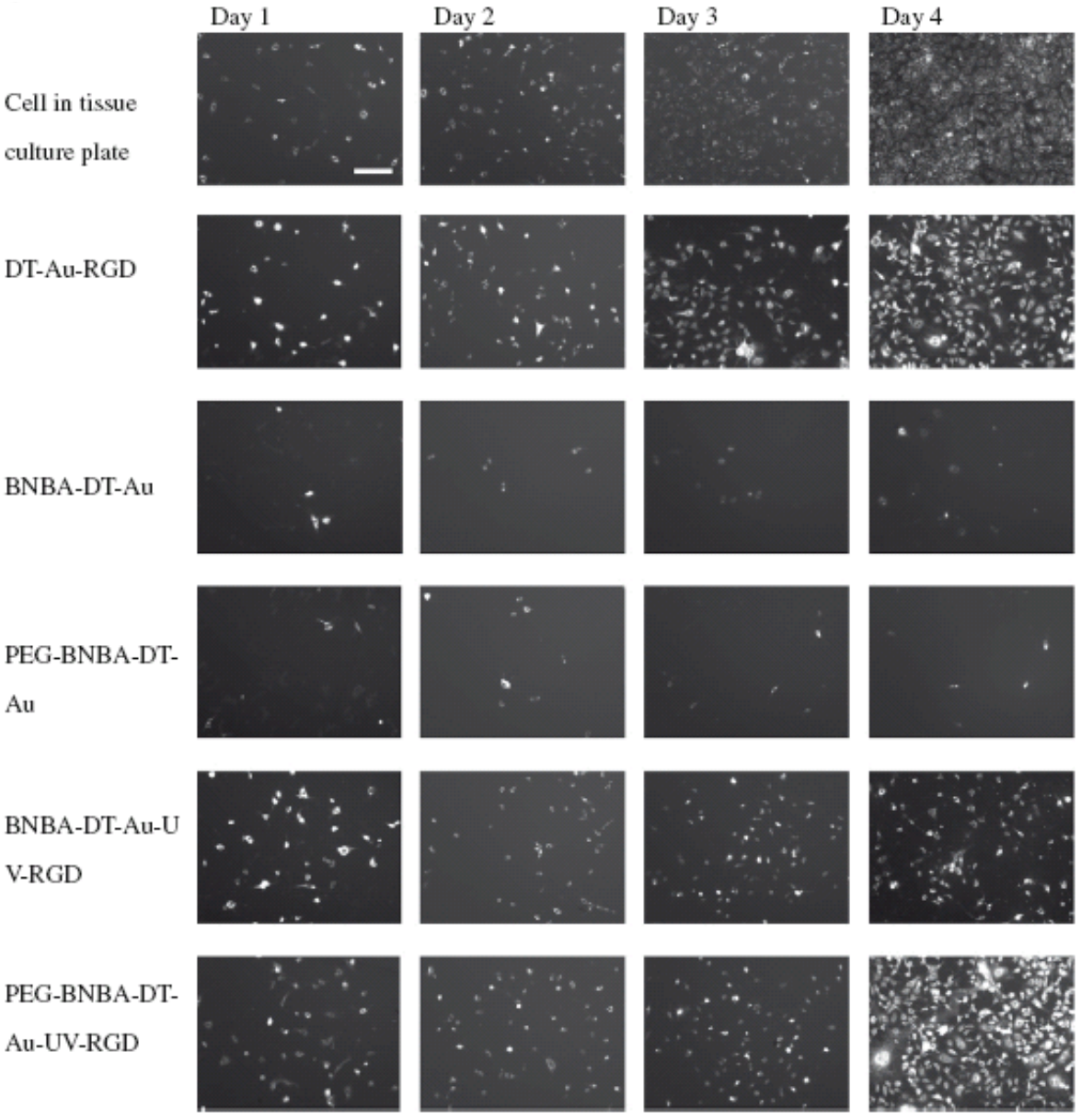
Day 1
Day 2
Day 3
Day 4
Cell in tissue culture plate
DT-Au-RGD
BNBA-DT-Au
PEG-BNBA-DT-Au
BNBA-DT-Au-UV-RGD
PEG-BNBA-DT-Au-UV-RGD

B.

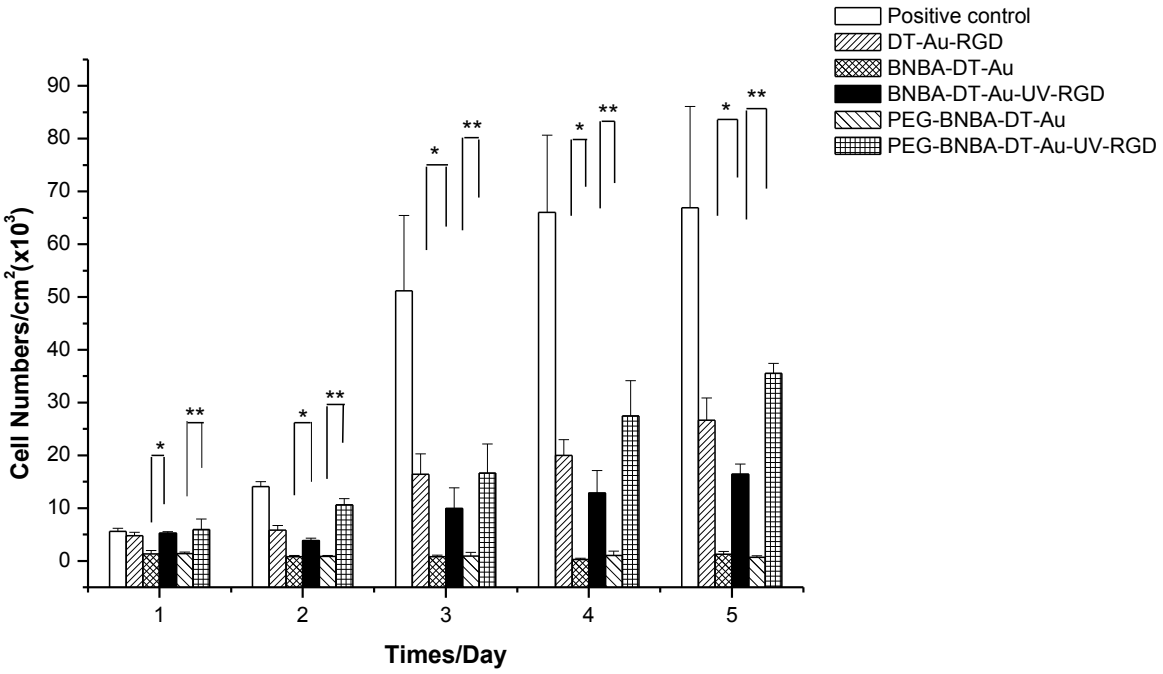

Figure 6 Cell culture on different surfaces over time, scale bar = 100um. A. Fluorescent images of cells on different surfaces after 4 days of culture; B. Cell density on different surfaces. *BNBA-DT-Au and BNBA-DT-Au-UV-RGD are significantly different at the p = 0.05 level from 1 day to 5 days. **PEG-BNBA-DT-Au and PEG-BNBA-DT-Au-UV-RGD are significantly different at the p = 0.05 level from 1 day to 5 days.

3.5 Conclusions

We have demonstrated that cell attachment can be manipulated using a photoactive SAM surface. The incorporation of PEG molecules to the surfaces via a photolabile nitrobenzyl caging groups not only drastically reduces the non-specific binding of biomolecules and forms cell non-permissive surfaces to repel cells, but also likely facilitates the uncaging reaction by creating a better leaving group during the photo uncaging process. This results in more effective photo uncaging reactions and more uncaged thiol function groups for subsequent RGD peptide immobilization for better cell attachment. This notion has been confirmed by a NIH/3T3 cell culture study. We believe that this method has a great

potential to create different cell patterns on a surface and can be used for guidance of cell growth and migration in the future.

3.6 Acknowledgement

The authors would like to acknowledge financial support from a Discovery Grant by the Natural Sciences and Engineering Research Council of Canada (NSERC).

3.7 References

1. Orsello, C.E., D.A. Lauffenburger, and D.A. Hammer, *Molecular properties in cell adhesion: a physical and engineering perspective.* Trends in Biotechnology, 2001. **19**(8): p. 310-316.
2. Veiseh, M., M.H. Zareie, and M.Q. Zhang, *Highly selective protein patterning on gold-silicon substrates for biosensor applications.* Langmuir, 2002. **18**(17): p. 6671-6678.
3. Prime, K.L. and G.M. Whitesides, *Adsorption of Proteins onto Surfaces Containing End-Attached Oligo(Ethylene Oxide) - a Model System Using Self-Assembled Monolayers.* Journal of the American Chemical Society, 1993. **115**(23): p. 10714-10721.
4. Assoian, R.K. and E.A. Klein, *Growth control by intracellular tension and extracellular stiffness.* Trends in Cell Biology, 2008. **18**(7): p. 347-352.
5. Vonrecum, A.F. and T.G. Vankooten, *THE INFLUENCE OF MICRO-TOPOGRAPHY ON CELLULAR-RESPONSE AND THE IMPLICATIONS FOR SILICONE IMPLANTS.* Journal of Biomaterials Science-Polymer Edition, 1995. **7**(2): p. 181-198.
6. Hertz, A. and I.J. Bruce, *Inorganic materials for bone repair or replacement applications.* Nanomedicine, 2007. **2**(6): p. 899-918.
7. Kang, G.D., et al., *A novel method of surface modification on thin-film composite reverse osmosis membrane by grafting poly(ethylene glycol).* Polymer, 2007. **48**(5): p. 1165-1170.
8. Goubko, C.A. and X.D. Cao, *Patterning multiple cell types in co-cultures: A review.* Materials Science & Engineering C-Materials for Biological Applications, 2009. **29**(6): p. 1855-1868.
9. Lee, E.J., E.W.L. Chan, and M.N. Yousaf, *Spatio-Temporal Control of Cell Coculture Interactions on Surfaces.* Chembiochem, 2009. **10**(10): p. 1648-1653.
10. Sebra, R.P., et al., *Controlled polymerization chemistry to graft architectures that influence cell-material interactions.* Acta Biomaterialia, 2007. **3**(2): p. 151-161.
11. Park, S. and M.N. Yousaf, *An interfacial oxime reaction to immobilize ligands and cells in patterns and gradients to photoactive surfaces.* Langmuir, 2008. **24**(12): p. 6201-6207.
12. Nakanishi, J., et al. *Spatiotemporal control of cell adhesion on a self-assembled monolayer having a photocleavable protecting group*. 2006: Elsevier Science Bv.
13. Chaulk, S.G. and A.M. MacMillan, *Caged RNA: photo-control of a ribozyme reaction.* Nucleic Acids Research, 1998. **26**(13): p. 3173-3178.
14. Luo, Y. and M.S. Shoichet, *Light-activated immobilization of biomolecules to agarose hydrogels for controlled cellular response.* Biomacromolecules, 2004. **5**(6): p. 2315-2323.
15. Doh, J. and D.J. Irvine, *Immunological synapse arrays: Patterned protein surfaces that modulate immunological synapse structure formation in T cells.* Proceedings of the National Academy of Sciences of the United States of America, 2006. **103**(15): p. 5700-5705.
16. Feng, C.L., et al., *Reactive thin polymer films as platforms for the immobilization of biomolecules.* Biomacromolecules, 2005. **6**(6): p. 3243-3251.

17. Shah, S.S., et al., *Micropatterning of Proteins and Mammalian Cells on Indium Tin Oxide.* Acs Applied Materials & Interfaces, 2009. **1**(11): p. 2592-2601.
18. Suh, K.Y., et al., *A simple soft lithographic route to fabrication of poly(ethylene glycol) microstructures for protein and cell patterning.* Biomaterials, 2004. **25**(3): p. 557-563.
19. Rundqvist, J., J.H. Hoh, and D.B. Haviland, *Substrate effects in poly(ethylene glycol) self-assembled monolayers on granular and flame-annealed gold.* Journal of Colloid and Interface Science, 2006. **301**(1): p. 337-341.
20. Barth, A., et al., *Time-resolved infrared spectroscopy of intermediates and products from photolysis of 1-(2-nitrophenyl)ethyl phosphates: Reaction of the 2-nitrosoacetophenone byproduct with thiols.* Journal of the American Chemical Society, 1997. **119**(18): p. 4149-4159.
21. Valiokas, R., et al., *Self-assembled monolayers of oligo(ethylene glycol)-terminated and amide group containing alkanethiolates on gold.* Langmuir, 1999. **15**(10): p. 3390-3394.
22. Kondo, T. and K. Uosaki, *Self-assembled monolayers (SAMs) with photo-functionalities.* Journal of Photochemistry and Photobiology C-Photochemistry Reviews, 2007. **8**(1): p. 1-17.
23. Marriott, G., H. Miyata, and K. Kinosita, *Photomodulation of the Nucleating Activity of a Photocleavable Cross-Linked Actin Dimer.* Biochemistry International, 1992. **26**(5): p. 943-951.
24. Erdamar, O., et al., *Experimental investigation of the conduction mechanism of hydrogenated PEG thin films at high relative humidities.* Solid State Ionics, 2006. **177**(37-38): p. 3217-3221.
25. Ernst, O., et al., *Control of cell detachment in a microfluidic device using a thermo-responsive copolymer on a gold substrate.* Lab on a Chip, 2007. **7**(10): p. 1322-1329.
26. Tlili, A., et al., *Adsorption characteristics of self-assembled thiol and dithiol layer on gold.* Materials Science & Engineering C-Biomimetic and Supramolecular Systems, 2007. **27**(4): p. 620-624.
27. Benhabbour, S.R., et al., *Protein resistance of surfaces prepared by chemisorption of monothiolated poly(ethylene glycol) to gold and dendronization with aliphatic polyester dendrons: Effect of hydrophilic dendrons.* Macromolecules, 2008. **41**(7): p. 2567-2576.
28. Lv, Z.J., et al., *Preparation and Characterization of Covalently Binding of Rat Anti-human IgG Monolayer on Thiol-Modified Gold Surface.* Nanoscale Research Letters, 2009. **4**(12): p. 1403-1408.
29. Ernst, O., et al., *Tuning of thermo-responsive self-assembly monolayers on gold for cell-type-specific control of adhesion.* Langmuir, 2008. **24**(18): p. 10259-10264.
30. Jun, Y., X.Y. Zhu, and J.W.P. Hsu, *Formation of alkanethiol and alkanedithiol monolayers on GaAs(001).* Langmuir, 2006. **22**(8): p. 3627-3632.
31. Rieley, H., et al., *X-ray studies of self-assembled monolayers on coinage metals. 1. Alignment and photooxidation in 1,8-octanedithiol and 1-octanethiol on Au.* Langmuir, 1998. **14**(18): p. 5147-5153.
32. Onoa, G.B. and V. Moreno, *Palladium and platinum famotidine complexes.* Journal of Inorganic Biochemistry, 1998. **72**(3-4): p. 141-153.
33. Laiho, T., J.A. Leiro, and J. Lukkari, *XPS study of irradiation damage and different metal-sulfur bonds in dodecanethiol monolayers on gold and platinum surfaces.* Applied Surface Science, 2003. **212**: p. 525-529.
34. Laffineur, F., et al., *Formation of a bilayer film on gold substrates for connector applications: spectroscopic study of the deposition process.* Journal of Materials Chemistry, 2005. **15**(47): p. 5054-5062.
35. Merzlikin, S.V., et al., *Resolving the depth coordinate in photoelectron spectroscopy - Comparison of excitation energy variation vs. angular-re solved XPS for the analysis of a self-assembled monolayer model system.* Surface Science, 2008. **602**(3): p. 755-767.

36. Shchukarev, A.V., *A study of the SiO2-aqueous electrolyte (NaCl, CsCl) interface by X-ray photoelectron spectroscopy.* Colloid Journal, 2007. **69**(4): p. 514-525.
37. Legrand, J., et al., *Synthesis and XPS characterization of nickel boride nanoparticles.* Langmuir, 2002. **18**(10): p. 4131-4137.
38. Lebugle, A., et al., *XPS Study of elastin-solubilized peptides binding onto apatite in orthopaedic biomaterials.* Journal of Materials Science-Materials in Medicine, 1996. **7**(4): p. 223-226.
39. Cumpson, P.J., *The Thickogram: a method for easy film thickness measurement in XPS.* Surface and Interface Analysis, 2000. **29**(6): p. 403-406.
40. *Biopolymers at interfaces* Surfactant science series ; v. 110 ed. M. Malmsten. 2003: New York ; Basel : M. Dekker, c2003. 641.
41. Hoffmann, N., *Photochemical reactions as key steps in organic synthesis.* Chemical Reviews, 2008. **108**(3): p. 1052-1103.
42. Hoffmann, N., J.C. Gramain, and H. Bouas-Laurent, *Photochemistry in organic synthesis.* Actualite Chimique, 2008(317): p. 6-13.
43. Alberto Diaspro, G.C., Maddalena Collini, *Quarterly Reviews of Biophysics*, in *Two-photon Fluorescence Excitation and related techniques in biological microscopy*, A.G. Steve Goldstein, Gerhard Wagner, Peter Wolynes, Editor. 2005, Cambridge University Press.
44. Pollitt, S.K. and P.G. Schultz, *A photochemical switch for controlling protein-protein interactions.* Angewandte Chemie-International Edition, 1998. **37**(15): p. 2104-2107.
45. Du, X.L., H. Frei, and S.H. Kim, *Comparison of nitrophenylethyl and hydroxyphenacyl caging groups.* Biopolymers, 2001. **62**(3): p. 147-149.
46. Han, X.J., et al., *Supported bilayer lipid membrane arrays on photopatterned self-assembled monolavers.* Chemistry-a European Journal, 2007. **13**(28): p. 7957-7964.
47. Yamazoe, H., T. Uemura, and T. Tanabe, *Facile cell patterning on an albumin-coated surface.* Langmuir, 2008. **24**(16): p. 8402-8404.
48. Takahashi, H., et al., *Imaging surface immobilization chemistry: Correlation with cell patterning on non-adhesive hydrogel thin films.* Advanced Functional Materials, 2008. **18**(14): p. 2079-2088.

Chapter 4 Neuron-like PC12 cell patterning on a photoactive self-assembled monolayer (SAM)

Nan Cheng and Xudong Cao

Journal of Colloid and Interface Science

(Submitted)

4.1 Abstract

An approach to control cell initial attachment using photochemistry and self-assembled monolayer (SAM) was described. Photocleavable 4,5-dimethoxy-2-nitrobenzyl chloroformate (NVOC) protected amine on an alkanethiol-gold SAM was developed for cell adhesion. The cleavage of NVOC and deprotection of amines was controlled spatially and temporally by two UV irradiations with a photomask. The following biomolecule immobilizations after each UV irradiation with deprotected amines on specific regions were done by introducing cell non-adhesive poly(ethylene glycol) (PEG) after the first irradiation and cell adhesive protein laminin (LAM) after the second irradiation to create surface heterogeneity for cell adhesion. Different surface properties were characterized before cell culture. UV-Vis spectrophotometry was used to determine the photolysis of caged self-assembled molecules; water contact angle (WCA) was to characterize the surface wettability; atomic force microscopy (AFM) was to describe the different surface microstructures; cyclic voltammetry (CV) was used to elaborate electrochemical properties of intermediate and the resulting surfaces; X-ray photoelectron spectroscopy (XPS) was obtained to show the presence of elements on different surfaces. Cell adhesion was processed with neuron-like cell line, PC12 cell. Cell studies demonstrated the successful control over cell initial attachment on our designed surface and cell differentiation could be further controlled by the addition of diffusible nerve growth factor (NGF) after selective cell adhesion.

4.2 Introduction

The natural environment of a living cell is critical to cell functions and behaviours. Studies have shown that many molecular processes in a cell are dependent on cell adhesion and spreading. This phenomenon is known as anchorage dependence, and most normal mammalian cells are anchorage dependent. Therefore, by controlling the cell microenvironment, the correct positioning of cells on biomaterials can be achieved, and this is believed to be very important for cell behaviours such as proliferation, differentiation, migration, and apoptosis. For example, 3T3 fibroblasts are documented to reduce mRNA production and eventually lose cell viability when cultured in suspension for 8-9 days [1, 2]. In addition, corneal epithelial cells are shown to maintain a fibroblastoid morphology and sensitivity to fibroblast growth factor (FGF) on tissue culture polystyrene plates, whereas they are shown to maintain a cuboidal morphology and sensitivity to epidermal growth factor (EGF) when they are cultured on collagen [3]. To date, the mechanisms of how extracellular environment controls cell behaviour are far from fully understood, and there is no well-accepted studies to show how cells recognize and respond to different surface properties. However, based on our current knowledge, we have already started to understand that the presence of certain biomolecules on a material surface can control cell adhesion, and that if these biomolecules are patterned, cell attachment and subsequent cell functions and behaviour can be further tailored. This patterning approach is especially useful for tissue engineering in which by manipulating targeted cell microenvironments one can try to regulate cell behaviours, which subsequently could help to reconstruct or regenerate damaged tissues [4-6]. In order to create well controlled microenvironments, surface functionalization is commonly used to immobilize different biomolecules for well-controlled cell adhesion on material surfaces.

There are many methods to control the surface functionalities – especially for applications of controlling cell adhesion – such as soft lithography [7-10], photolithography [11-13], photoimmobilization [4, 14-18] and ink-jet technology [19, 20]. For the application of *in vitro* studies, particularly those to study cell-cell or cell-material interactions, a self-assembled monolayer (SAM) provides a facile way to modify the surface functionalities, and control physical and chemical properties of the resulting surface. Mimicking micrometric

biological surface properties on a SAM is a powerful tool to study and manipulate cell growth *in vitro* for several reasons: 1) for a SAM surface, it is easy to control surface functionalities by changing the tail group of the self-assembled molecule; 2) the single molecular layer will minimize the effect of topographical structure on cell adhesion and growth; 3) there are many powerful techniques developed to characterize the SAM surface, such as atomic force microscopy (AFM), X-ray photonspectroscopy (XPS), ellipsometry and water contact angle (WCA). Among all the SAM surfaces, alkane-thiol on gold is a well-documented SAM and has been extensively studied. It has also been shown that the thiol-gold SAM is very stable under a variety of conditions, such as UV irradiations [21, 22] , heat treatments [23] and electrochemical potentials [24].

In order to create patterns that exhibit different chemical or physical properties to control cell attachment in specific areas, i.e. cell patterns, several techniques have been explored on SAM surfaces. Micro-contact printing (μCP) and dip-pen nanolithography are two commonly used techniques to deposit SAMs on specific regions of an otherwise homogeneous surface to create surface patterns for selective cell adhesion [25-28]. Other methods such as microfluidics [29] and photochemistry can also be applied to SAMs to create surface heterogeneity to control cell adhesion. In comparison with other methods, the most important advantage of using photochemistry and photosensitive molecules is the ease to control the patterned size and the shape in micron- or nano- scale in both spatial and temporal manners. In addition, other advantages of using photochemistry to pattern a surface include avoidance of using harsh solvents on the surface of interest, which will otherwise likely to cause denaturation of biomolecules during the patterning process. For photosensitive molecules used for surface patterning, *o*-nitrobenzyl derivatives are commonly used [30-32]. They can react with (i.e. protect or cage) many functional groups and act as a cage to protect these functional groups. Subsequently, these caged functional groups can be released when they are exposed to light at a proper wavelength. These photolabile cages have been successfully used to pattern proteins and cells in many studies [17, 33, 34]. In our previous papers, we utilized different *o*-nitrobenzyl derivatives to control a fibroblast cell adhesion on different substrates [35, 36]. In this current study, we attempt to pattern PC12 cells using an *o*-nitrobenzyl derivative on a SAM surface by a two light exposure approach. Specifically, *o*-nitrobenzyl derivative caged self-assembled molecules

were first synthesized and were subsequently used to form a photocage protected SAM on gold surface by alkanethiol-gold interaction. When exposed with UV light through a photomask, the caging groups on selected regions (defined by the patterns on the photomask) of the SAM surface were photo-cleaved thus deprotecting the originally caged function groups, amines. These selected regions on the SAM were then rendered cell non-adhesive by immobilizing cell non-permissive poly(ethylene glycol) (PEG) molecules via the photo deprotected amine groups on the surface. This was followed by a second illumination without a photomask to uncage the amine functional groups on the rest of the SAM surface, and subsequently a cell adhesive molecule, laminin (LAM), was patterned on the surface via the amine groups uncaged in the second exposure to render the remaining cell-adhesive. By using double UV illuminations to different regions of the same SAM surface followed by sequentially immobilizing two different biomolecules, we attempted to realize the control of surface properties in a spatial manner for cell attachment. The general approach of our strategy is shown in Figure 1. In this paper, we report the preparation and characterization of our photoactive SAM surfaces before and after the two UV exposures. To test the ability of such surfaces to control cell adhesion and their efficacy to pattern cells, PC12 cells were used. Our results show that PC12 cell patterns can be achieve by this double light exposure approach to individually create cell non-adhesive and adhesive regions. This study may provide an another strategy to direct cell attachment and axonal extension, which has the potential to mimic neuronal outgrowth and to obtain *in vitro* neural-like networks, thus providing an *in vitro* platform to study nerve regeneration and nerve guidance [37-39].

4.3 Experimental

4.3.1 Materials

All chemicals were used as received without any further purification. Bovine serum albumin (BSA), 11-amino-1-undecanethiol hydrochloride (AUT), *o*-(2-aminoethyl) polyethylene glycol 2,000 (PEG), and 4,5-dimethoxy-2-nitrobenzyl chloroformate (NVOC) were obtained from Sigma-Aldrich (St. Louis, MO). Dichloromethane, *N*,*N*-Diisopropylethylamine (DIEA), and chloroform were purchased from Fisher Scientific (Ottawa, ON). Anhydrous ethanol was purchased from Commercial Alcohols (Toronto, ON).

4.3.2 Preparation of caged self-assembling molecule (NVOC-AUT)

In order to cage the self-assembled molecule for SAM, DIEA (10.78 mg) was added to a 3 ml solution of AUT (10 mg) in dichloromethane to adjust the pH to 8. To this resulting solution, a NVOC (11.5 mg) solution in dichloromethane was dropwisely added at 0℃ over a period of 30 min followed by 2 hrs of incubation. The mixture was left to react overnight at room temperature with continuous agitation followed by sequential washes with 1M aq. HCl (1 x 5 ml), sat. aq. $NaHCO_3$ (3 x 10ml) and sat. aq. NaCl (1 x 10 ml). The product was dried over Na_2SO_4 and finally purified by flash chromatography eluting with 10% methanol in ethyl acetate. The obtained product was referred to as NVOC-AUT.

4.3.3 SAM preparation ((NVOC-AUT)-Au)

Gold coated glass surface prepared by thermo-evaporation method was purchased from Arrandee™ Company, Germany. The squares were 11 × 11 mm in size with a 2.5 ± 1.5 nm thickness chromium under-layer and a 250 ± 50 nm gold coating as the upper layer. Immediately before use, the surfaces were cleaned by piranha solution (3:1 (v/v) of 98% H_2SO_4 and 30% H_2O_2, *caution: piranha solution is a very corrosive solution and appropriate safety precaution should be utilized, including the use of acid-resistant gloves and adequate shielding.*), wash extensively by Milli-Q water, anhydrous ethanol, and finally dried under nitrogen flow at room temperature. To prepare the SAM layer with NVOC-AUT, the previously cleaned gold coated surfaces were immersed and kept in anhydrous ethanol solution with 1mM NVOC-AUT at room temperature for 24 h. The resulting surfaces were rinsed extensively with anhydrous ethanol and then dry with nitrogen flow. The obtained surfaces were referred to as (NVOC-AUT)-Au.

4.3.4 Photoactivation

To cleave the photoactive NVOC from the (NVOC-AUT)-Au surface, UV irradiation from a 365 nm Longwave UV lamp (Black-Ray B-100 Longwave UV lamp, 100W, UVP, Upland, CA) was used on the (NVOC-AUT)-Au surface. Specifically, (NVOC-AUT)-Au surfaces were submerged in a 1M glycine aqueous solution before the UV irradiation. The

distance between the lamp and the sample was approximately 5 cm, and the light intensity was 15.50 mW/cm^2 as determined by a digital radiometer (Model UVX, UVP, Upland, CA). The irradiation time was 5 min. In order to pattern surfaces, two irradiations were sequentially applied to different regions of the surface with the use of a photomask (MPC Circuits, Ottawa, ON) in the first illumination -- the photomask was placed directly on top of the surface during the first light exposure to minimize light scattering. After each irradiation, the uncaged surfaces were washed extensively and dried as mentioned in the previous step.

4.3.5 Biomolecule immobilization

PEG or protein was immobilized on the surface after UV exposure. Briefly, a photo-uncaged surface (with or without a photomask) was reacted with PEG to create cell non-permissive patterns in selected regions of the surface or on the whole surface. To achieve this, an initially illuminated surface was put into a well of a 24-well plate (Corning, Lowell, MA), and 1ml of 10 mg/ml PEG solution in PBS (Pierce, Rockford, IL) was added into the well with 1mg bis(sulfosuccinimidyl) suberate (BS^3) (Pierce, Rockford, IL). The reaction was allowed to take place at 4˚C with minimum agitation overnight.

Alternatively, for protein immobilization, BSA was used as a model protein to generate a homogeneous protein immobilized surface for subsequent surface characterizations. Finally, to create a patterned surface for PC12 cell studies, after the first irradiation with a photomask, PEG immobilization, and the second irradiation without a photomask, LAM (BD Bioscience, Bedford, MA) was immobilized on selected regions defined by the second exposure. Specifically, for BSA immobilization, 1ml BSA (10 mg /ml) solution with 1 mg BS^3 was reacted with photo-uncaged amines on the SAM surface using the same reaction conditions as mentioned above. For LAM immobilization, 1 ml LAM (500 ug/ml) solution was reacted with the photoactive SAM surface after the second exposure (i.e. PEG patterned surface after the first illumination through a photomask) by the BS^3 chemistry. The resulting surfaces were stored in PBS at 4˚C for future use.

4.3.6 PC12 cell culture

4.3.6.1 Cell culture and seeding

The PC12 rat pheochromocytoma cell line is an established model for nerve growth factor (NGF)-induced neurite formation. PC12 cells (ATCC, **Manassas, VA)** were routinely cultured and maintained in Dulbecco's Modified Eagle Medium (DMEM) (Thermo Fisher Scientific, Ottawa, ON) with 10% (v/v) horse serum (Thermo Fisher Scientific) and 5% (v/v) fetal bovine serum (Thermo Fisher Scientific).

For cell experiments, PC12 cells were detached from the culturing flask by repeated gentle pipetting. Needle and syringe were used, if necessary, to break up cell clumps and form a single cell suspension. Cells were seeded on different surfaces in wells of a 24-well plate at a cell density of 3×10^5 cells/cm^2. In order to induce PC12 differentiation and neurite outgrowth for the LAM patterned samples, NGF (2.5s, beta subunit) (Cedarlane, Burlington, ON) was added to the culture 2h after cell seeding to achieve a final NGF concentration of 50 ng/ml. Tissue culture polystyrene (TCPS) was used as a control surface for the studies.

4.3.6.2 Microscopy

In order to visualize cell growth and cell morphologies, PC12 cells were stained with fluorescent Calcein AM (Invitrogen, Carlsbad, CA) immediately before observation based on a protocol provided by the vendor. Briefly, the cells to be stained were gently rinsed with DMEM followed by the treatment of a 2 μM Calcein AM working solution in DMEM to stain the cells for 30 min at 37℃. The fluorescent dye was then removed from the culture which was further gently washed with pre-warmed DMEM. Stained cells were observed using a fluorescence microscope (Olympus IX81) and the observation was documented by Image-Pro Plus software (Media Cybemetics, Silver Spring, MD).

4.3.7 Surface characterizations

4.3.7.1 UV-Vis spectrophotometry

To confirm the formation and photolysis of caged self-assembled molecule, UV-Vis spectroscopy was used to study the absorbance spectra of NVOC-AUT as a function of different irradiation durations in chloroform. Specifically, 0.25 mg/ml NVOC-AUT chloroform solution was prepared for this study. Various pre-determined irradiation time from 0 min to 30 min was used to photo-uncage the NVOC-AUT. The spectra were recorded and analyzed using a Lambda 25 spectrophotometer (PerkinElmer, Waltham, MA).

4.3.7.2 Water contact angle (WCA)

Water contact angles of different modified surfaces were obtained using the sessile drop method with a VCA Optima XE system (AST product, Billerica, MA). The surfaces of (NVOC-AUT)-Au, UV-(NVOC-AUT)-Au, PEG-UV-(NVOC-AUT)-Au and BSA-UV-(NVOC-AUT)-Au were tested immediately after surface modifications. Five random (and different) spots on each surface and two surfaces for each sample were analyzed. Both advancing and receding contact angles were recorded.

4.3.7.3 Atomic force microscopy (AFM)

To study the surface microstructures after different modifications and the surface topography changes before and after UV irradiation, AFM imaging was carried out using a Veeco Multimode AFM Nanoscope V (Veeco Instruments, Santa Barbara, CA). All images were collected in tapping mode in air at room temperature using a low-force Si tip. Multiple testing areas on each sample surface were analyzed. Surface roughness of 5 areas of each sample was quantified with the roughness function in the Nanoscope software.

4.3.7.4 Cyclic voltammetry (CV)

Cyclic voltammetry was performed using a VSP-Modular 5 Channels Potentiostat/Galvanostat/EIS (BioLogic Science Instrument, Claix, France). A platinum wire was used as the counter electrode; an Hg/Hg_2SO_4 (K_2SO_4) electrode was used as the reference; different sample surfaces were used individually as the working electrode. An

alligator clip was used to attach the samples, and a surface area of ~0.6 cm^2 was immersed into the electrolyte solution. The electrolyte solution was an aqueous solution with 1 mM potassium ferricyanide and 0.1 M potassium chloride. Voltammograms were scanned from -0.8 V to + 0.2 V at a scanning rate of 50 mV/s.

4.3.7.5 X-ray Photoelectron Spectroscopy (XPS)

XPS spectra of different sample surfaces were obtained using Axis Ultra DLD (Kratos Analytical, Chestnut Ridge, NY) with a monochromatic Al Kα source. A fixed take-off angle of 90° was used in the study. The spectra were analyzed by CasaXPS software.

4.4 Results and Discussion

In this study, we developed a new method to control cell attachment through the introduction of photocleavable molecules to initially inactivate the tail groups of a SAM, forming a photoactive SAM. This photoactive SAM was subsequently photo-activated by a UV exposure to selectively release the caged tail functional groups in a specific time and location on the SAM. The caging agent protected self-assembled molecule was synthesized and used to form a self-assembled monolayer on gold. In the current study, AUT was utilized as the self-assembled molecule with two functional groups, thiol and primary amine. While the thiol groups interacted with the gold surface to form a highly-ordered SAM layer, the primary amines, the tail groups of the SAM, were caged by photo-cleavable NVOC. Therefore when irradiated by UV with a photomask, the caged primary amines on selected regions of the photoactive SAM were uncaged and thereby recovered, enabling further PEG immobilization on the illuminated areas to render these regions cell non-adhesive. Similarly, a second UV irradiation without a photomask followed by immobilization of LAM on the remaining SAM surfaces rendered the rest of the surface cell-adhesive. Therefore, after two UV irradiations and subsequent surface modifications, an alternating pattern of PEG and LAM was achieved. PC12 cells that can mimic neurite outgrowth were used for cell attachment studies and cell patterning. LAM is known as an ECM protein to promote neural cell attachment and it usually used as a cell-adhesive molecule in PC12 cell studies [40]. In addition, the existence of LAM in cell patterns could help enhance the contrast of surface property with cell non-adhesive PEG.

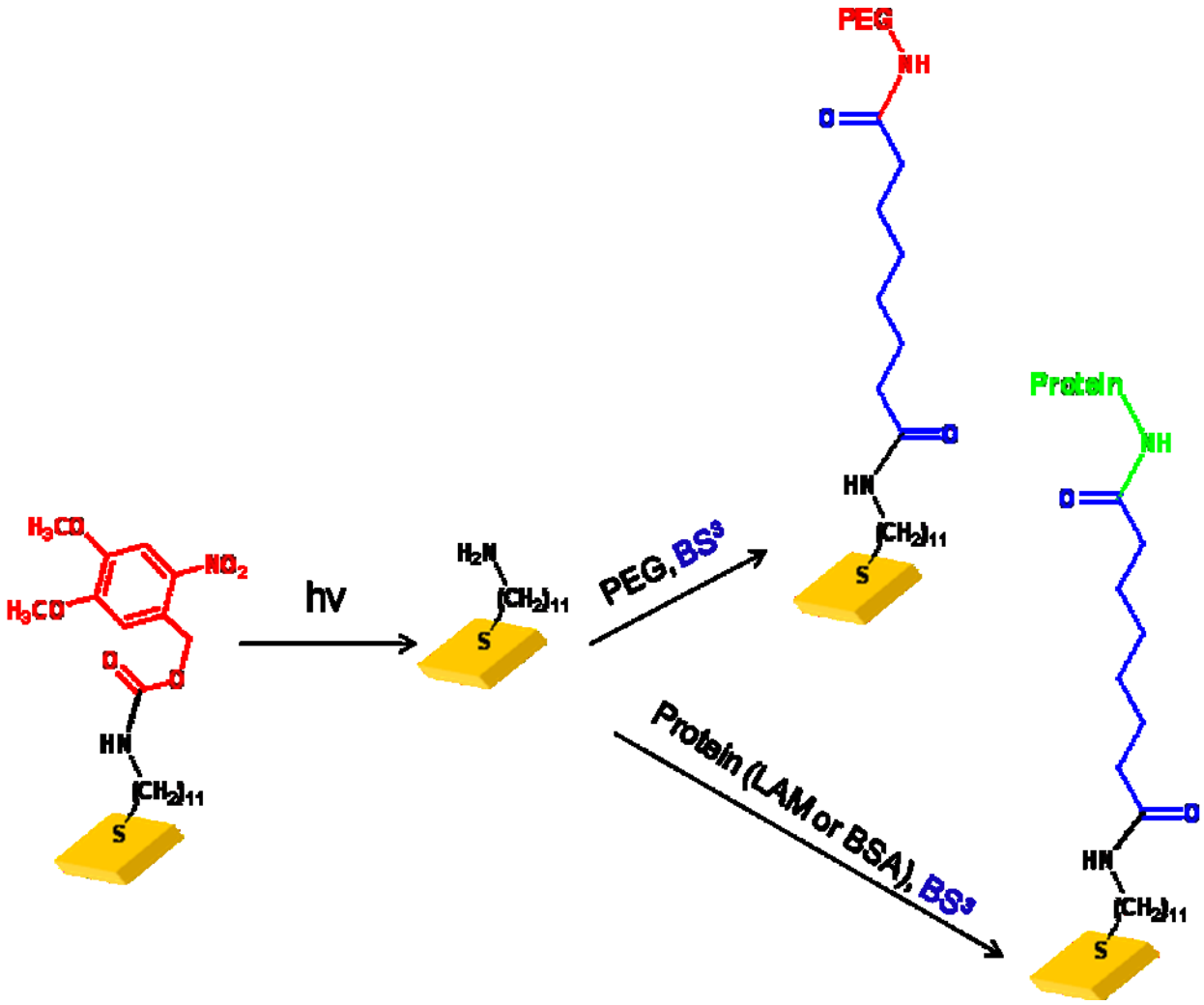

Figure 1 Structure, irradiation, and different immobilizations of photocleavable SAM on a gold surface.

4.4.1 Characterizations

4.4.1.1 Photolysis of NVOC-AUT

As shown in Figure 1, the photocleavable self-assembled molecule was used to form SAM with the nitrobenzyl group as the tail group before irradiations. The chemical reaction to synthesize NVOC-AUT, the photocaged self-assembled molecule, has been addressed in the experimental section. The formation of NVOC-AUT is through the reaction between primary amine and chloride, and then caging group NVOC was linked to the self-assembled

molecule AUT. The successful formation of NVOC-AUT was confirmed by UV-Vis. As shown in Figure 2, the original spectrum (at 0 min) of NVOC-AUT exhibited two maxima at 243 and 344 nm and a shoulder at 298 nm. This is a typical absorption spectrum of nitrobenzyl derivatives and has been well documented by many previous reports [41, 42]. Spectra for samples that received 10 min, 20 min or 30 min of irradiation showed significant changes in spectra, likely due to the photolysis of NVOC-AUT. Specifically, after the irradiation, two new peaks appeared at approximately 479 nm and 511 nm, each having slightly increasing intensities with increasing exposure times, suggesting formations of new photoreaction by-products. At the same time, the peak originally seen at 243 nm gradually shifted to a longer wavelength around 257 nm with increasing exposure times. In addition, the strong absorption at 344 nm decreased in intensity with increasing exposure times while slightly shifting to a longer wavelength. This is in good agreement with Li et al. who reported that aromatic carbamate residues, as a result of the nitrobenzyl photolysis, caused red-shift of the maximum absorption peak [43]. Taken together, all the changes in UV-Vis spectra strongly suggest that photolysis of NVOC-AUT can be successfully carried out in solutions.

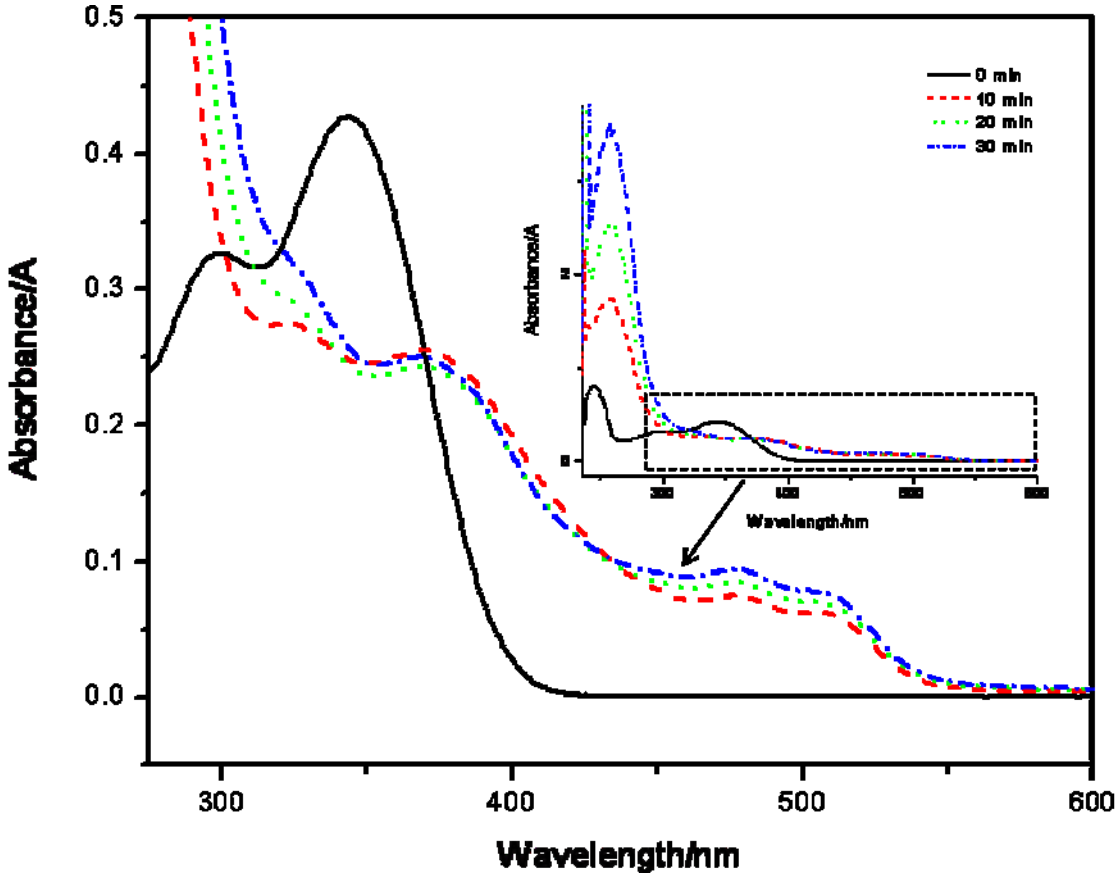

Figure 2 UV photolysis of NVOC-AUT in chloroform with different irradiation times from 0 to 30 min.

4.4.1.2 Water contact angle (WCA)

To further confirm formations of various surfaces after different surface treatments, WCAs of different surfaces were measured. Water contact angle is a parameter to characterize the surface wettability, and it is directly related to the surface energy. It is also used as a parameter to correlate with different chemical and physical property changes of the surfaces [44, 45]. As shown in Figure 3, for the photoactive SAM surface (i.e. (NVOC-AUT)-Au) the advancing water contact angle (AWCA) was measured at 64.1 ± 1.3. This can be explained by the presence of NVOC-AUT on the SAM surface, whose AWCA was mainly affected by two methoxyls with aromatic ring structure in the NVOC molecule. This

is in a good agreement with previously published results about methoxyl as the tail group of SAMs (57° and 63°) [46]. After the UV irradiation, the AWCA of the UV-(NVOC-AUT)-Au was increased to 75.0 ± 1.8, suggesting the removal of NVOC from the SAM surface and the appearance of primary amines as the tail group of the SAM layer. While this value is slightly higher than previously reported AWCAs of amine terminated SAM surfaces (63.3° and 52.9°) [47, 48] we attribute this discrepancy to the long alkane chains we used in this study and different treatment on the substrates. Interestingly, a similar AWCA result (73.2 ± 0.6) was obtained by Wang et al. on a similar amine-terminated gold surface [49]. When immobilized with PEG, the AWCA was decreased from 75.0 ± 1.8 to 61.9 ± 1.2, reflecting the hydrophilic property of the PEG molecules and confirming the success of PEG immobilization on the surface. Alternatively, when the model protein BSA was immobilized on the surface, the AWCA value was decreased from 75.0 ± 1.8 to 65.8 ± 2.7, confirming the success of BSA immobilization on the surface.

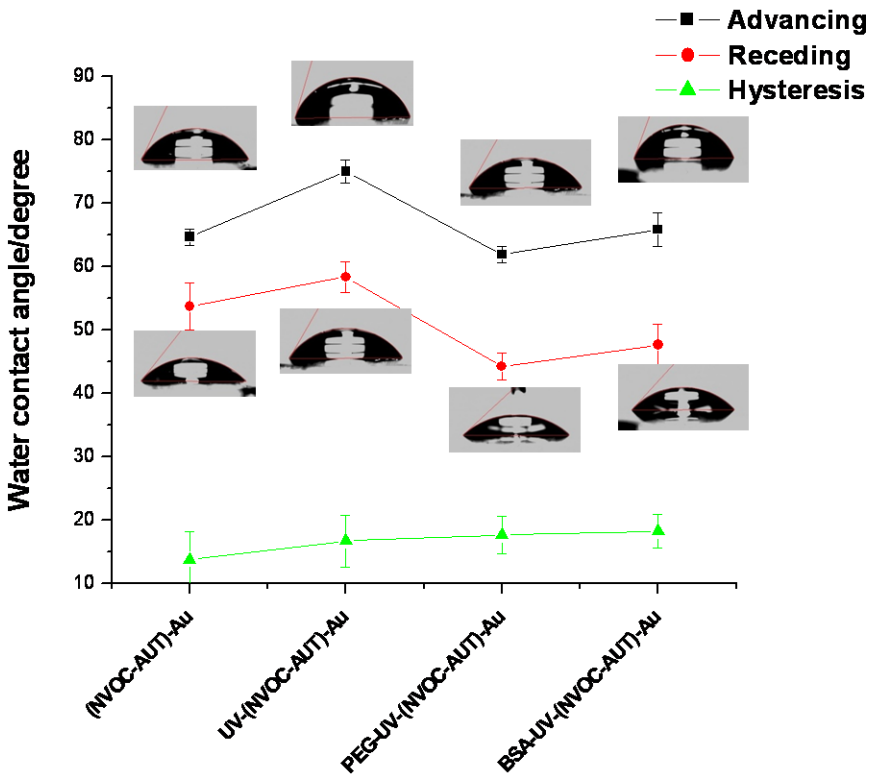

Figure 3 Water contact angle of SAM and the following surfaces after each modification.

4.4.1.3 Atomic force microscopy

AFM images and roughness data provided us with another way to characterize the surface, and provided additional information on topographical structures of the surface of our interest during surface modifications. As shown in Figure 4, four different surfaces were investigated: (NVOC-AUT)-Au, UV-(NVOC-AUT)-Au, PEG-UV-(NVOC-AUT)-Au, and BSA-UV-(NVOC-AUT)-Au. It can be concluded that the most significant topographical change was between (NVOC-AUT)-Au and UV-(NVOC-AUT)-Au. AFM images of these two surfaces showed significantly different molecular packing on gold surface, providing an additional evidence for the successful photolysis of NVOC-AUT-Au. In addition, the surface roughness was also significantly increased after the photolysis (i.e. (NVOC-AUT)-Au vs. UV-(NVOC-AUT)-Au). It is well documented that during photolysis of *o*-nitrobenzyl group, hydrogen transfer occurs from the benzyl position to the nitro functional group, and o-

nitrosobenzaldehyde is released. It is therefore likely for this free aldehyde residue to further react with the regenerated (photo-uncaged) amine on UV-(NVOC-AUT)-Au surface as a side reaction, thus resulting an increased roughness of the original surface after irradiation as measured by AFM [32, 50]. Therefore, to minimize the undesirable side reaction, a glycine solution was used during the photolysis procedure to scavenge the nitrosobenzaldehyde residues. After the immobilization of PEG on the irradiated surface, the surface roughness decreased from 2.00 to 1.63 for Rq and from 1.64 to 1.30 for Ra, respectively. It is also interesting to note that in comparison with the PEG immobilized surface (PEG-UV-(NVOC-AUT)-Au), BSA immobilized (BSA-UV-(NVOC-AUT)-Au) surface showed increased roughness. This could be explained by the different molecular structures of the two molecules. For example, the more flexible PEG molecule does not maintain a 3D molecular conformation, which would allow rearrangement on the surface even after immobilization and result in a smoother surface. In contrast, once BSA is immobilized on the surface, the 3D conformation of BSA is maintained on the surface, with no molecular rearrangement allowed, resulting in an more uneven surface [51].

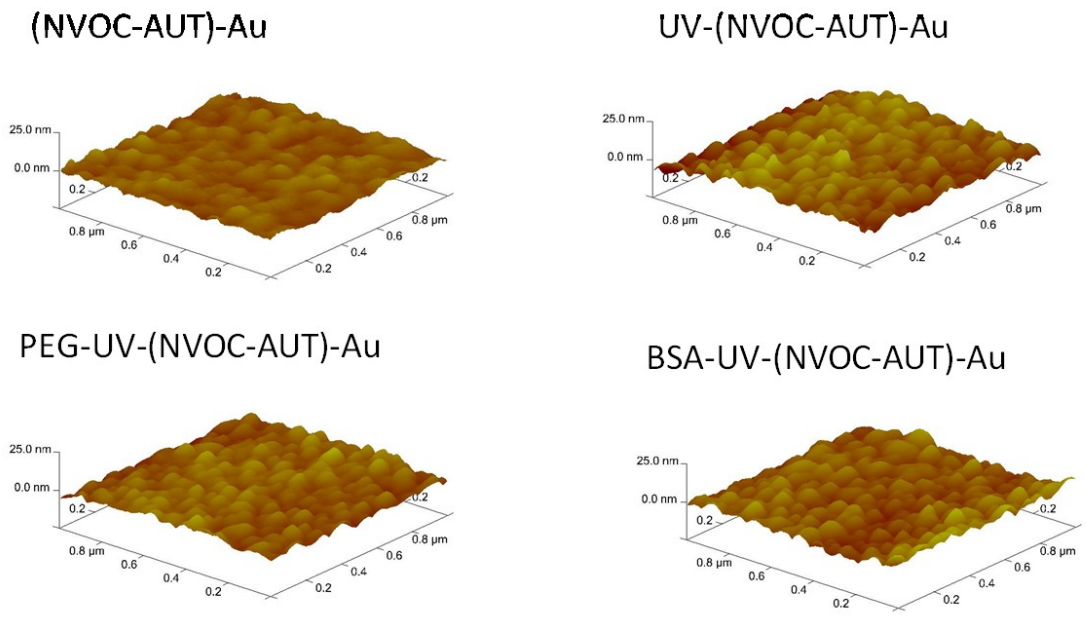

	Rq/nm	Ra/nm
(NVOC-AUT)-Au	1.20 ± 0.15	1.11 ± 0.14
UV-(NVOC-AUT)-Au	2.00 ± 0.15	1.64 ± 0.11
PEG-UV-(NVOC-AUT)-Au	1.63 ± 0.11	1.30 ± 0.10
BSA-UV-(NVOC-AUT)-Au	2.05 ± 0.16	1.63 ± 0.10

Figure 4 AFM images and roughness of SAMs after each step of modifications.

4.4.1.4 Cyclic voltammetry

Cyclic voltammetry is a potentiodynamic electrochemical measurement and it can also be used to demonstrate the different modification of SAMs. Cyclic voltammetry was performed on the bare gold surface and the surfaces after each modification step between - 0.8 V and + 0.2 V (*cf.* Figure 5). Attenuation of current for the redox process of ferricyanide in potassium chloride solution was used as an indicator to show the existence and stability of the SAM and modified SAMs. The curves confirmed the formation of a highly ordered monolayer, NVOC-AUT-Au, and the stability of this highly ordered film after each modification. CV curve for bare gold surface as the working electrode showed well-defined oxidation and reduction peaks corresponding to the redox process of ferricyanide/ferrocyanide with an anodic potential at - 0.08 V and a cathodic potential at - 0.24 V versus $Hg/HgSO_4$. After SAM formation, the presentation of NVOC-AUT on gold

surface works as an insulating layer to block electron penetration and transfer. As we saw in Figure 5, there is no redox peak when (NVOC-AUT)-Au SAM was used as the working electrode. After UV irradiation of this (NVOC-AUT)-Au, the caging agent, NVOC, was removed from the surface and amine groups are present as the tail groups. It is well documented that that different terminal groups on SAM affect electron transfer properties between the electrode and anionic ferricyanide ion [52-54]; in this study, the photo-uncaged amine groups on the SAM surface decreased the potential barrier for electron transfer between the electrode surface and $Fe(CN)_6^{4-}$ because they attracts anionic $Fe(CN)_6^{4-}$ more effectively. It is also worthwhile to note that the evolution of the voltammogram for UV-(NVOC-AUT)-Au has a good agreement with the conclusion that the longer of alkyl chain on SAM deceases the electron transfer rates compared with previous reports [55], which results in a large separation of current peaks. After the immobilization of an insulating PEG chain on the SAM, a significant decrease of the current in comparison to UV-(NVOC-AUT)-Au was found. The even larger separation of current peaks in the reversible redox process indicated a much slower electron transfer rate on PEG-UV-(NVOC-AUT)-Au. The similar blocking effect of BSA, in comparison to PEG, on the SAM gold surface was found in our CV testing and also by other researchers in their studies [56-58]. In shorts, from the electrochemical experiment, the peak presentation and evolution of different CV curves after each step of modifications confirm the stable presence of the monolayer in all modified SAM surfaces and also demonstrate the formation of the SAM, UV-irradiation, PEG and BSA immobilization proceed as expected.

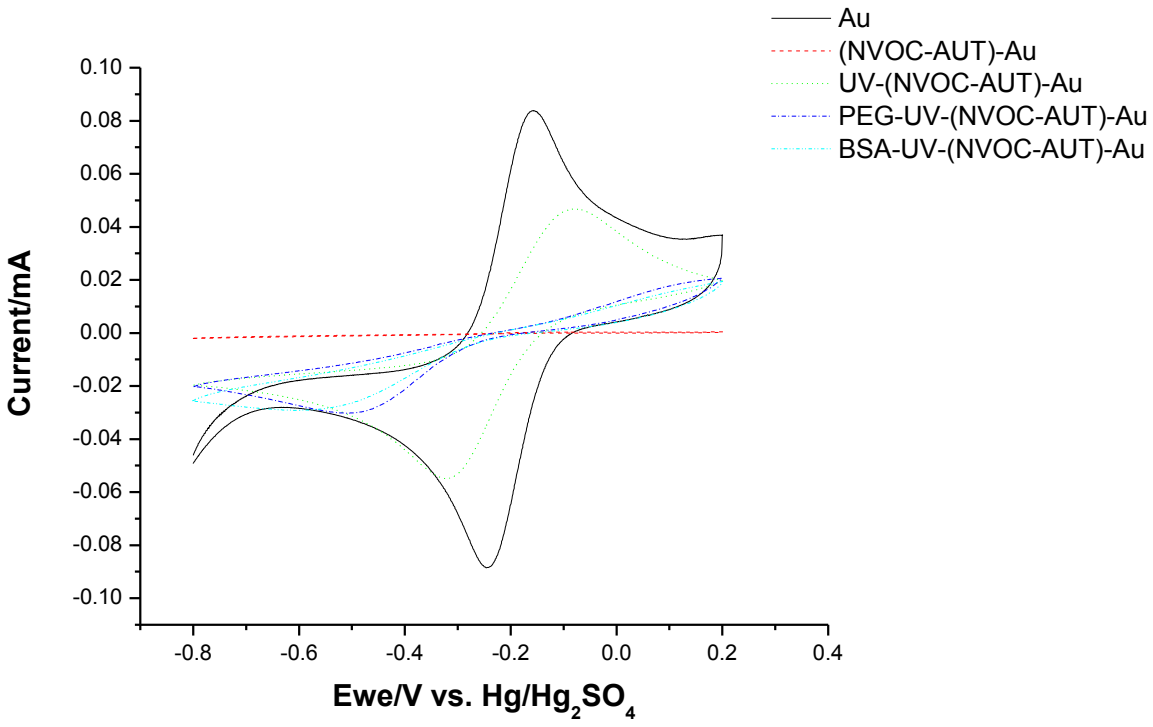

Figure 5 Cyclic voltammograms of different surfaces during the fabrication.

4.4.1.5 X-ray Photoelectron Spectroscopy (XPS)

The SAM surfaces were also be analyzed by XPS (Figure 6). XPS gives the information of relative atom concentration and the binding energies (BEs) of different atoms. On the C 1s spectrum of (NVOC-AUT)-Au surface, there were multiple overlapping peaks around 282.4 eV. These peaks arises from the 1s orbital of C-C/C-H, C-S, C-O, C-N, O=C-O and aromatic C binding. The BEs of carbon electrons change according to the different electronegativity of the adjacent atoms. The peak shifts to the higher BE with a more electronegative adjacent atom. These overlapping peaks are an evidence of different carbon binding presented on (NVOC-AUT)-Au surface. The peak at 282.4 eV is caused by the electron emission of the aromatic and aliphatic carbon; the shoulder peaks at 283.9 eV correspond to carbon atoms bonded to oxygen, nitrogen and sulphur; the distinguishing peak at 287.1 eV is a shake-up excitation caused by the $\pi \rightarrow \pi^*$ transition in the aromatic ring [59, 60]. After UV irradiation, a relatively decrease on the shoulder peak around 284.2 eV was

seen on UV-(NVOC-AUT)-Au, compared with (NVOC-AUT)-Au. Also, the disappeared wide peak of $\pi \rightarrow \pi^*$ transition around 287.1 eV is another evidence to confirm the removal of caging agent, nitrobenzyl ring, from the surface. After PEG linkage, wider peaks were observed around 284.0 eV, which could be assigned as overlapped peaks of C-O ether carbon and C-N; the wide peak at 287.0 eV is caused by carbon atoms in carbonyls. For the surface BSA-UV-(NVOC-AUT)-Au, there are peaks at 282.4 eV with a shoulder peak around 283.9 eV and a wide peak around 285.8 eV. These peaks are caused by the C-C and C-S bindings from the self-assembled molecule, AUT, and also, mainly, the carbon bonded with oxygen and nitrogen in amide and amine of the protein [61, 62].

In N 1s spectra, on (NVOC-AUT)-Au surface, there are two main peaks at 397.6 eV and 403.6 eV, respectively. The peak at lower BE (397.6 eV) is attributed to the existence of nitrogen in O=C-N. The peak at higher BE (403.6 eV), which is about 6.0 eV higher than the amide, is caused by the existence of the nitro group ($–NO_2$) in the aromatic ring of NVOC and an evidence to show NVOC molecules covalently bonded on the self-assembled molecules. After UV irradiation, NVOC is cleaved from the surface, just nitrogen in the amine left, so a single peak at 397.7 eV in N 1s spectrum is seen and it is caused by $C-NH_2$ binding in amine. After the immobilization of PEG with BS^3 crosslinker, the formation of amide bonding between BS^3 and PEG/AUT caused a peak with the BE at 397.4 eV in its N 1s spectrum. In addition, there is a BE peak at 403.4 eV in PEG-UV-(NVOC-AUT)-Au spectrum. It could be the residual component from BS^3 reaction, incompletely reacted BS^3 or BS^3 residue after crosslinking. After BSA immobilization, a sharper singlet peak with BE at 397.6 eV was shown in the spectrum and the predominant amide and amine bindings in BSA is attributed to this peak, which confirmed BSA immobilization to the surface.

Through the analysis of WCA, AFM, CV and XPS, we characterized the surface properties of different modified surfaces during our fabrication. WCA gave the wettability of surfaces and indirectly indicated the functional groups or tail groups changed on SAMs by UV irradiation and the following immobilization. AFM showed the microstructures of different surfaces and also indicated the successful modification as described in Figure 1. CV measurement provided characteristic data of different surfaces and demonstrated the formation of the SAM, UV irradiation and the different immobilization with different

performances of the potential. XPS also demonstrated different surface properties of the surfaces by investigating BEs of different elements and the shifts of these BEs.

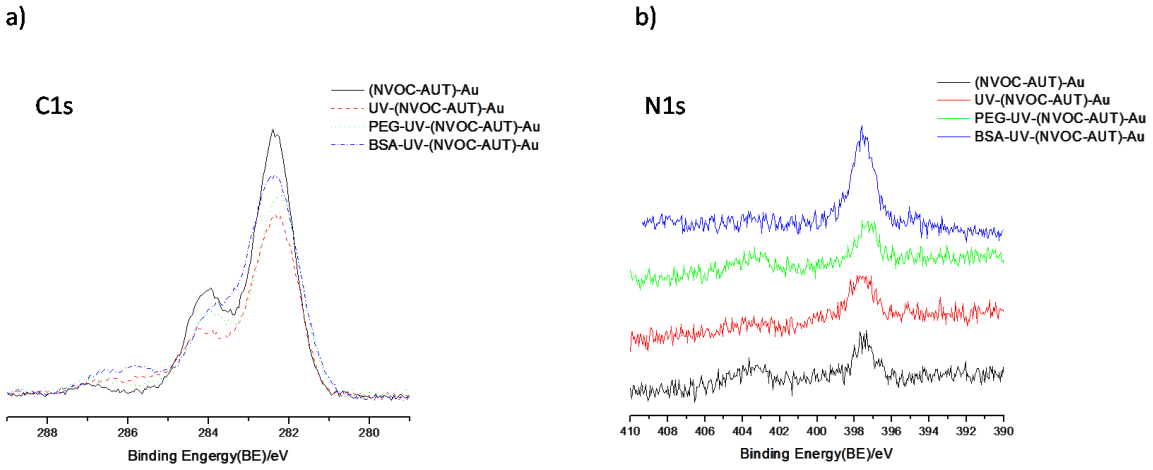

Figure 6 XPS spectrum of different modified surfaces: a) C1s spectrum of SAM surfaces; b) N1s spectrum of SAM surfaces.

4.4.2 Cell study

PC12 cell was used as a model cell line for neurons on our surface [63-65]. The cells halt proliferation and terminally differentiate when treated with NGF, which makes PC12 cells a useful model for neurite outgrowth studies.

As shown in Figure 7, it is evident that long and multiple PC12 cell strip patterns were achieved on the PEG/LAM patterned surface (Fig.7 a and b); a grid-shape patterned cell culture was observed as shown in Fig. 7 e. The shapes of cell patterns were consistent with the shapes of micro-print photomasks used to create the patterns. These different shapes of PC12 cell patterns on one flat surface suggest that double irradiation of a photoactive SAM surface followed by biomolecule immobilization allow one to successfully control chemical properties on the surfaces and thus PC12 cell initial attachment in a spatial manner. PC12 cell can selectively attach to immobilized LAM regions by specific binding between cell receptors and surface chemical cues, not PEG immobilized regions, which have a typical cell resistant property. A closer analysis of cell images at higher magnification (*cf.* Fig 7 d) reveals that that the PC 12 cells underwent a small but significant morphological change

when grown on LAM immobilized surface, as small neurites were seen on the micrographs. These small neurite outgrowths could be evidence of the existence of LAM on the surface and also suggests bioactivity of the immobilized LAM [66]. Through guided irradiation on caging agent protected SAM surface, the localization of cell adhesion was controlled. The control was relatively easy to achieve and cells were attached by specific binding between the surface and the cells.

Another cell patterns experiment was also performed on PEG/LAM patterned surfaces with diffusible NGF added. NGF was added into the cell culture medium to enhance neurite outgrowth. To avoid physical absorption of diffusible NGF onto our surface and not to interfere with cell initial attachment by immobilized LAM, the diffusible NGF was added after cell initial adhesion. The cell patterning results were shown in Figure 8. A similar cell patterning results were seen in Figure 8 a and c. Cells were patterned according to the shape of photomasks. A higher extent of morphological change and a long neurite extension were observed and indicate further PC12 differentiation (Figure 8 b and d) due to soluble signaling molecule NGF addition. Here, instead of only one biomolecules was immobilized and just for controlling cell initial adhesion, cell signaling could be further controlled on these patterned regions by the addition of soluble NGF to induce cell differentiation. Therefore, we introduced two different biomolecules into cell culture system, one is immobilized and one is diffusible in the medium. Cells can response to the two different chemical cues to attach to the specific areas and then induce the neurite growth at a specific time. In our cell culture, not only immobilized ECM protein, LAM, was studied in a patterned surface, but also the incorporation of immobilized LAM with NGF as a solute was studied. Generally, as shown in Figure 7 and 8, cell initial attachment can be controlled by applying different photomasks on the surface to control light pathway. As seen in the high-magnification images, neurite outgrowth can be found on both surfaces. However, the small extent of PC12 cell differentiation and neurite outgrowth was found on PEG/LAM patterned surfaces without diffusible NGF added while a long neurite extension was observed on PEG/LAM patterned surfaces with diffusible NGF added. The results are consistent with previous study done by Achyuta et al. [66]: on a LAM immobilized surface, the existence of diffusible NGF resulted in a dramatic increase in neurite outgrowth. Our results suggest that LAM has a specific impact on cell initial attachment while NGF plays a significant role on neurite sprouting.

Therefore, instead of controlling only the position of cell adhesive molecule LAM and eventually cells on one surface, the introduction of diffusible NGF in the cell culture medium helps to examine the effects of cell adhesion and cell differentiation separately and in a controllable temporal manner. The precise localized LAM on one flat surface has the potential to help create a 2D *in* vitro neuronal network, which could mimic the one in a native tissue, and the addition of NGF could provide further control on the network by modulating neurite outgrowth on a specific time. This strategy could potentially be exploited to design different neuronal networks for various applications in nerve tissue engineering.

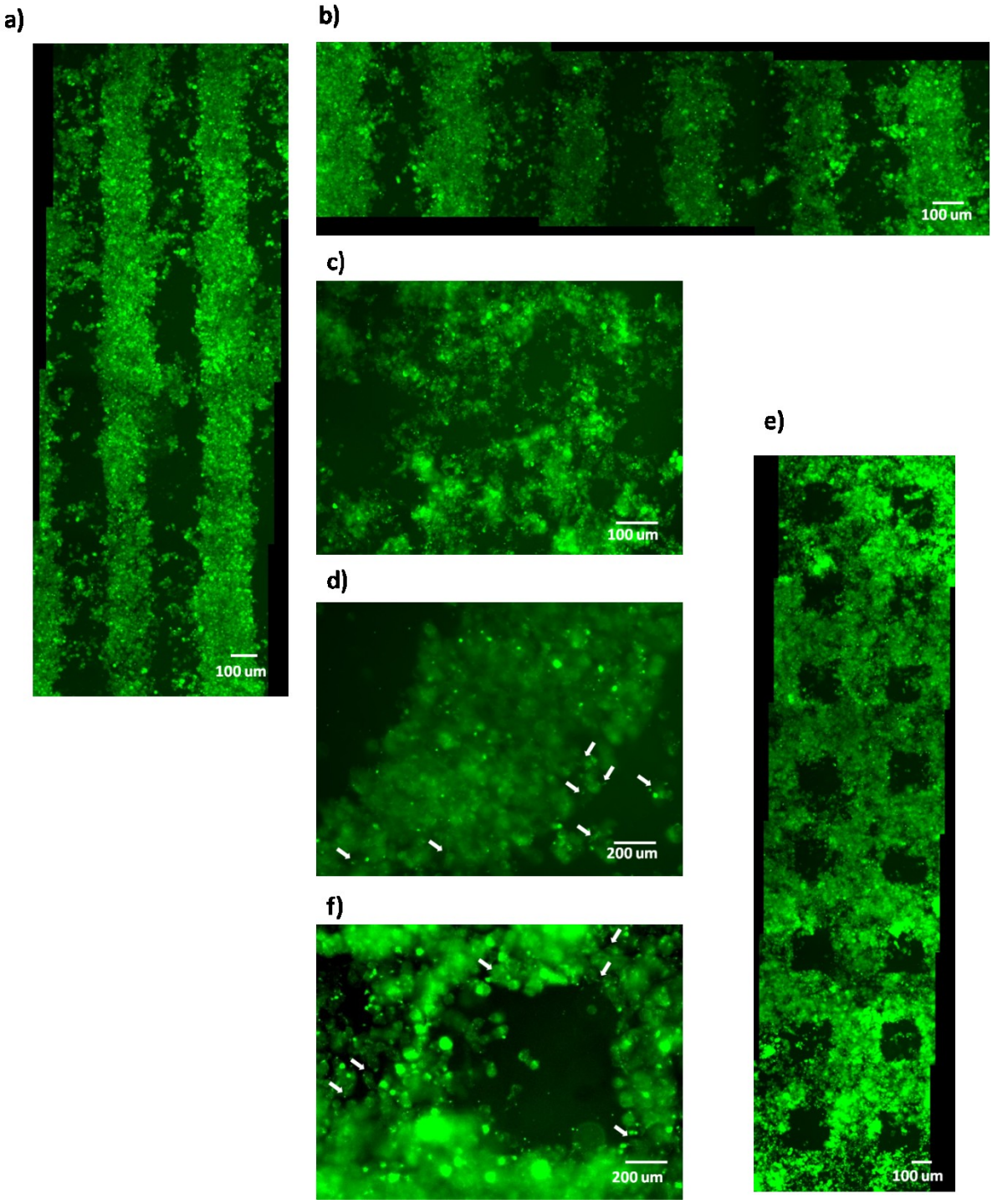

Figure 7 Microscopical images of PC12 cell labeled with Calcein AM after 3 days of seeding onto PEG/LAM surfaces. Tiled PC12 cell images to show the length and the width of PC12 cell patterning on PEG/LAM surfaces, a) and b); PC12 cell cultured in TCPS as a control, c); higher-magnification PC12 cell in the strip-pattern, d). The strip-photomask with alternating

100 um and 200 um transparent and black strips was applied on a), b) and d). Tiled PC12 cell patterning and high magnification with a square-photomask applied on e) and f). The square-photomask has 200 um x 200 um black squares and 250 um inter-square spacing. The arrows in d) and f) indicated the neurite outgrowth in the patterns.

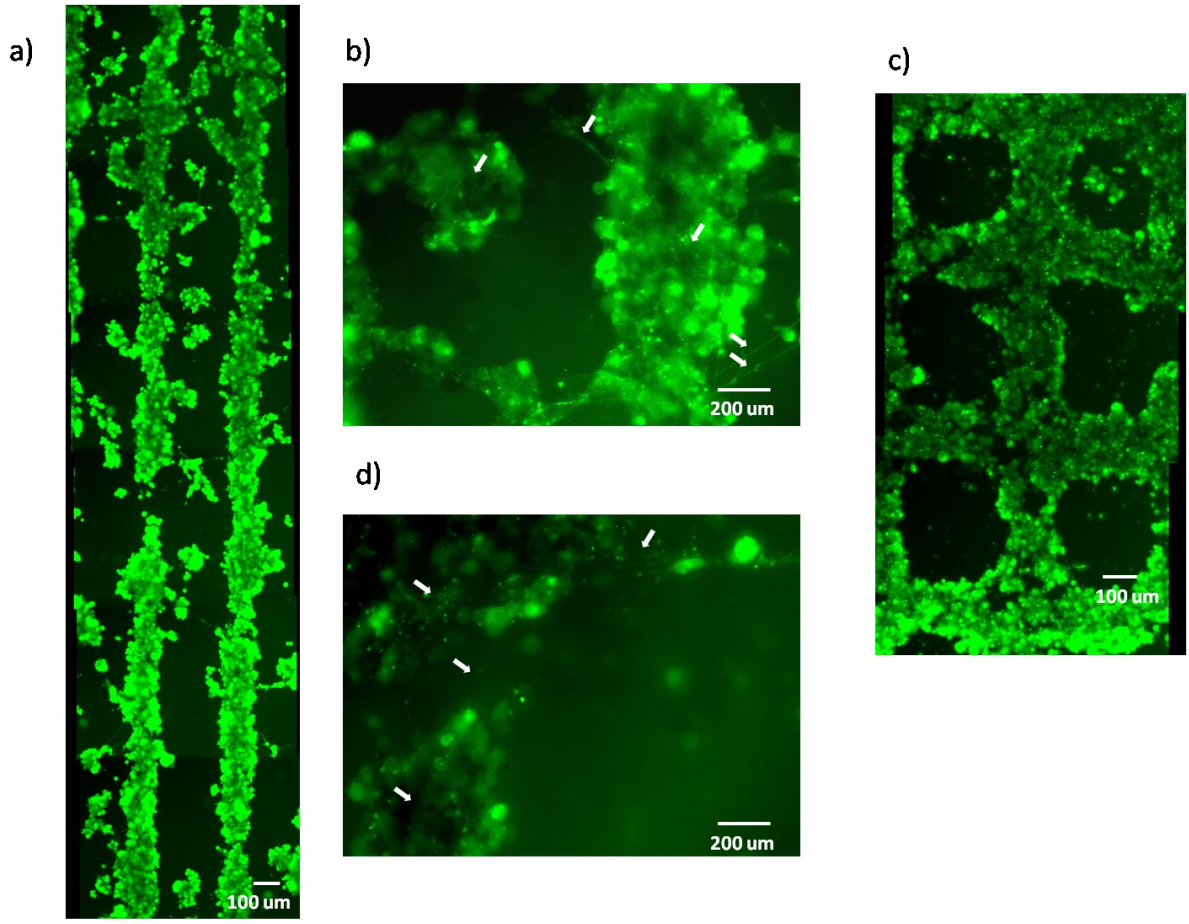

Figure 8 Microscopical images of PC12 cell labeled with Calcein AM after 3 days of seeding onto PEG/LAM surfaces with diffusible NGF addition. Tiled PC12 cell images to show the length of PC12 cell patterning on PEG/LAM surfaces, a); higher-magnification PC12 cell in the strip-pattern, b). The strip-photomask with alternating 100 um and 200 um transparent and black strips was applied on a) and b). Tiled PC12 cell patterning and high magnification with a square-photomask applied on c) and d). The square-photomask has 200 um x 200 um black squares and 250 um inter-square spacing. The arrows in b) and d) indicated the neurite outgrowth in the patterns.

4.5 Conclusion

In this paper, we addressed a new approach to control cell initial attachment on a SAM-gold surface. Differently from cell patterning on degradable materials, this surface is designed for *in vitro* studies. We took advantage of the well-known alkanethiol-gold SAM system to create a platform. By applying a photocleavable self-assembled molecule on gold which was used to protect and inactivate primary amines on the original self-assembled molecule, we can control the presence of amine functional groups in a spatial manner. By applying double UV irradiations with a photomask, the presence of reactive amines on a specific region could be controlled and heterogeneous properties of the surface for cell attachment and behaviors can be realized. Cell non-adhesive PEG and cell adhesive molecule, ECM protein LAM, were introduced into our system to react with recovered amines in a controllable manner. Finally the cell position can be precisely controlled. To characterize the surfaces, different surface characterization techniques were applied. WCA, CV, XPS and AFM provide the characterization of different surface properties including wettability, electrochemical property, element binding formation and microstructure. Overall cell culture results showed that by double UV irradiations on one surface on different time in different location with a photomask to control light pathway, controllable cell attachment with PC12 cells on PEG/LAM-patterned surfaces was achieved, and further neurite outgrowth on the patterned cells can be manipulated by NGF addition. The further addition of diffusible NGF in the system provided us an alternative way to study cell adhesion and cell differentiation separately in one system with controllable cell position. We believe this approach has the potential to be used as an *in vitro* cell-cell interaction platform to understand neuron behaviors and also design complex neuronal networks for nerve tissue engineering.

4.6 Reference

1. Benecke, B.J., A. Benzeev, and S. Penman, *CONTROL OF MESSENGER-RNA PRODUCTION, TRANSLATION AND TURNOVER IN SUSPENDED AND REATTACHED ANCHORAGE-DEPENDENT FIBROBLASTS.* Cell, 1978. **14**(4): p. 931-939.
2. Folkman, J. and A. Moscona, *ROLE OF CELL-SHAPE IN GROWTH-CONTROL.* Nature, 1978. **273**(5661): p. 345-349.
3. Gospodarowicz, D., G. Greenburg, and C.R. Birdwell, *DETERMINATION OF CELLULAR SHAPE BY EXTRACELLULAR MATRIX AND ITS CORRELATION WITH CONTROL OF CELLULAR GROWTH.* Cancer Research, 1978. **38**(11): p. 4155-4171.

4. Saneinejad, S. and M.S. Shoichet, *Patterned glass surfaces direct cell adhesion and process outgrowth of primary neurons of the central nervous system.* Journal of Biomedical Materials Research, 1998. **42**(1): p. 13-19.
5. Hsiao, Y.S., et al., *Manipulating location, polarity, and outgrowth length of neuron-like pheochromocytoma (PC-12) cells on patterned organic electrode arrays.* Lab on a Chip, 2011. **11**(21): p. 3674-3680.
6. Saha, K., et al., *Substrate Modulus Directs Neural Stem Cell Behavior.* Biophysical Journal, 2008. **95**(9): p. 4426-4438.
7. Singhvi, R., et al., *ENGINEERING CELL-SHAPE AND FUNCTION.* Science, 1994. **264**(5159): p. 696-698.
8. Mrksich, M., et al., *Using microcontact printing to pattern the attachment of mammalian cells to self-assembled monolayers of alkanethiolates on transparent films of gold and silver.* Experimental Cell Research, 1997. **235**(2): p. 305-313.
9. Oliva, A.A., et al., *Patterning axonal guidance molecules using a novel strategy for microcontact printing.* Neurochemical Research, 2003. **28**(11): p. 1639-1648.
10. Nishizawa, M., K. Takoh, and T. Matsue, *Micropatterning of HeLa cells on glass substrates and evaluation of respiratory activity using microelectrodes.* Langmuir, 2002. **18**(9): p. 3645-3649.
11. VandeVondele, S., J. Voros, and J.A. Hubbell, *RGD-Grafted poly-l-lysine-graft-(polyethylene glycol) copolymers block non-specific protein adsorption while promoting cell adhesion.* Biotechnology and Bioengineering, 2003. **82**(7): p. 784-790.
12. Keselowsky, B.G., D.M. Collard, and A.J. Garcia, *Surface chemistry modulates focal adhesion composition and signaling through changes in integrin binding.* Biomaterials, 2004. **25**(28): p. 5947-5954.
13. Falconnet, D., et al., *A combined photolithographic and molecular-assembly approach to produce functional micropatterns for applications in the biosciences.* Advanced Functional Materials, 2004. **14**(8): p. 749-756.
14. Dillmore, W.S., M.N. Yousaf, and M. Mrksich, *A photochemical method for patterning the immobilization of ligands and cells to self-assembled monolayers.* Langmuir, 2004. **20**(17): p. 7223-7231.
15. Hypolite, C.L., et al., *Formation of microscale gradients of protein using heterobifunctional photolinkers.* Bioconjugate Chemistry, 1997. **8**(5): p. 658-663.
16. Brown, A.A., O. Azzaroni, and W.T.S. Huck, *Photoresponsive Polymer Brushes for Hydrophilic Patterning.* Langmuir, 2009. **25**(3): p. 1744-1749.
17. Chen, S.Y. and L.M. Smith, *Photopatterned Thiol Surfaces for Biomolecule Immobilization.* Langmuir, 2009. **25**(20): p. 12275-12282.
18. Luo, Y. and M.S. Shoichet, *A photolabile hydrogel for guided three-dimensional cell growth and migration.* Nature Materials, 2004. **3**(4): p. 249-253.
19. Pardo, L., W.C. Wilson, and T.J. Boland, *Characterization of patterned self-assembled monolayers and protein arrays generated by the ink-jet method.* Langmuir, 2003. **19**(5): p. 1462-1466.
20. Sanjana, N.E. and S.B. Fuller, *A fast flexible ink-jet printing method for patterning dissociated neurons in culture.* Journal of Neuroscience Methods, 2004. **136**(2): p. 151-163.
21. Fox, M.A. and M.D. Wooten, *Characterization, adsorption, and photochemistry of self-assembled monolayers of 10-thiodecyl 2-anthryl ether on gold.* Langmuir, 1997. **13**(26): p. 7099-7105.
22. Li, W.J., et al., *Self-assembled monolayers of 7-(10-thiodecoxy)coumarin on gold: Synthesis, characterization, and photodimerization.* Journal of the American Chemical Society, 1997. **119**(31): p. 7211-7217.
23. Delamarche, E., et al., *THERMAL-STABILITY OF SELF-ASSEMBLED MONOLAYERS.* Langmuir, 1994. **10**(11): p. 4103-4108.

24. Beulen, M.W.J., et al., *Electrochemical stability of self-assembled monolayers on gold.* Langmuir, 1998. **14**(26): p. 7463-7467.
25. Mrksich, M., et al., *Controlling cell attachment on contoured surfaces with self-assembled monolayers of alkanethiolates on gold.* Proceedings of the National Academy of Sciences of the United States of America, 1996. **93**(20): p. 10775-10778.
26. Song, Y.F., et al., *Micropatterned Surfaces with Covalently Grafted Unsymmetrical Polyoxometalate-Hybrid Clusters Lead to Selective Cell Adhesion.* Journal of the American Chemical Society, 2009. **131**(4): p. 1340-+.
27. Zhao, C., et al., *Microelectrochemical modulation of micropatterned cellular environments.* Langmuir, 2008. **24**(14): p. 7605-7613.
28. Jing, G., S.F. Perry, and S. Tatic-Lucic, *Precise cell patterning using cytophobic self-assembled monolayer deposited on top of semi-transparent gold.* Biomedical Microdevices, 2010. **12**(5): p. 935-948.
29. Zhao, B., J.S. Moore, and D.J. Beebo, *Pressure-sensitive microfluidic gates fabricated by patterning surface free energies inside microchannels.* Langmuir, 2003. **19**(5): p. 1873-1879.
30. Nakanishi, J., et al., *Photoactivation of a substrate for cell adhesion under standard fluorescence microscopes.* Journal of the American Chemical Society, 2004. **126**(50): p. 16314-16315.
31. Hoffmann, C. and G.E.M. Tovar, *Mixed self-assembled monolayers (SAMs) consisting of methoxy-tri(ethylene glycol)-terminated and alkyl-terminated dimethylchlorosilanes control the non-specific adsorption of proteins at oxidic surfaces.* Journal of Colloid and Interface Science, 2006. **295**(2): p. 427-435.
32. Hoffmann, N., *Photochemical reactions as key steps in organic synthesis.* Chemical Reviews, 2008. **108**(3): p. 1052-1103.
33. Jang, K., et al., *Single-cell attachment and culture method using a photochemical reaction in a closed microfluidic system.* Biomicrofluidics, 2010. **4**(3).
34. Kikuchi, Y., et al., *Arraying Heterotypic Single Cells on Photoactivatable Cell-Culturing Substrates.* Langmuir, 2008. **24**(22): p. 13084-13095.
35. Cheng, N. and X.D. Cao, *Photosensitive chitosan to control cell attachment.* Journal of Colloid and Interface Science. **361**(1): p. 71-78.
36. Cheng, N. and X.D. Cao, *Photoactive SAM surface for control of cell attachment.* Journal of Colloid and Interface Science, 2010. **348**(1): p. 71-79.
37. Barille, R., et al., *Photo-responsive polymer with erasable and reconfigurable micro- and nano-patterns: An in vitro study for neuron guidance.* Colloids and Surfaces B-Biointerfaces, 2011. **88**(1): p. 63-71.
38. Gustavsson, P., et al., *Neurite guidance on protein micropatterns generated by a piezoelectric microdispenser.* Biomaterials, 2007. **28**(6): p. 1141-1151.
39. Yang, I.H., C.C. Co, and C.C. Ho, *Controlling neurite outgrowth with patterned substrates.* Journal of Biomedical Materials Research Part A. **97A**(4): p. 451-456.
40. Koh, H.S., et al., *Enhancement of neurite outgrowth using nano-structured scaffolds coupled with laminin.* Biomaterials, 2008. **29**(26): p. 3574-3582.
41. Katz, J.S. and J.A. Burdick, *Light-Responsive Biomaterials: Development and Applications.* Macromolecular Bioscience, 2010. **10**(4): p. 339-348.
42. Blawas, A.S., et al., *Step-and-repeat photopatterning of protein features using caged/biotin-BSA: Characterization and resolution.* Langmuir, 1998. **14**(15): p. 4243-4250.
43. Li, Y., et al., *Photoresponsive Nanocarriers Based on PAMAM Dendrimers with a o-Nitrobenzyl Shell.* Journal of Polymer Science Part a-Polymer Chemistry, 2010. **48**(3): p. 551-557.
44. Rotta, J., et al., *Parameters of color, transparency, water solubility, wettability and surface free energy of chitosan/hydroxypropylmethylcellulose (HPMC) films plasticized with sorbitol.*

Materials Science & Engineering C-Biomimetic and Supramolecular Systems, 2009. **29**(2): p. 619-623.
45. Lopez-Perez, P.M., et al., *Effect of chitosan membrane surface modification via plasma induced polymerization on the adhesion of osteoblast-like cells.* Journal of Materials Chemistry, 2007. **17**(38): p. 4064-4071.
46. Harder, P., et al., *Molecular conformation in oligo(ethylene glycol)-terminated self-assembled monolayers on gold and silver surfaces determines their ability to resist protein adsorption.* Journal of Physical Chemistry B, 1998. **102**(2): p. 426-436.
47. Contreras, A.E., et al., *Studying the Role of Common Membrane Surface Functionalities on Adsorption and Cleaning of Organic Foulants Using QCM-D.* Environmental Science & Technology, 2011. **45**(15): p. 6309-6315.
48. Arima, Y. and H. Iwata, *Effects of surface functional groups on protein adsorption and subsequent cell adhesion using self-assembled monolayers.* Journal of Materials Chemistry, 2007. **17**(38): p. 4079-4087.
49. Wang, M.S., et al., *Evaluating protein attraction and adhesion to biomaterials with the atomic force microscope.* Langmuir, 2004. **20**(18): p. 7753-7759.
50. Hoffmann, N., J.C. Gramain, and H. Bouas-Laurent, *Photochemistry in organic synthesis.* Actualite Chimique, 2008(317): p. 6-13.
51. Rundqvist, J., J.H. Hoh, and D.B. Haviland, *Substrate effects in poly(ethylene glycol) self-assembled monolayers on granular and flame-annealed gold.* Journal of Colloid and Interface Science, 2006. **301**(1): p. 337-341.
52. Garcia-Raya, D., et al., *Electrochemical characterization of a 1,8-octanedithiol self-assembled monolayer (ODT-SAM) on a Au(111) single crystal electrode.* Electrochimica Acta, 2008. **53**(27): p. 8026-8033.
53. Takehara, K. and Y. Ide, *ELECTROCHEMICAL PROPERTIES OF A GOLD ELECTRODE MODIFIED WITH A MIXED MONOLAYER.* Bioelectrochemistry and Bioenergetics, 1992. **27**(2): p. 207-219.
54. Molinero, V. and E.J. Calvo, *Electrostatic interactions at self assembled molecular films of charged thiols on gold.* Journal of Electroanalytical Chemistry, 1998. **445**(1-2): p. 17-25.
55. Becka, A.M. and C.J. Miller, *ELECTROCHEMISTRY AT OMEGA-HYDROXY THIOL COATED ELECTRODES .3. VOLTAGE INDEPENDENCE OF THE ELECTRON-TUNNELING BARRIER AND MEASUREMENTS OF REDOX KINETICS AT LARGE OVERPOTENTIALS.* Journal of Physical Chemistry, 1992. **96**(6): p. 2657-2668.
56. Balasubramanian, S., A. Revzin, and A. Sirnonian, *Electrochemical desorption of proteins from gold electrode surface.* Electroanalysis, 2006. **18**(19-20): p. 1885-1892.
57. Fu, Y.Z., et al., *Study on the immobilization of anti-IgG on Au-colloid modified gold electrode via potentiometric immunosensor, cyclic voltammetry, and electrochemical impedance techniques.* Colloids and Surfaces B-Biointerfaces, 2005. **40**(1): p. 61-66.
58. Tang, D.P., R. Yuan, and Y.Q. Chai, *Novel immunoassay for carcinoembryonic antigen based on protein A-conjugated immunosensor chip by surface plasmon resonance and cyclic voltammetry.* Bioprocess and Biosystems Engineering, 2006. **28**(5): p. 315-321.
59. Dieckhoff, S., et al., *XPS STUDIES OF THIN POLYCYANURATE FILMS ON SILICON-WAFERS.* Fresenius Journal of Analytical Chemistry, 1995. **353**(3-4): p. 278-281.
60. Schmidt, R., et al., *Azobenzene-functionalized alkanethiols in self-assembled monolayers on gold.* Applied Physics a-Materials Science & Processing, 2008. **93**(2): p. 267-275.
61. Wen, X.G., et al., *Self-assembled monolayers of hexapeptides on gold: Surface characterization and orientation distribution analysis.* Journal of Physical Chemistry A, 2004. **108**(45): p. 9673-9681.
62. Ramanathan, T., et al., *Amino-functionalized carbon nanotubes for binding to polymers and biological systems.* Chemistry of Materials, 2005. **17**(6): p. 1290-1295.

63. Gomez, N. and C.E. Schmidt, *Nerve growth factor-immobilized polypyrrole: Bioactive electrically conducting polymer for enhanced neurite extension.* Journal of Biomedical Materials Research Part A, 2007. **81A**(1): p. 135-149.
64. Das, K.P., T.M. Freudenrich, and W.R. Mundy, *Assessment of PC12 cell differentiation and neuritc growth: a comparison of morphological and neurochemical measures.* Neurotoxicology and Teratology, 2004. **26**(3): p. 397-406.
65. Rudkin, B.B., et al., *CELL CYCLE-SPECIFIC ACTION OF NERVE GROWTH-FACTOR IN PC12 CELLS - DIFFERENTIATION WITHOUT PROLIFERATION.* Embo Journal, 1989. **8**(11): p. 3319-3325.
66. Achyuta, A.K.H., et al., *Synergistic Effect of Immobilized Laminin and Nerve Growth Factor on PC12 Neurite Outgrowth.* Biotechnology Progress, 2009. **25**(1): p. 227-234.

Chapter 5 Photosensitive Chitosan to Control Cell Attachment

Nan Cheng and Xudong Cao

Journal of Colloid and Interface Science

2011, 361(1), 71-78

5.1 Abstract

An approach to control cell adhesion using a photocleavable molecule on chitosan has been developed and studied. Photocleavable 4,5-dimethoxy-2-nitrobenzyl chloroformate (NVOC) was introduced into chitosan to control the surface properties. The two UV illuminations with a photomask controlled the cleavage of NVOC and the presentation of deprotected amines on one chitosan surface spatially and temporally. The following immobilizations of cell repulsive poly(ethylene glycol) after the first illumination and cell adhesive sequence Arg-Gly-Asp-Ser (RGDS) after the second illumination on the surface helped create surface heterogeneity. Fourier transform infrared spectroscopy (FTIR), water contact angle and UV-Visible spectroscopy were used to characterize the surfaces and photoactivation during the process. To study cell attachment and morphology on our designed surfaces, NIH/3T3 fibroblast cell was used. Cell number and morphology on the surfaces were investigated. The cell study demonstrated the feasibility of the surfaces on the control of cell adhesion and the formation of cell patterns by UV illuminations and the following immobilizations of different biomolecules.

5.2 Introduction

Cells are essential to all biological processes. Many cell functions and behaviors are modulated by environmental conditions. For example, most cells must first attach to a surface in order to spread on the surface and respond to complex surface cues such as substrate rigidity and ligand presentation. Therefore spatial control of material properties at the micron scale – comparable to that of a cell -- is of great importance, and the presentation of surface cues in a spatial and temporal manner will be beneficial to cell related studies, such as the applications of cell-based biosensor and tissue engineering [1]. But currently most cell-based studies are based on a large groups of cells and the cells are less controlled spatially and temporally on the designed surfaces [2, 3]. To carry out cell studies on a reduced number of cells, which are well controlled in space and time, will improve the precision of the results and help speed up the process. Here we will present a new approach to get cell patterning on polymer film through photochemistry.

One of the most promising methods to create a surface that presents multiple surface cues is by using photoliable molecules and light to selectively change surface functional groups and signaling molecules [3, 4]. The use of photoliable molecules, especially photocleavable molecules in the design, provides a convenient and precise way to control the locations of proteins and cells. Light, as a stimulus, is particularly attractive choice in controlling biomaterial functionalities [5]. In addition, the chemistry is "clean" with no reagents added during the photo-activation. Most importantly, it can be easily controlled using wavelength and intensity [6]. Particularly, it allows complex exposure areas with high spatial resolution by simply using photomasks, micro-mirror arrays or lasers [7-11]. Therefore using light to alter surface properties and achieve protein and cell patterning is a promising strategy to develop a platform for a wide range of biological applications such as tissue engineering, studies on cell-cell interactions and high-throughout drug screenings [12-14].

Chitosan (CS) is a naturally occurring polysaccharide, and its derivatives have been widely studied as promising biomaterials in many applications due to its biocompatibility, biodegradability, non-toxicity and antimicrobial activities [15, 16]. In addition, modified

chitosans have been used as gene delivery carriers [17-20], tissue engineering scaffolds [21, 22], and wound dressings biomaterial [23, 24]. In this study, we report a two-step UV-irradiation method on a photoactive chitosan substrate to achieve cell patterning. To achieve this, the photoactive chitosan is created by covalently binding 2-nitrobenzyl photocleavable functional groups via primary amines on the chitosan molecules. By applying near-UV illuminations to different selected regions of the modified chitosan substrate, the photoactive 2-nitrobenzyl is photocleaved from the chitosan molecules upon irradiation thereby releasing the protected primary amine groups for further reactions with both cell non-adhesive – upon the first exposure -- and cell adhesive molecules – upon the second exposure -- to render different cell adhesiveness properties on different region of the same chitosan surface. By grafting the photocleavable molecule on primary amines of CS, UV light and photomask designed, we demonstrate that the two-step UV illuminations followed by immobilizations of different biofunctional molecules can achieve spatial and temporal control over surface properties on a two-dimensional substrate. In comparison with other efforts to use single UV illumination to realize the control of surface functionality and achieve protein or cell patterns [8, 25, 26], our control of functional groups on the surface is through two UV illuminations. This enables a better control of surface cues for cell adhesion, generating a surface heterogeneity that is ultimately independent of remnant of the unreacted photocleavable molecules; after two UV illuminations, the photocleavable molecules used to cage the functional groups will be totally removed, and the surface properties of the substrate are no longer controlled by the photocleavable molecules and instead determined by the subsequently immobilized biomolecules.

5.3 Experimental

5.3.1 Materials

All chemicals were obtained from Sigma-Aldrich (St. Louis, MO) and used as received without any further purification unless otherwise indicated. In addition, N-hydroxysulfosuccinimide (NHS) was purchased from Pierce (Rockford, IL); glutaradehyde (GA) solution in PBS (30%) was from Fisher Scientific Canada (Ottawa, ON); peptide Arg-Gly-Asp-Ser (RGDS) was obtained from the Ottawa Hospital Research Institute (Ottawa,

ON); NIH/3T3 cell line was purchased from ATCC (Manassas, VA). Deionized distilled water (ddH_2O) was obtained from Milli-RO 10 Plus and Milli-Q UF Plus system (Bedford, MA) with an 18MΩ resistance.

5.3.2 Preparation of NVOC-CS films

5.3.2.1 CS films

Chitosan films were prepared by casting chitosan solutions in Petri dishes and let dry. Specifically, 2 ml 1 % (w/v) CS solution in acetic acid was cast into glass Petri dish (60 mm × 5 mm), transferred into an oven and kept for 16 h at 37℃. Subsequently, the dried chitosan film was first rinsed with PBS (pH 7.4) (Invitrogen, Carlsbad, CA) for 2 h with gentle vibration, and then with ddH_2O for 3 additional rinses, 2 h each. The films were finally dried again in the oven under the conditions (i.e. 37℃, 16 h) as mentioned above.

5.3.2.2 NVOC-CS films

Caged chitosan (NVOC-CS) was fabricated using the following procedures according to procedures by Alonso et al.'s [26] with minor modifications: 50 mg of 4,5-dimethoxy-2-nitrobenzyl chloroformate (NVOC) was dissolved in 5 ml anhydrous 1, 4-dioxane to obtain a NVOC solution at 10 mg/ml, which was subsequently transferred to react with the dry CS film prepared in the previous step. To the reaction mixture, a total of 5 ml 10 mM $NaHCO_3$ (JT Baker, Phillipsburg, NJ) solution was slowly added over a period of 2 h under gentle vibration. The mixture was allowed to react for an additional 16 h at room temperature under gentle vibration. At the end of the reaction, the reaction mixture was removed from the CS films. The films were subsequently washed once with anhydrous 1, 4-dioxane and then with ddH_2O for 3 times with 2 h each time, respectively. The films were finally dried at 37℃ for 16 h in an oven.

5.3.3 Photoactivation (NVOC-CS)

To cleave photoactive NVOC groups from NVOC-CS, UV irradiation at 365 nm using an UV lamp (Black-Ray B-100 longwave UV lamp, 100 W, UVP, Upland, CA) was carried out. Specifically, the dry NVOC-CS films obtained from the previous step were submerged in 1M glycine in PBS (pH 7.4) for 1 h. The wetted films were then placed directly under the UV lamp, and exposed to the UV light for 5 min. The distance between the sample and the lamp was kept constant at 5 cm. After the light exposure, the films were washed extensively with ddH_2O and dried in at 37℃ for 16 h in an oven. When needed, a line photomask (MPC Circuits, Ottawa, ON) was placed directly on top of the films during light exposure to create line patterns. For the convenience of discussion, photoactive NVOC groups that have undergone UV exposure will be identified by underlining it in the document (i.e. NVOC for single exposure and NVOC for double exposure) hereinafter.

5.3.4 Preparation of PEG-NVOC-CS, RGDS-NVOC-CS and RGDS/PEG-NVOC-CS films

5.3.4.1 PEG -NVOC-CS homogeneous films

Dry homogeneously irradiated NVOC-CS films were reacted with o-(2-aminoethyl)polyethylene glycol 2,000 (PEG), an amine terminated PEG (10 mg/ml in PBS solution), using glutaradehyde (GA) (0.1% in PBS, 1:1 volume ratio to PEG solution) at 37˚C for 0.5 h to achieve a homogeneous cell non-adhesive PEG covered CS film surface (PEG-NVOC-CS). At the end of the reaction, excessive 1M glycine solution was added to the reaction mixture to quench the unreacted GA. The resulting films were extensively washed using ddH_2O for 3 times, and dried at 37˚C for 16 h.

5.3.4.2 RGDS-NVOC-CS homogeneous films

Similarly, dry NVOC-CS films were reacted with cell adhesive peptide RGDS (0.2 mg/ml PBS solution) to link the primary amine groups on the film with carboxylic acid groups on the peptide. Specifically, 3 mg ethyl(dimethylaminopropyl) carbodiimide (EDC) and 2 mg N-hydroxysuccinimide (NHS) were added into 5 ml RGDS solution (0.2 mg/ml)

and incubated at room temperature for 15 min with agitation to activate the carboxyl groups on the peptide. After the activation, the resulting mixture was added onto the homogeneously irradiated NVOC-CS films to carry out the reaction for 2 h at room temperature. Subsequently, the resulting films were thoroughly washed and dried. The final product was cell adhesive RGDS peptide covered homogeneous films (i.e. RGDS-NVOC-CS).

5.3.4.3 RGDS/PEG-NVOC-CS patterned films

Patterned NVOC-CS film with selective irradiation achieved through line photomask (first exposure) was reacted with PEG in the same fashion as mentioned above in the homogeneous surface preparation. To pattern the cell adhesive RGDS peptide to the remaining part of the same surface after the first exposure, a second irradiation was applied to the initially un-irradiated regions (i.e. after the first irradiation) to photo-cleave the remaining NVOC in the rest areas thereby enabling RGDS peptide immobilization. The RGDS peptide was subsequently immobilized to the regions defined by the second exposure in the same fashion as outlined above in the RGDS homogeneous surface preparation. The surface thus obtained was patterned by both cell non-adhesive PEG, after the first exposure, and cell adhesive RGDS, after the second exposure, noted as RGDS/PEG-NVOC-CS. The surfaces were dried and stored at 4℃ for future use.

5.3.5 Cell culture

To test the relative cell adhesiveness of different films, NIH/3T3 fibroblasts were used as model adherent cells. The cells were routinely maintained in medium containing Dulbecco's Modified Eagle's Medium (DMEM) (Invitrogen) supplemented with 10% fetal bovine serum (FBS) (Invitrogen), 100 U/mL penicillin (Invitrogen), and 0.1 mg/mL streptomycin (Invitrogen), and kept in T-75 flasks (BD Biosciences, San Jose, CA) at 37˚C in incubator with 100% relative humidity and 5% CO_2.

Dry NVOC-CS, NVOC-CS, PEG-NVOC-CS, RGDS-NVOC-CS and RGDS-/PEG-NVOC-CS films were sterilized by 70% ethanol and washed extensively with sterile PBS (pH 7.4) (Invitrogen) before cell cultures.

Prior to cell seeding on the experimental surfaces, cells were trypsinized, centrifuged into a pellet, re-suspended in the medium without FBS (serum-free DMEM) and counted by a hemocytometer. The cells were subsequently seeded onto the experimental surfaces at a density of 5×10^3 cells/cm^2 in a serum-free DMEM medium. After 2 h of seeding, the medium was changed to serum-contained medium. Tissue culture polystyrene (TCPS) was used as a control surface for the studies. Cells were observed using a fluorescence microscope (Olympus IX81, Olympus, Mississauga, ON) every 24 h and the observations were documented using an Image-Pro Plus software (Media Cybernetics, Silver Spring, MD). To study the cell morphology parameters, cell outlines were manually traced in captured phase contrast images and quantified using the Image-Pro Plus software. For every surface, at least 60 cells from more than five different 10x magnification frames were randomly selected for tracing. Cell morphology parameters, such as cell area, perimeter, aspect ratio and roundness were automatically calculated by the software [27].

In some cases, fluorescent CellTracker^{TM} Green (Invitrogen) was used to label the fibroblasts according to the vendor's protocol for better visualization of the cells before seeding. Briefly, 10 mM stock solution of the dye in DMSO (Fisher Scientific) was prepared and subsequently dissolved in DMEM to produce a 2.5 μM working solution. One milliliter of the working solution was added to stain the fibroblasts and allowed to incubate for 45 min at 37ºC. The staining solution was then replaced with pre-warmed fresh medium and allowed to incubate for additional 30 min at 37ºC.

5.3.6 Surface characterization

5.3.6.1 Fourier transform infrared spectroscopy

To characterize the chemical compositions of CS, NVOC and NVOC-CS, attenuated total reflectance Fourier transform infrared spectroscopy (ATR -FTIR) was used. The samples were placed on a zinc selenide crystal and the spectra were recorded in ATR-FTIR mode in a Varian FTIR spectrometer (Varian 7000, Agilent Technologies, Santa Clara, CA).

5.3.6.2 Water contact angle

Water contact angles (WCA) for dry homogeneous CS, NVOC-CS, NVOC-CS, PEG-NVOC-CS and RGDS-NVOC-CS – all prepared on glass slides in Petri dishes -- were obtained using a sessile drop method on a VCA Optima XE system (AST product, Billerica, MA, USA). Five random (and different) spots on each slide were analyzed and one slide for each sample was tested. Both advancing and receding angles were measured and recorded.

5.3.6.3 UV-Vis spectrum of NVOC-CS at different irradiation time

Dry NVOC-CS film was weighed and then dissolved into 2% acetic acid solution to obtain a 0.5 mg/ml NVOC-CS solution. To the wells of a 96-well plate (Corning, Lowell, MA), 200 μl NVOC-CS solution per well was transferred and subsequently irradiated at 365 nm using the longwave UV lamp at different time intervals. A BioTek microplate reader (Fisher Scientific) was used to record the spectrum change as a function of irradiation times.

5.3.7 Statistics

To determine statistical significant differences of four cell morphology parameters among different surfaces, One-Way ANOVA analysis was applied to the cell morphology data, and a significant level of $p < 0.05$ was considered to be statistically significant.

5.4 Results and discussion

In this study, we developed a new photocleavable biomaterial to control cell attachment. The bulk material, chitosan, is a naturally occurring cationic material that exhibit favorable properties, such as biocompatibility and biodegradability, which are much desirable for tissue engineering applications. In addition, the existence of active primary amines on chitosan provides the possibility for further chemical modifications for various applications [28, 29]. Nitrobenzyl derivatives are a series of photocleavable molecules that usually undergo photolysis at near-UV range [7, 30, 31]. Here we combine the advantages of chitosan and photocleavable nitrobenzyl derivatives to generate a controllable surface for cell attachment. The chemical reactions and fabrication scheme are shown in Figure 1. By caging the primary amine groups in the chitosan molecules with photocleavable molecules NVOC,

we can realize spatial and temporal controls on the chitosan surface by multiple and sequential light illuminations on different regions of one chitosan surface. More specifically, we demonstrate that cell repulsive PEG and cell adhesive peptide RGDS can be sequentially patterned to a chitosan surface by two near-UV exposures in sequence. We also show that the patterned surfaces obtained this way can be used to influence cell attachment.

As shown in Figure 1, through modification of the chitosan surface by photoactive NVOC, UV irradiation to uncage the protected amine groups of the chitosan and subsequently modifying the chitosan surface with either cell non-adhesive PEG or cell adhesive RGDS, the control of the chitosan surface functionality is achieved.

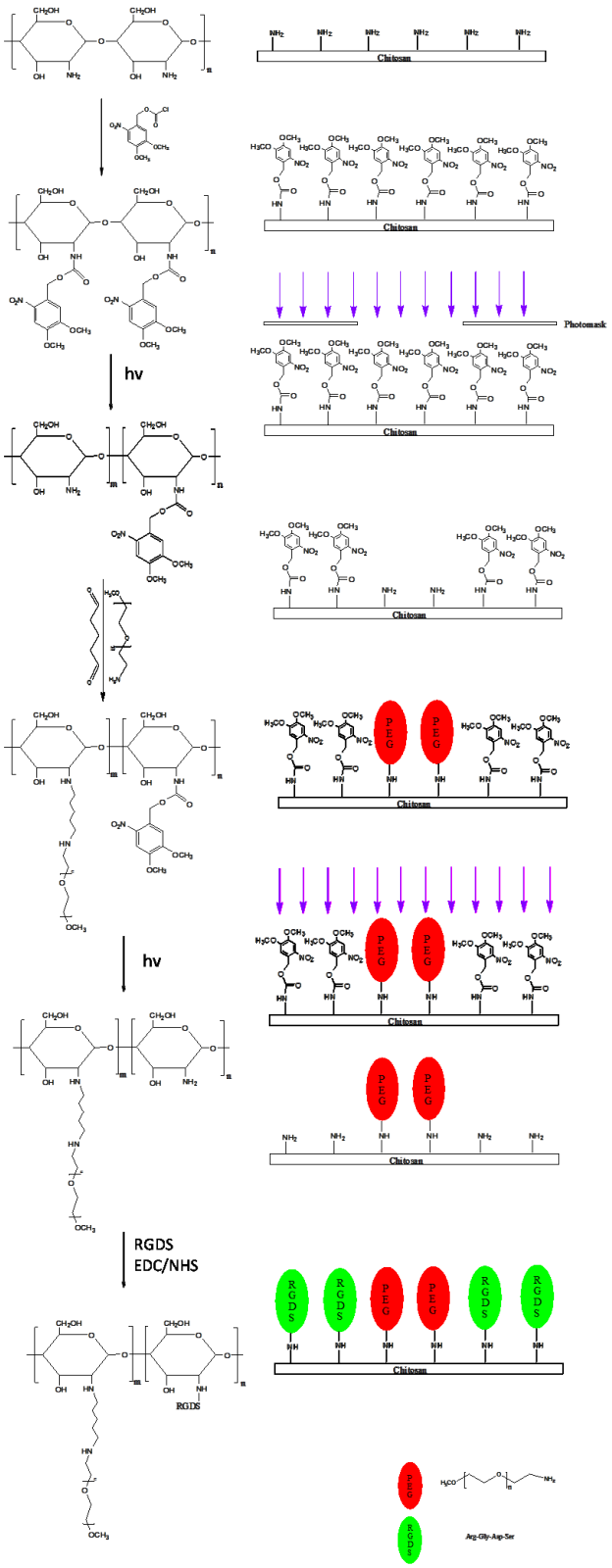

Figure 1 Surface preparation schemes for different surfaces

5.4.1 Surface characterization

To confirm the chemical properties of different prepared surfaces, ATR-FTIR was used. As shown in Figure 2, the chitosan spectrum (i.e. CS trace) depicts the characteristic absorption peaks of stretching of –OH and –NH groups around 3311 cm^{-1} with a broad peak. The peak around 2879 cm^{-1} is believed to be the stretching of –CH bonds in methyl or methylene of the chitosan molecule. The peaks at 1649, 1320 and 1026 cm^{-1} are typically for chitosan and represent the stretching of C=O, primary C-N and C-O groups in the sugar rings of the chitosan. Furthermore, the peak at 1580 cm^{-1} can be attributed to the typical absorption of the symmetrical stretching of amino groups. The peak at 1422 cm^{-1} could be assigned as the bending of –OH and –CH on the ring [32]. The spectrum of NVOC shows the characteristic peaks at 2981, 1683, 1530, 1351, 908 and 690 cm^{-1}. These peaks can be assigned as –CH stretching in aromatics, C=O stretching, N-O symmetric stretching [31], N-O symmetric stretching, O-H bending and C-Cl stretching on the NVOC structure, respectively. The spectrum of NVOC-CS shows the characteristic peaks at 2978, 1712, 1526, 1359 and 976 cm^{-1}. The peak at 2978 cm^{-1} can be identified as –CH stretching in aromatics from NVOC. Importantly, in comparison with the NVOC trace, the disappearance of C-Cl peak at 690 cm^{-1} in NVOC-CS trace confirms bonding formation between NVOC and CS to eliminate C-Cl linkage as a result. By identifying the chemical structures of both reactants and products through ATR-FTIR, we conclude that NVOC-CS has been successfully synthesized.

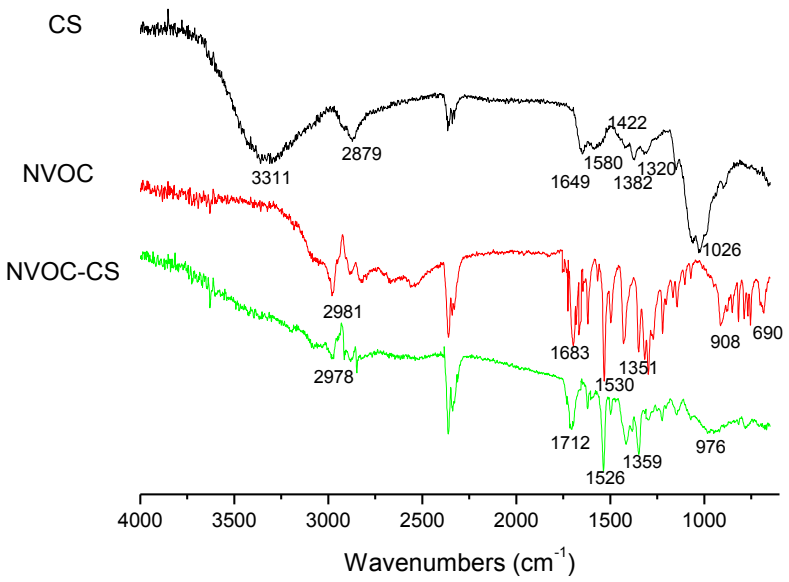

Figure 2 FTIR spectra of chitosan, NVOC and NVOC-CS

The identities of different surfaces were further confirmed by water contact angle data as it has been shown that surface wettability is directly related to the surface energy and it is a useful parameter to correlate with cell-biomaterials interactions on the interface [33, 34]. As demonstrated in Table 1, both advancing and receding water contact angles change after each step of chemical reaction and photoactivation, suggesting possible surface composition changes. In particular, the most dramatic change took place after PEG immobilization (PEG-NVOC-CS vs. NVOC-CS), dropping the measured advanced water contact angle (AWCA) from 78.1 ± 3.0° to 52.3 ± 7.9° and the measured receding water contact angle (RWCA) from 52.0 ± 5.6° to 40.3 ± 6.9°. This is most likely due to the introduction of the hydrophilic PEG molecules on the surface, suggesting successful photoactivation and subsequent PEG immobilization by crosslinker GA. The pure CS film has an AWCA about 77.6 ± 3.6°, which is acceptable and in a good agreement with previous reports. There are literatures reported the water contact angles of chitosan are 80 ± 4.6° [35], 60.7 ± 1.25° [36], 69.4° [37], 85.6° [38] and 84.54° [39]. We believed that the variation of water contact angle values of chitosan is due to non-equilibrium state of the testing and the swelling of materials. The wettability of chitosan is known from the hydrophilic groups like hydroxyls and amines on the chitosan chain [39]. So the percentage of amines could change

the surface free energy and thus affect the wettability of the films. After caging reaction, we saw a slight increase on advancing water contact angle, 85.2 ± 4.3°. It could be evident for the presentation of hydrophobic 2-nitrobenzyl groups on the surface [40, 41]. After photoactivation, because of the removal of hydrophobic caging agent NVOC, a slight decrease on advancing water contact angle was been observed on NVOC-CS. It proved that the surface is altered from NVOC-CS to CS surface by light. PEG immobilization on the deprotected surfaces caused the bigger change on advancing water contact angle. It is 52.3 ± 7.9° for PEG -NVOC-CS, which is acceptable [42]. But the relative high water contact angle for PEG covered surface suggest us that the coverage of PEG on chitosan is limited. RGDS linkage introduces RGDS peptide on the surfaces. The result of RGDS -NVOC-CS is 61.6 ± 5.0°, which is acceptable by comparison with other researchers' results [43].

Table 1 Water contact angles of different homogeneous surfaces

Samples	**Advancing water contact angles/∘**	**Receding water contact angles/∘**
CS	77.6 ± 3.6	55.1 ± 10.9
NVOC-CS	85.2 ± 4.3	57.8 ± 7.8
NVOC-CS	78.1 ± 3.0	52.0 ± 5.6
PEG-NVOC-CS	52.3 ± 7.9	40.3 ± 6.9
RGDS-NVOC-CS	61.6 ± 5.0	47.0 ± 5.8

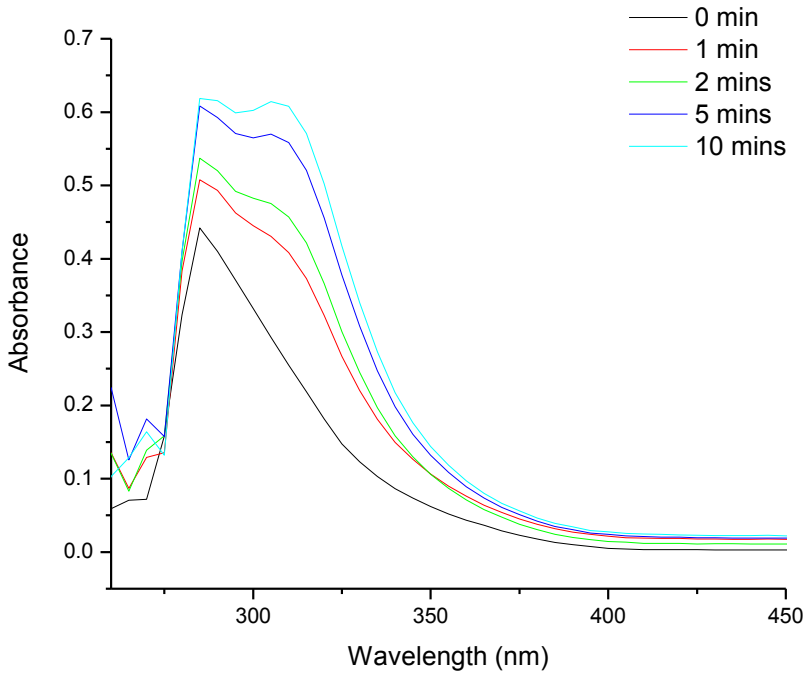

Figure 3 Absorption spectra of NVOC-CS on different UV-irradiation times

5.4.2 Photoactivation

The feasibility and efficiency of 2-nitrobenzyl derivatives removed from the base materials has been investigated and proved by many researchers [3, 13]. Because of the strong absorption of photocleavable NVOC at near-UV range, the scanning spectra of NVOC-CS in acetic acid solution were recorded with different UV irradiation times. Figure 3 is shown the absorption spectra of NVOC-CS after 0-10 min irradiation by UV lamp (365 nm). After the first irradiation, we could see a slight increase in the absorption maximum and a general baseline shift. These observations indicated that a certain rearrangement occurring in the solution. By increasing the irradiation times, a slight shoulder was observed and a constant increase of the shoulder peak was shown following the time increased. The compound with a red-shift on the maximum absorption is an aromatic carbamate residue of the protecting group removed by light from the bulk NVOC-CS and became free in the solution[44]. It indicated the decomposition of NVOC induced by light and the extent of decomposition would be increased with a longer exposure time.

5.4.3 Cell culture study

To assess if our surfaces could control cell attachment and modulate cell behavior, NIH/3T3 cell line was used as a model to study cell attachment on our designed and intermediate surfaces. Images of cells incubated on different homogeneous surfaces which represent the different stages of the whole process were collected and quantified for cell densities by manually counting (Figure 4). The cells on different surfaces were counted until the 4th day of culture due to the continuing decrease in fluorescent intensity of CellTracker^{TM} Green in each cell. From the images, we could conclude that NVOC-CS has a few cells attached but less than the surface after UV illumination, NVOC-CS. On NVOC-CS surface, the primary amines are caged by photocleavable NVOC reagent, which reduces the positive charge on the surface and at the same time a hydrophobic group, benzyl group with two methoxyls, is introduced to the surface. The decline of positive charge on the surface will result in the decrease on the attraction to cell membrane, negatively charged, by the primary amine, positive charged, but the addition of hydrophobic group from NVOC will increase the hydrophobicity of the surface, which help cells attached. So the cell attachment is the result of the competition of the decline of primary amines and the increase of hydrophobicity. On our NVOC-CS surfaces, the cell attachment images showed the prominent influence of positive charge on cell attachment, which causes the less cell density on NVOC-CS. On NVOC-CS, it is an opposite condition, compared with NVOC-CS. Because of the cleavage of NVOC and the deprotection of primary amines, there is an increase of positive charges and decline of hydrophobicity. More cells were attached. It is consistent with our conclusion that the charges are important for cell attachment in our system. PEG-NVOC-CS surface has the least cells attached and the least cell density in all these surfaces, because hydrophilic PEG reduces the positive charge and increases the hydrophilicity on the surface. PEG is known for its ability to form hydrogen bonding with water by oxygen ether. The hydrophilicity of PEG and the decline of positive charge causes the cell is hard to initially attached to the surface, so the cell density on PEG covered chitosan surface is the minimum in all designed surfaces. It also showed the capability of PEG to repulse cell. After UV illumination and RGDS linkage, a cell adhesive peptide was introduced onto chitosan surface. The attraction of cell adhesive peptides with cells is

specific and it is a ligand-receptor interaction. From the cell image of RGD-NVOC-CS, we saw an increase on cell density and it is believed because of the introduction of cell adhesive peptide RGDS. Unfortunately, because of the existence of primary amines, which cause strong positive charge density on the surface after UV illumination, we couldn't see the big difference on cell densities of NVOC-CS and RGDS -NVOC-CS.

a) 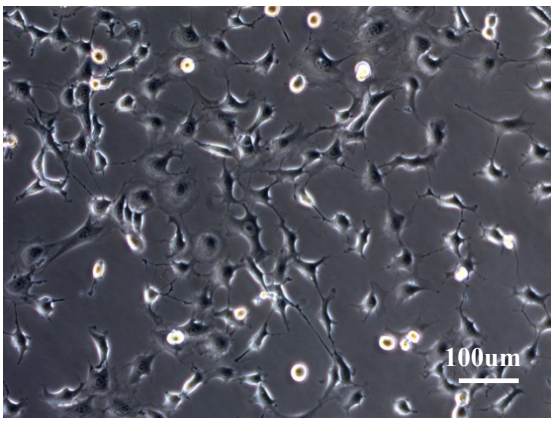

b) 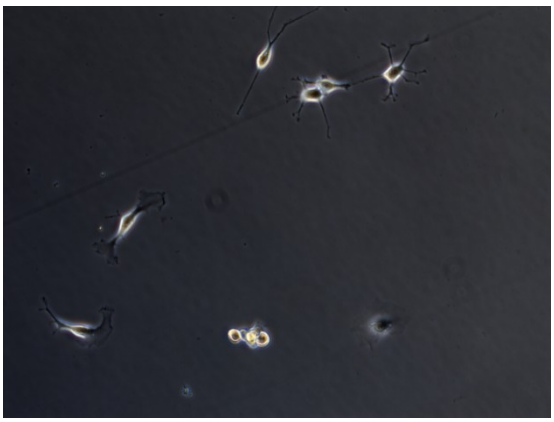

c) 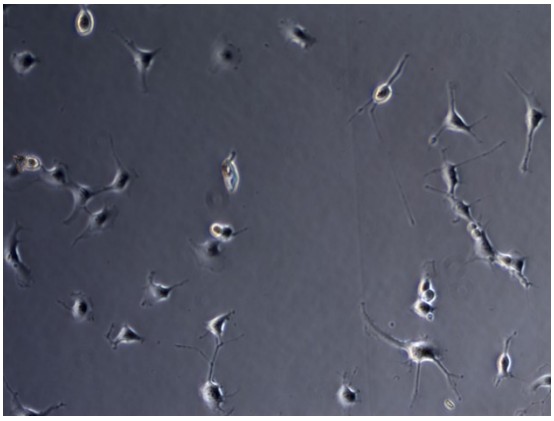

d) 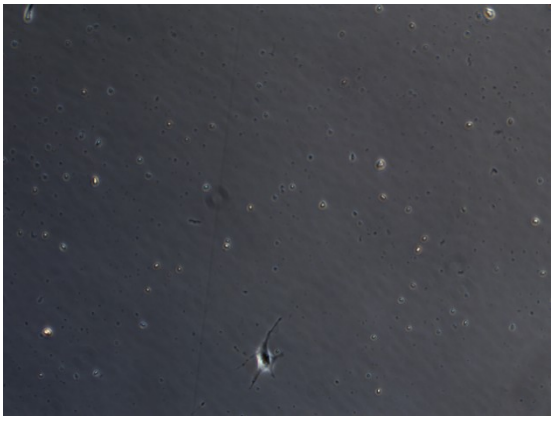

e) 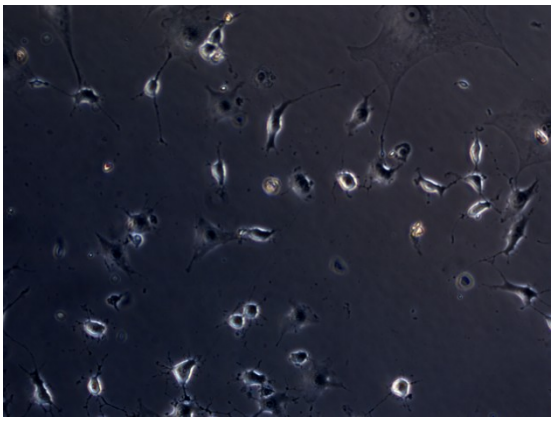

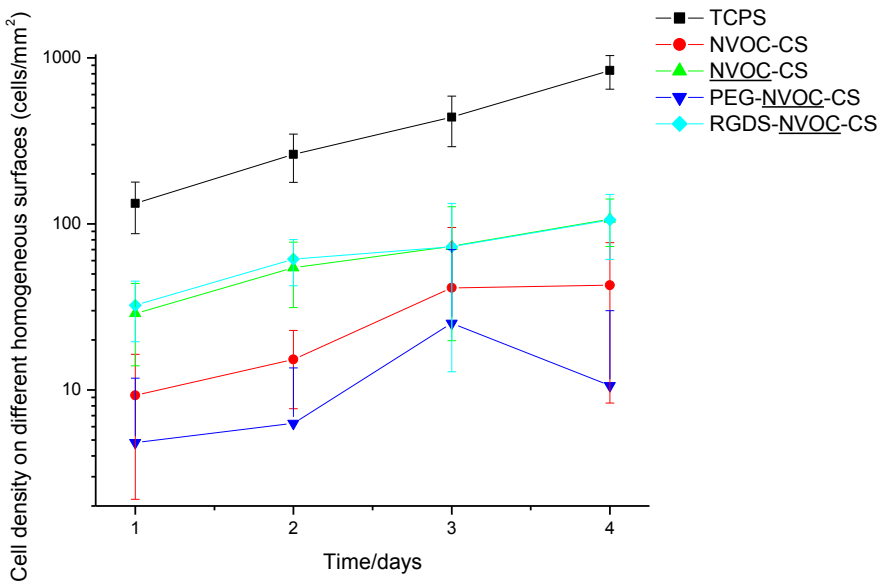

f)

Figure 4 Microscopical images of homogeneous surfaces after 2 days of seeding: a) TCPS (tissue culture polystyrene); b) NVOC-CS; c) NVOC-CS; d) PEG- NVOC-CS; e) RGDS-NVOC-CS. Cell densities on different homogeneous surfaces, f).

Quantification of cell morphology parameters at 48 h after seeding was studied to show how cell behaves with different surface functionality. In the figure 5, mean cell areas on different homogeneous surface are significantly different ($p < 0.05$). Cell has low spread-out on NVOC-CS surface and PEG-NVOC-CS. Mean cell area was increased after UV irradiation and RGDS linkage, as expected. The results showed that even a few cells attached to NVOC protected surface and PEG covered surface but the spreading of these cells is not as good as the control, TCPS, and RGDS covered surface. Due to biospecific binding between cells and RGDS peptides on RGDS-NVOC-CS, it has the best cell spreading on all the surfaces. Cell perimeter on different surfaces showed the same trend as mean cell area. They all indicated that the RGDS modified surface has competitive cell spreading as TCPS. Caging reagent and PEG coverage cause a poor spreading of cells based on the mean cell area and perimeter data, and also there is no significant difference ($p > 0.05$) for the parameters of cell aspect ratio and cell roundness on these two surfaces. Based on the definitions of the two parameters, it indicated that there is no different on cell elongation on these surfaces. Overall, from the analysis of cell morphology, RGDS covered surface

conducts better cell spreading. Combined with cell images, we could conclude that after UV irradiation and the following modifications, the surface cues could be changed and the influence is not just on the cell initial attachment and proliferation, but also on the cell spreading.

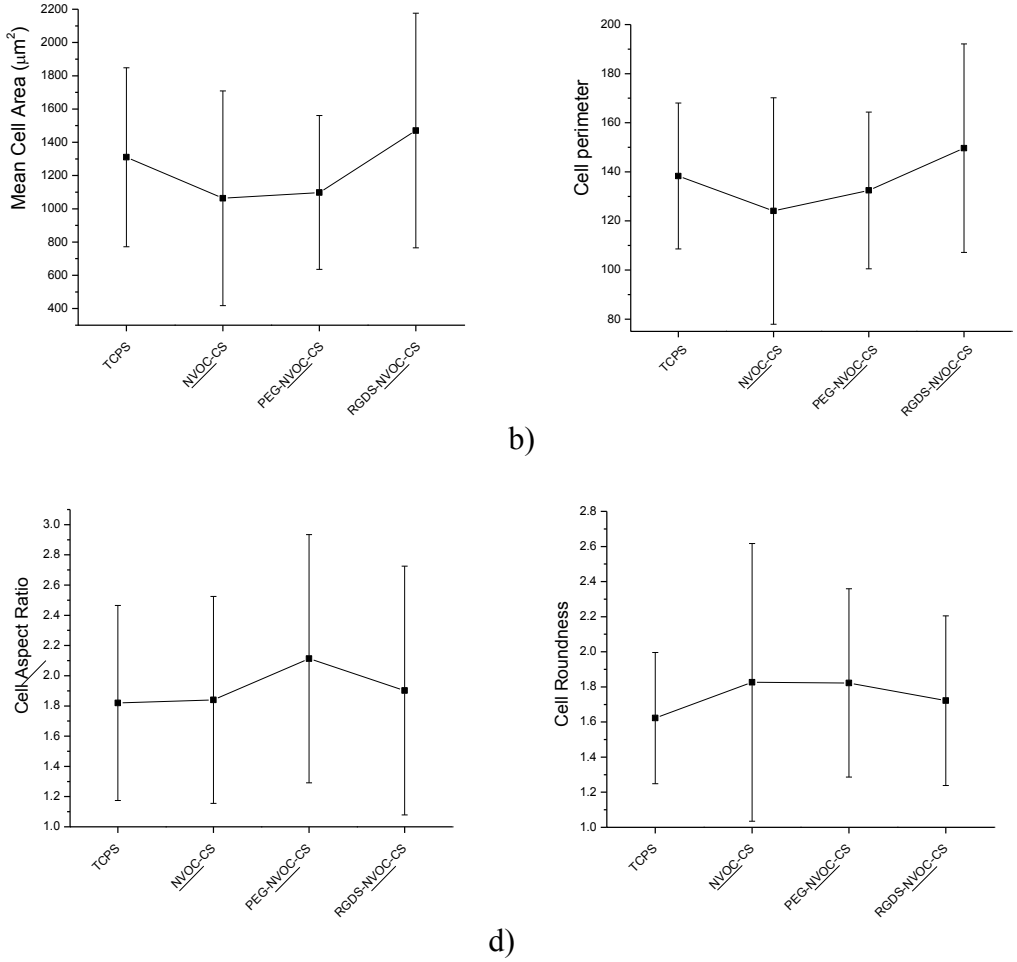

Figure 5 Quantification of cell morphological parameters in different surfaces at 48h. Error bars indicate standard deviation. a) Mean cell area, b) cell perimeter, c) cell aspect ratio (the ratio of the major and the minor axes of a best-fit ellipse), d) cell roundness (defined as $p^2/(4\pi A)$ where p is the object perimeter and A is the object area).

To show the control of cell attachment by multiple illuminations on our surfaces, site-specific cell attachment was studied by applying a micro-printed line mask when the first illumination took place. Our results showed successful cell patterns formed in Figure 6. The tiled images were processed by using “tile images” function in Image-Pro Plus software.

These NIH/3T3 cell patterns on RGDS/PEG-NVOC-CS film are consistent with the shape of photomask. By using caging agent NVOC, first, we protected primary amines on chitosan and introduced light as a stimulus to realize site-specific control. Then, the multiple illuminations following with different linkages realized the control of cell repulsion and cell adhesion by the introduction of different molecules on the different regions of one surface. In detail, the first illumination is applied to the surface with the mask directly contacted with NVOC-CS film. After the illumination, cell non-adhesive PEG was immobilized on these amine-activated regions by crosslinker GA. The second illumination was applied without photomask, followed by RGDS linkage. Through our illumination steps, we could create alternative cell permissive and cell non-permissive lines on RGDS/PEG-NVOC-CS film, where the black strips regions correspond to cell permissive regions.

From the images, we could see that the pattern on RGDS/PEG-NVOC-CS didn't reach confluence after days and cell proliferation was slow. We believed it could be explained by the limited NVOC coverage. The limited NVOC coverage on the initial chitosan surface will result in the existence of remained primary amines. After first step of illumination, PEG was introduced to the surface by homofunctional crosslinker GA for amine groups. GA helped immobilization of PEG; at the same time, it helped to eliminate the remained amine groups by crosslinking and stabilized the surface for further chemistry by crosslinking chitosan through these remained amines. During our process, we speculate the limitation of NOVC coverage finally caused the existence of PEGs on the whole surface because the PEG could react with remained amines on the surface. Therefore, after the first illuminations and the following linkages, it is possible that PEG exists on the second illumination regions for RGDS immobilization and it is due to crosslinking of remained amine groups with PEGs by GA. The existence of PEGs on the second illumination regions could explain the slow proliferation of cells. The PEGs on these regions probably prevent cell spreading and migration to certain locations which are immobilized with PEG and consequently result in a relative low cell growth. It is possible that optimization of NVOC-CS reaction could help create completely alternative cell patterns and it will be one focus to improve our design and control of cell behaviors.

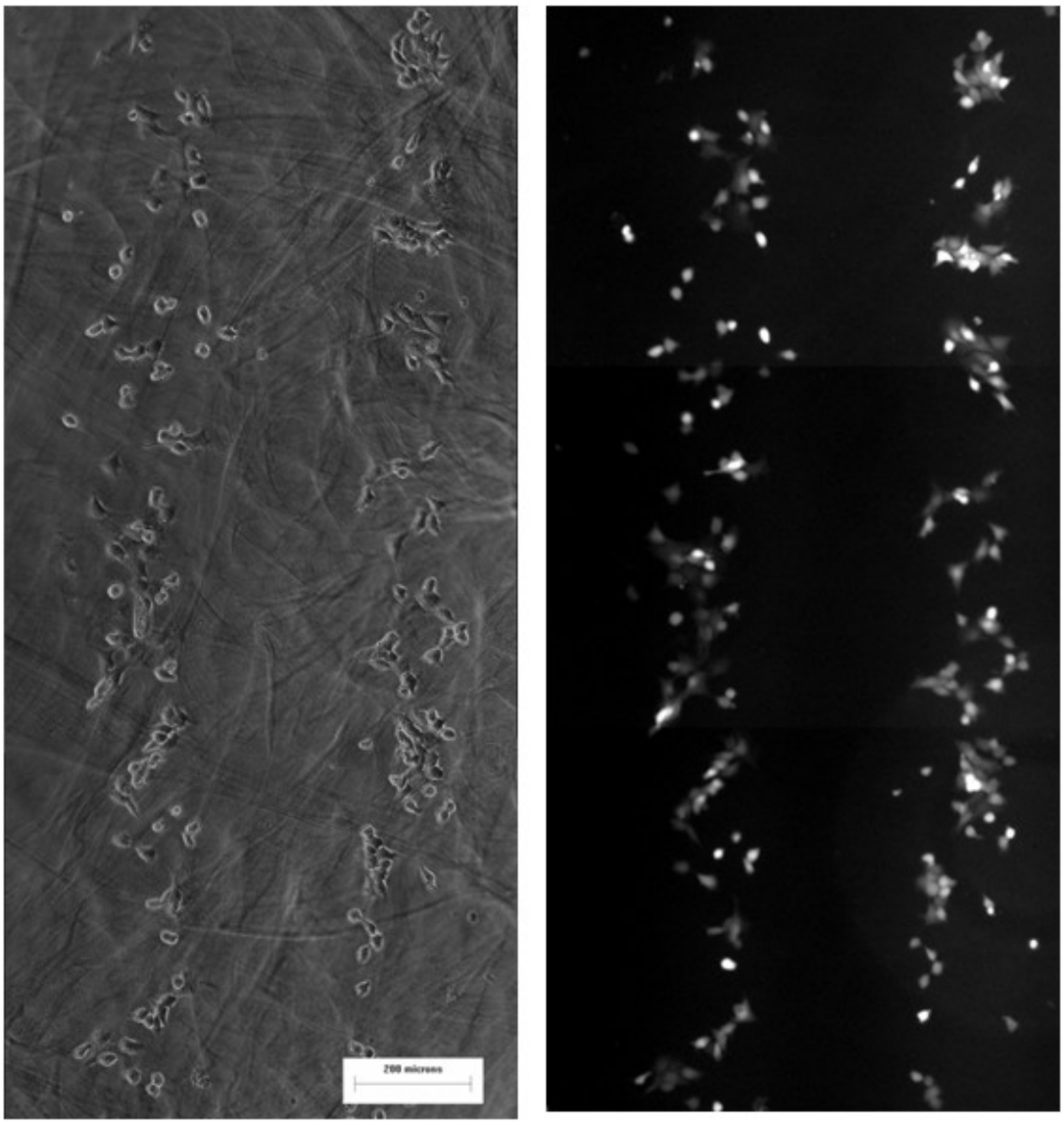

Figure 6 Tiled cell pattern images to show NIH/3T3 cell patterns on RGDS/PEG-NVOC-CS films after 2 days of seeding. Two images represent the phase contrast and fluorescent images for the same surface, respectively. The mask applied is with 100μm width of blank strips and 200 μm width of spaces (Transparent strip).

5.5 Conclusion

In native tissue, changes in microenvironment are linked to cell growth, migration, proliferation and differenation. The approach described in our paper, based on a natural polymer and light as a switch of surfce properties, provided a way to manipulate chemical

cues on surface and a platform to study cell behaviors [2]. The base mateiral, chitosan, is a promising natural polycation with the advantages of biocompatability and biodegradation. The photosensitive molecule, NVOC, is responsive to the near UV light, which will limit the concerns of UV-cytotoxicity and not be impacted by the *in vitro* environment. It may be benifical to many applications in tissue engineering. In this paper, we studied the novel materials with the photosensitve moities and the changes of surface functionalities to affect cell attachment by UV illumiantions and the following reactions. FTIR was used to characterize NVOC-CS. The water contact angle results showed the successful switch of surface properties by using chemical reaction on the soft material chitosan. The feasibility of photoactivation was proved by the UV-Vis spectra of NVOC-CS solution with different UV exposure times. For the cell culture study, the results show the success of photosensitive NVOC modified chitosan surface, NVOC-CS, in controlling cell attachment by multiple illuminations and the following linkage of cell repulsive or cell adhesive molecule after each illumination. From cell culture on the homogeneous surfaces, control of cell attachment has been observed and analyzed by cell density and different cell morphology parameters. The results show the surface properties not only played an impact on cell attachment but also change cell spreading and morphology. On RGDS/PEG- NVOC-CS films, line-patterned cells formed and maintained for a long period time. In brief, our study shows an approach to achieve selective cell adhesion and growth on a two-dimensional surface. It is based on soft material, chitosan, which is biocompatible and well studied, and can be applied to study cell-materials interaction and guide cell growth, not only in two-dimensional surface but also three-dimensional structure can be envisaged. We think it has great potential use on engineering tissue development [3, 31].

5.6 Acknowledgement

The authors would like to acknowledge financial support from a Discovery Grant by the Natural Sciences and Engineering Research Council of Canada (NSERC).

5.7 Reference

1. Jang, K., et al., *Single-cell attachment and culture method using a photochemical reaction in a closed microfluidic system.* Biomicrofluidics, 2010. **4**(3).

2. Langer, R. and D.A. Tirrell, *Designing materials for biology and medicine.* Nature, 2004. **428**(6982): p. 487-492.
3. Katz, J.S. and J.A. Burdick, *Light-Responsive Biomaterials: Development and Applications.* Macromolecular Bioscience, 2010. **10**(4): p. 339-348.
4. Katz, J.S., J. Doh, and D.J. Irvine, *Composition-tunable properties of amphiphilic comb copolymers containing protected methacrylic acid groups for multicomponent protein patterning.* Langmuir, 2006. **22**(1): p. 353-359.
5. Zipfel, W.R., R.M. Williams, and W.W. Webb, *Nonlinear magic: multiphoton microscopy in the biosciences.* Nature Biotechnology, 2003. **21**(11): p. 1368-1376.
6. Helmchen, F. and W. Denk, *Deep tissue two-photon microscopy.* Nature Methods, 2005. **2**(12): p. 932-940.
7. Kikuchi, Y., et al., *Arraying Heterotypic Single Cells on Photoactivatable Cell-Culturing Substrates.* Langmuir, 2008. **24**(22): p. 13084-13095.
8. Lee, K.N., et al., *Protein patterning by virtual mask photolithography using a micromirror array.* Journal of Micromechanics and Microengineering, 2003. **13**(1): p. 18-25.
9. Hoffmann, J.C. and J.L. West, *Three-dimensional photolithographic patterning of multiple bioactive ligands in poly(ethylene glycol) hydrogels.* Soft Matter, 2010. **6**(20): p. 5056-5063.
10. Nakanishi, J., et al., *Photoactivation of a substrate for cell adhesion under standard fluorescence microscopes.* Journal of the American Chemical Society, 2004. **126**(50): p. 16314-16315.
11. Chen, S.Y. and L.M. Smith, *Photopatterned Thiol Surfaces for Biomolecule Immobilization.* Langmuir, 2009. **25**(20): p. 12275-12282.
12. Sundberg, S.A., et al., *SPATIALLY-ADDRESSABLE IMMOBILIZATION OF MACROMOLECULES ON SOLID SUPPORTS.* Journal of the American Chemical Society, 1995. **117**(49): p. 12050-12057.
13. Blawas, A.S., et al., *Step-and-repeat photopatterning of protein features using caged/biotin-BSA: Characterization and resolution.* Langmuir, 1998. **14**(15): p. 4243-4250.
14. Blawas, A.S. and W.M. Reichert, *Protein patterning.* Biomaterials, 1998. **19**(7-9): p. 595-609.
15. Hsiao, S.W., et al., *Interactions between chitosan and cells measured by AFM.* Biomedical Materials, 2010. **5**(5).
16. Mano, J.F., *Stimuli-responsive polymeric systems for biomedical applications.* Advanced Engineering Materials, 2008. **10**(6): p. 515-527.
17. Kumbar, S.G., K.S. Soppimath, and T.M. Aminabhavi, *Synthesis and characterization of polyacrylamide-grafted chitosan hydrogel microspheres for the controlled release of indomethacin.* Journal of Applied Polymer Science, 2003. **87**(9): p. 1525-1536.
18. Jiang, H.L., et al., *Preparation and characterization of ibuprofen-loaded poly(lactide-co-glycolide)/poly(ethylene glycol)-g-chitosan electrospun membranes.* Journal of Biomaterials Science-Polymer Edition, 2004. **15**(3): p. 279-296.
19. Satoh, T., et al., *In vitro gene delivery to HepG2 cells using galactosylated 6-amino-6-deoxychitosan as a DNA carrier.* Carbohydrate Research, 2007. **342**(11): p. 1427-1433.
20. Sun, S.J., et al., *A thermoresponsive chitosan-NIPAAm/vinyl laurate copolymer vector for gene transfection.* Bioconjugate Chemistry, 2005. **16**(4): p. 972-980.
21. Feng, Z.Q., et al., *The effect of nanofibrous galactosylated chitosan scaffolds on the formation of rat primary hepatocyte aggregates and the maintenance of liver function.* Biomaterials, 2009. **30**(14): p. 2753-2763.
22. Zhang, Y., et al., *Electrospun biomimetic nanocomposite nanofibers of hydroxyapatite/chitosan for bone tissue engineering.* Biomaterials, 2008. **29**(32): p. 4314-4322.
23. Chen, J.P., G.Y. Chang, and J.K. Chen, *Electrospun collagen/chitosan nanofibrous membrane as wound dressing.* Colloids and Surfaces a-Physicochemical and Engineering Aspects, 2008. **313**: p. 183-188.

24. Ignatova, M., N. Manolova, and I. Rashkov, *Novel antibacterial fibers of quaternized chitosan and poly(vinyl pyrrolidone) prepared by electrospinning.* European Polymer Journal, 2007. **43**(4): p. 1112-1122.
25. Braun, F., et al., *Novel labile protected amine terpolymers for the preparation of patterned functionalized surfaces: Synthesis and characterization.* Macromolecular Chemistry and Physics, 2003. **204**(12): p. 1486-1496.
26. Alonso, J.M., et al., *Photopatterned surfaces for site-specific and functional immobilization of proteins.* Langmuir, 2008. **24**(2): p. 448-457.
27. Gillette, B.M., et al., *Dynamic Hydrogels: Switching of 3D Microenvironments Using Two-Component Naturally Derived Extracellular Matrices.* Advanced Materials, 2010. **22**(6): p. 686-+.
28. Pillai, C.K.S., W. Paul, and C.P. Sharma, *Chitin and chitosan polymers: Chemistry, solubility and fiber formation.* Progress in Polymer Science, 2009. **34**(7): p. 641-678.
29. Mourya, V.K. and N.N. Inamdar, *Chitosan-modifications and applications: Opportunities galore.* Reactive & Functional Polymers, 2008. **68**(6): p. 1013-1051.
30. Nakayama, H., et al., *Silane coupling agent bearing a photoremovable succinimidyl carbonate for patterning amines on glass and silicon surfaces with controlled surface densities.* Colloids and Surfaces B-Biointerfaces, 2010. **76**(1): p. 88-97.
31. Ramanan, V.V., et al., *Photocleavable side groups to spatially alter hydrogel properties and cellular interactions.* Journal of Materials Chemistry, 2010. **20**(40): p. 8920-8926.
32. Brugnerotto, J., et al., *An infrared investigation in relation with chitin and chitosan characterization.* Polymer, 2001. **42**(8): p. 3569-3580.
33. Rotta, J., et al., *Parameters of color, transparency, water solubility, wettability and surface free energy of chitosan/hydroxypropylmethylcellulose (HPMC) films plasticized with sorbitol.* Materials Science & Engineering C-Biomimetic and Supramolecular Systems, 2009. **29**(2): p. 619-623.
34. Lopez-Perez, P.M., et al., *Effect of chitosan membrane surface modification via plasma induced polymerization on the adhesion of osteoblast-like cells.* Journal of Materials Chemistry, 2007. **17**(38): p. 4064-4071.
35. Tanuma, H., et al., *Preparation and characterization of PEG-cross-linked chitosan hydrogel films with controllable swelling and enzymatic degradation behavior.* Carbohydrate Polymers, 2009. **80**(1): p. 260-265.
36. Shi, G.Q., et al., *Study on the preparation of chitosan-alginate complex membrane and the effects on adhesion and activation of endothelial cells.* Applied Surface Science, 2008. **255**(2): p. 422-425.
37. Zheng, Z.H., et al., *Surface Properties of Chitosan Films Modified with Polycations and Their Effects on the Behavior of PC12 Cells.* Journal of Bioactive and Compatible Polymers, 2009. **24**(1): p. 63-82.
38. Hamilton, V., et al., *Characterization of chitosan films and effects on fibroblast cell attachment and proliferation.* Journal of Materials Science-Materials in Medicine, 2006. **17**(12): p. 1373-1381.
39. Tsai, H.S. and Y.Z. Wang, *Properties of hydrophilic chitosan network membranes by introducing binary crosslink agents.* Polymer Bulletin, 2008. **60**(1): p. 103-113.
40. Brown, A.A., O. Azzaroni, and W.T.S. Huck, *Photoresponsive Polymer Brushes for Hydrophilic Patterning.* Langmuir, 2009. **25**(3): p. 1744-1749.
41. Jensen, A.W., et al., *Photohydrolysis of substituted benzyl esters in multilayered polyelectrolyte films.* Macromolecules, 2004. **37**(11): p. 4196-4200.
42. Tanuma, H., et al., *Characterization and Enzymatic Degradation of PEG-Cross-Linked Chitosan Hydrogel Films.* Journal of Applied Polymer Science, 2009. **114**(3): p. 1902-1907.
43. Lin, H.B., et al., *ENDOTHELIAL-CELL ADHESION ON POLYURETHANES CONTAINING COVALENTLY ATTACHED RGD-PEPTIDES.* Biomaterials, 1992. **13**(13): p. 905-914.

44. Li, Y., et al., *Photoresponsive Nanocarriers Based on PAMAM Dendrimers with a o-Nitrobenzyl Shell.* Journal of Polymer Science Part a-Polymer Chemistry, 2010. **48**(3): p. 551-557.

Chapter 6 General discussion and Conclusions

6.1 Introduction

Highly ordered structure is an important feature of biological systems. Surface modification with controlled functionality is a useful tool to realize this ordered structure on surfaces for different *in vitro* and *in vivo* applications. *In vitro* studies with controlled surface properties provide platforms for fundamental research on cellular behaviours and response to different stimuli, including drugs, growth factors and so on. These studies can determine the surface features influence on cell adhesion, proliferation, apoptosis, migration, and differentiation. Subsequently this will help understand the interaction of cell-cell and cell-material in the native environment. *In vivo* studies provide a method to create well controlled scaffolds for implantations. These organized structures could help regulate cell adhesion and assembly for further dynamic morphogenetic movements and transitions to stable tissues. Finally these scaffolds will help mimic native tissues and eventually regenerate damaged tissues.

In order to control surface features and cell adhesion, light was introduced to our system to generate surface heterogeneity for further biomolecule immobilization. Two different photocleavable molecules were utilized on two kinds of surfaces in this project. The chosen photocleavable molecules are *o*-nitrobenzyl derivatives with mono- and bifunctionality. The nitrobenzyl caged functional group can undergo photolysis under UV irradiation and release the functional group initially protected by nitrobenzyl. The control-release of functional groups in designed regions can be utilized to generate surface heterogeneity. The stronger interaction between surfaces and cells could be created by the subsequently different biomolecule immobilization to the designed regions in order to form specific ligand-receptor bindings. At the same time, to increase the contrast on one surface, a cell non-adhesive molecule was introduced to provide non-fouling to resist cell adhesion. Based on these purposes, PEG, RGDS peptide sequence, LAM protein were applied to the surfaces after UV irradiation to create specific interaction between cell and surface.

6.2 Discussion

The first attempt to control cell adhesion was to use bifunctional BNBA for the linkage of PEG on its one terminal and protect the active functional group with the other

terminal group of BNBA. To simply the system, a SAM with thiols was used to provide functionality and also for the control of biomolecule immobilization. The results showed the capability to manipulate cell attachment using a SAM with BNBA working as a photo-switch. Through UV and the subsequent RGD immobilization, the surface is switched from PEG to RGD covered. The change on the presence of different biomolecules facilitates the surface from cell non-adhesive to cell-adhesive. Meanwhile, it was found that the limited yield of BNBA protection on the surface resulted in a lack of precisely control on surface heterogeneity. However, on this BNBA modified SAM, the possibility to switch surface features to control cell attachment using nitrobenzyl chemistry was demonstrated.

Because of the limitation to use BNBA on the surface to control surface features, a second attempt was focused on creation of heterogeneous features on a SAM. To achieve this, a well-studied nitrobenzyl derivative, NVOC, was introduced into the system as the photosensitive molecule. Due to the single functionality and specific amine-reactivity of NVOC, we chose AUT, an amine-terminated alkanethiol, as the self-assembled molecule and subsequently the multiple-exposure strategy to create the heterogeneity. Specifically, NVOC was immobilized to inactivate primary amine groups on the surface; upon two steps of UV irradiation with a photomask in the first step, deprotection of primary amines was activated in spatial and temporal manners; with the subsequently different biomolecule immobilization after each exposure of double UV exposures, a controlled surface patterning with alternative cell non-adhesive/adhesive regions by PEG/LAM immobilization was achieved. A successful cell pattern was generated on this properties-heterogeneous surface with PC12 cell line. For further control over cell behaviours on this surface, other than the immobilized cell adhesive molecule on the surface to control cell adhesion, NGF was introduced to provide cell signalling after cells attached. It is a good model to localize cell adhesion and control cell signalling simultaneously *in vitro*. As shown in Chapter 4, different shapes of patterns were obtained by simply using different photomasks. It elucidated the feasibility to immobilize various proteins aiming to the adhesion of different cell types. As demonstrated, through selective immobilization of LAM, low-adhesive PC12 cell could adhere to a SAM and be induced to neurite outgrowth. It suggested potential to use this platform to study a wide variety of cell-cell or cell-material interactions simply by choosing different cell

adhesive molecules. It can also be useful as a platform for further development of cell-based biochips.

The NVOC immobilized SAM is based on a flat solid substrate and it is not biodegradable and biocompatible. Therefore, it cannot be further developed for *in vivo* applications and impossible to be used in the development of regenerative medicines. The successful cell patterning on a NVOC modified SAM provided a possibility to utilize the same chemistry on a biocompatible and biodegradable material. Through the same multiple exposure approach and the following biomolecule immobilization, the surface heterogeneity could be created for cell adhesion and cell patterning on chitosan. In this project, the biocompatible and biodegradable polysaccharide, amine-rich chitosan, was used as a substrate for NVOC immobilization and protection. Different from SAM substrate, chitosan surface is more difficult to pattern cells utilizing photochemistry. The first difficulty is the fibrous microstructure of chitosan, as seen in Chapter 5 Figure 6. This microstructure on chitosan surface could increase the unevenness of its 2D surface and the topographical effect on cell adhesion, which could cause non-specific binding of cells. The second difficulty is that chitosan is widely accepted as a material that can promote cell viability and adhesion. There are studies suggesting that chitosan can increase the adhesion of fibroblast and neuronal cells, and also promote neurite outgrowth [1, 2]. Cell adhesive properties of chitosan increased the difficulty to convert a chitosan film to cell non-adhesive. Due to these difficulties to control surface properties on a biodegradable polymeric material, especially a natural polymer, which has less stable properties compared with synthetic polymers as described in Chapter 2, cell patterning on a natural polymer film is challenging. Here, we successfully developed a chitosan film with a photosensitive moiety. It can change surface functionality upon UV irradiation and affect cell attachment by different biomolecule immobilization afterwards. The control over cell adhesion on this NVOC-CS was investigated by the model cell line for cell-surface interaction, NIH/3T3 fibroblast, and successful cell attachment / detachment was seen on these surfaces after different treatment. Cell patterns were achieved in a heterogeneous surface by multiple illuminations and the following immobilization. It was also found that different surface properties affected cell morphology and spreading after cell initial attachment, and it could result in different cell behaviours with different cell types.

6.3 Conclusion

In my thesis, the main objective is to provide a platform that can precisely control cell attachment. Due to two different types of base materials we chose, two different platforms to control cell attachment were developed for *in vitro* and *in vivo* applications, respectively. Here are different strategies used: (1) As shown in Chapter 3, by introducing a bifunctional photocleavable molecule onto the SAM and the following chemical reaction, the surface could be switched to cell non-adhesive PEG covered surface and repel cell attaching; after UV irradiation and the subsequent immobilization of cell adhesive peptide sequence, the surface was altered to cell adhesive and attract cells. (2) Through the immobilization of a monofunctional photocleavable molecule on the surface, two steps of irradiation were applied to completely remove the photo residues from the surface and immobilize different biomolecules on the surface in spatial and temporal manners. for a SAM, the surface was patterned with cell non-adhesive PEG and cell adhesive protein LAM after two steps of irradiation with different photomasks for different shapes of patterning; PC12 cells were then cultured on these functionality-heterogeneous surfaces to achieve neuronal-like cell patterning (Chapter 4). (3) The other surface, a biodegradable chitosan targeting *in vivo* applications, was also introduced as a base material for cell patterning on a soft material. The same NVOC chemistry was utilized to primary amine groups on chitosan. Through multiple UV exposures with a photomask, surface patterning with different biomolecules was realized and fibroblast cells were attached on the chitosan surface in line pattern.

In general, by introducing photocleavable molecules on the surfaces, biomolecules were successfully immobilized on different kinds of surfaces in controlled spatial and temporal manners. By using a photomask during UV irradiation, the spatial control of surface functionality can be achieved and the following immobilization of cell adhesive/non-adhesive molecules on the exposure regions further controlled the presence and location of cells. The major advantage to introduce a photocleavable molecule in the system is to introduce light to control surface properties for cell adhesion. Light as a versatile stimulus is easy to control on the movement and intensity, which is important to control a micro or ever nano-scale feature for cell adhesion. Not like other stimuli (such as heat and pH), light can be easily controlled on the dose and the affected area. At the same time, light is a non-invasive

stimulus and wouldn't cause structural damage on the material. Secondly, photocleavable molecules can be completely removed from the system without any residue left ideally, and cell adhesion will be not affected by any photocleavable molecule used and will be only related to the base material and the biomolecules in the strategy. Thirdly, the technique was able to control the presence of different surface functionality and feasible for different biomolecules immobilization targeting various applications. Finally, this technique allows spatial control of surface functionality in 3D and therefore provides a powerful alternative to generate a complex 3D structure for tissue engineering.

6.4 Recommendation

The following are a few recommendations for future research directions regarding to this study.

To simplify our system for cell initial attachment, a widely-studied cell line for cell-surface interaction, fibroblast, was utilized in cell studies. But in order to study cell behaviours after attachment, a specific cell type targeting the studied tissues or effects is more desirable. Highly organization of cells is a nature of tissues and a major goal of tissue engineering is to produce tissues equivalent to native tissues. To study the precise position of cells is a preliminary stage of understanding cell organization. Many researchers have shown the need to develop a platform or scaffold to precisely control cell attachment for different purposes on tissue engineering and related studies. For example, a skeletal muscle whose function highly depends on its structure from the molecular up to macroscopic dimensions. Its structure allows force to be generated and transmitted effectively throughout the muscle. In order to control its microstructure and mimic physiologic process of muscle formation, a control on the cellular level needs to be introduced. A study of muscle cell alignment to affect its function has been explored with a wavy micropatterned substrate. However, more aligning cells are seen and needed in a native tissue, and it is considered to be useful to create more complex structure for understanding the relationship between cell alignment and force production [3]. Our designed surface could be applied in these studies as a very good model surface due to the ease to create complex microstructures by light and to create a precisely controlled microstructure mimicking the native tissue and study how these structures

enhance force production. Another possible application of our surface could be a mimicking of neural network. As we know, neurons form interconnection to transmit signals. Therefore, the study of neural network is beneficial to build up an artificial neural network and understand how a brain works. Patterned growth of neurons and the formation of a neural network on a surface *in vitro* are prerequisite to studies related neural networks. A few studies have been done to create patterns for neural growth and form a network. Most current research involves in photolithography [4], soft lithography [5], and microfluidic system [6] to create surface heterogeneity for neuron attachment. Our surfaces based on SAM and chitosan could provide an alternative choice for biologists to create *in vitro* neural network.

The current method is not advocating for high-precise single cell patterning. The resolution is hundreds of microns and still too large for individual cell patterning. To localize single cell on our surfaces, a control upon surface functionality was recommended to be modified and extended into a smaller size even a nano-scale. To narrow cell adhesive regions to a single-cell width for cell alignment or reduce them to create controlled single cell-cell interactions could be a future direction for many applications, especially for neuron studies. It is believed that single neuron patterning with complex interconnections can provide more insight about neural networks in the body [6, 7].

Particularly for the SAM system, due to its well-defined surface functionality on 2D, it could be developed as a biochip for regulating cell-cell interactions in controlled microenvironment and the study of cell attachment phenomena, like interactions to specific extracellular matrix components with cells. Here are some examples that can be adapted. (1) An immediate application of this surface is to create small cellular colonies for rapid cytotoxicity testing and drug screening. For example, multiple chemicals could be immobilized to the surface and then study the effects of these chemical (e. g. drugs) on adhesion of different cell types [8]. (2) By changing the immobilized biomolecules, the system could be used to introduce biotin-streptavidin complexation on this two-dimensional surface to immumocapture different types of cells [9]. (3) An important exploration of this SAM is that it could be used with controlled light pathway and light intensity to create chemical gradient which is believed important to guide neuron growth [10].

For chitosan, known for its biodegradability and biocompatibility, it can be developed to an implantable scaffold with controllable microstructure. Chemical reaction employed in 2D is recommended to apply on a 3D chitosan scaffold or hydrogel. The ultimate goal to develop and study cell patterning is to understand and mimic tissue development from the cellular level to the organ. With the development of tools for light pathway or two-photon microscopy [11], the method combining photochemistry and a biodegradable material may be able to create complex 3D architectures in order to control cell growth. Optimization over UV irradiation can be expected to provide precise control on light pathway and minimize light scattering.

6.5 Scientific contribution

The following lists the scientific contributions from this study.

Generally, new approaches to create controllable surface heterogeneity for cell patterning were proposed and demonstrated from surface characterizations to cell studies.

For BNBA-DT-Au surface,

(1) A novel photocleavable SAM was developed involving a bifunctional nitrobenzyl derivative and PEG to control cell attachment.
(2) A full examination by different surface techniques was provided to demonstrate successful fabrication.
(3) The capability to switch its property from cell non-adhesive to cell adhesive was demonstrated.
(4) It was proven that the surface also helped decrease the side effect of nitrobenzyl residue after photoactivation.

For NVOC-AUT-Au surface,

(1) The fabrication for a new photocleavable SAM involving monofunctional NVOC was described and the detailed examination of surface properties was provided by different surface techniques.
(2) Precise control on the presence of surface functionality and cell initial attachment was achieved on this surface.

(3) Spatial and temporal control on cell initial attachment was achieved on NVOC-AUT-Au surface. PC12 cells were able to pattern in different shapes on NVOC-AUT-Au surface.

(4) Cell attachment and differentiation were controlled separately and precisely by selective immobilization and diffusion.

For NVOC-CS surface,

(1) A methodology to synthesize photocleavable NVOC immobilized chitosan was first described.

(2) Multiple exposure strategy was applied on biodegradable chitosan. Controllable cell attachment was achieved on this chitosan 2D surface, which is feasible to apply with different types of cell patterning.

6.6 References

1. Chatelet, C., O. Damour, and A. Domard, *Influence of the degree of acetylation on some biological properties of chitosan films.* Biomaterials, 2001. **22**(3): p. 261-268.
2. Freier, T., et al., *Controlling cell adhesion and degradation of chitosan films by N-acetylation.* Biomaterials, 2005. **26**(29): p. 5872-5878.
3. Lam, M.T., et al., *Microfeature guided skeletal muscle tissue engineering for highly organized 3-dimensional free-standing constructs.* Biomaterials, 2009. **30**(6): p. 1150-1155.
4. Jing, G.S., et al., *Cell patterning using molecular vapor deposition of self-assembled monolayers and lift-off technique.* Acta Biomaterialia, 2011. **7**(3): p. 1094-1103.
5. Heller, D.A., et al., *Patterned networks of mouse hippocampal neurons on peptide-coated gold surfaces.* Biomaterials, 2005. **26**(8): p. 883-889.
6. Romanova, E.V., et al., *Engineering the morphology and electrophysiological parameters of cultured neurons by microfluidic surface patterning.* Faseb Journal, 2004. **18**(9): p. 1267-+.
7. Morin, F., et al., *Constraining the connectivity of neuronal networks cultured on microelectrode arrays with microfluidic techniques: A step towards neuron-based functional chips.* Biosensors & Bioelectronics, 2006. **21**(7): p. 1093-1100.
8. Roth, E.A., et al., *Inkjet printing for high-throughput cell patterning.* Biomaterials, 2004. **25**(17): p. 3707-3715.
9. Li, N. and C.M. Ho, *Photolithographic patterning of organosilane monolayer for generating large area two-dimensional B lymphocyte arrays.* Lab on a Chip, 2008. **8**(12): p. 2105-2112.
10. Herbert, C.B., et al., *Micropatterning gradients and controlling surface densities of photoactivatable biomolecules on self-assembled monolayers of oligo(ethylene glycol) alkanethiolates.* Chemistry & Biology, 1997. **4**(10): p. 731-737.
11. Lee, S.H., J.J. Moon, and J.L. West, *Three-dimensional micropatterning of bioactive hydrogels via two-photon laser scanning photolithography for guided 3D cell migration.* Biomaterials, 2008. **29**(20): p. 2962-2968.